AN INVESTIGATION ON THE GAIT ANALYSIS PROTOCOL OF THE "KISS" MOTION ANALYSIS SYSTEM

A THESIS SUBMITTED TO
THE GRADUATE SCHOOL OF NATURAL AND APPLIED SCIENCES
OF
THE MIDDLE EAST TECHNICAL UNIVERSITY

BY

BURCU SÖYLEMEZ

IN PARTIAL FULFILLMENT OF THE REQUIREMENTS FOR THE DEGREE
OF MASTER OF SCIENCE
IN
THE DEPARTMENT OF MECHANICAL ENGINEERING

JUNE 2002

Approval of the Graduate School of Natural and Applied Sciences

Prof. Dr. Tayfur Öztürk
Director

I certificate that this thesis satisfies all the requirements as a thesis for the degree of Master of Science.

Prof. Dr. Eres Söylemez
Head of Department

This is to certify that we have read this thesis and that in opinion it is fully adequate, in scope and quality, as a thesis for the degree of Master of Science.

Prof. Dr. S. Turgut Tümer
Supervisor

Examining Committee Members

Prof. Dr. M. Kemal Özgören

Prof. Dr. Bülent E. Platin

Prof. Dr. S.Turgut Tümer

Assoc. Prof. Dr. İsmet Erkmen

Asst. Prof. Dr. Ergin Tönük

ABSTRACT

AN INVESTIGATION ON THE GAIT ANALYSIS PROTOCOL OF THE "KISS" MOTION ANALYSIS SYSTEM

Söylemez, Burcu

M.S., Department of Mechanical Engineering

Supervisor: Prof. Dr. S. Turgut Tümer

June 2002, 164 pages

This thesis aims to evaluate and refine the gait analysis protocol employed in the Biomechanics Laboratory at the Mechanical Engineering Department of the Middle East Technical University.

The current gait analysis protocol used in the laboratory, namely KissGAIT, was tested to observe the effects of hip joint center location and centering device placement on the reliability and repeatability of the gait analysis results. The evaluation has been performed through a set of experiments.

Based upon the outcomes of the evaluation, a new protocol has been proposed for the gait analysis and it has been validated via new experiments.

The protocol proposed in this study allows gait analysis without the use of centering devices so that the joint centers are determined all through the motion using real-time data. This new protocol is simpler than KissGAIT to apply during the experiments and the results came out to be in agreement with the data given in literature, data obtained using the KissGAIT protocol and a commercially available system.

Keywords: Gait analysis, anatomic landmark calibration, centering devices.

ÖZ

"KISS" HAREKET ANALİZİ SİSTEMİNİN YÜRÜYÜŞ ANALİZİ PROTOKOLÜNÜN İNCELENMESİ

Söylemez, Burcu

Yüksek Lisans, Makina Mühendisliği Bölümü

Tez Yöneticisi: Prof. Dr. S. Turgut Tümer

Haziran 2002, 164 sayfa

Bu tezde Orta Doğu Teknik Üniversitesi, Makina Mühendisliği Bölümü Biyomekanik Laboratuarında kullanılan yürüme analizi protokolünün değerlendirilmesi ve iyileştirilmesi amaçlanmıştır.

Şu anda laboratuarda kullanılmakta olan yürüyüş analizi protokolü, KissGAIT ile kalça eklemi merkezinin konumu ve merkezleme aparatı yerleştirmenin yürüyüş analizi sonuçlarının güvenilirlik ve tekrarlanabilirliğine etkilerini incelemek üzere bir dizi deney yapılmıştır. Yapılan deneylerin sonuçlarına dayanarak yeni bir yürüyüş analizi protokolü teklif edilmiş ve bu protokol yeni deneylerle doğrulanmıştır.

Bu çalışmada önerilen protokol diz ve bilek merkezleme aparatları olmaksızın yürüyüş analizine olanak sağlamakta, böylelikle diz ve ayak bileği eklem merkezleri hareket esnasında gerçek zamanlı veriler kullanılarak hesaplanmaktadır. Deneylerde uygulanması daha kolay olan bu yeni protokol ile elde edilen sonuçlar, literatürden sağlanan, KissGAIT ve ticari bir sistem kullanılarak elde edilen verilerlerle de uyuşmaktadır.

Anahtar kelimeler: Yürüme analizi, anatomik nokta kalibrasyonu, merkezleme aparatları.

ACKNOWLEDGEMENTS

First of all, I would like to express my great appreciation and thanks to my family, who supported and encouraged me all through my life.

I also want to thank my supervisor Prof. Dr. S. Turgut Tümer, my co-worker and friend Behzat B. Kentel for the guidance they provided in this study. I also deeply appreciate the valuable comments of Prof. Dr. Kemal Özgören.

I hereby, would like to state my gratefulness to those who participated in long and tiring experiments and whose names are not mentioned.

TABLE OF CONTENTS

LIST OF TABLES

TABLE

LIST OF FIGURES

FIGURE

CHAPTER I

INTRODUCTION

1.1 Gait Analysis

Locomotion is the action with which the entire bulk of an animal's body moves through aerial, aquatic or terrestrial space (Cappozzo, 1984). Although locomotion is a very complex phenomenon, which can only be thoroughly described through a multidisciplinary approach, the most quantifying approach comes from the domain of classical mechanics.

The quantitative description of all mechanical aspects of walking is referred to as the gait analysis. The gait analysis is a systematic measurement, description and assessment of those quantities thought to characterize human locomotion (Davis et al, 1991). In gait analysis, the motion data and ground reaction forces are obtained simultaneously; later this data is used to calculate time-distance parameters, joint angles, joint moments and joint powers depending upon a model.

Through gait analysis, kinematic and kinetic data are acquired and analyzed to provide information which describes fundamental gait characteristics and which is ultimately interpreted by the clinicians to form an assessment (Davis et al, 1991).

A more detailed description of the gait analysis can be found in the Ph.D. thesis by Dr. H. Cenk Güler (1998).

The clinical use of gait analysis has expanded due to an improved understanding and interpretation of the information that the measurement systems provide, the development of software packages for collection of data and the advances in hardware technology.

Today, gait analysis is a powerful tool for:

- Pre-surgical and post-surgical evaluation for clinicians,
- The evaluation during rehabilitation,
- The evaluation of prosthetic joint replacements,
- The study of athletic injuries, amputees, orthotics and assistive devices, and
- The study of neuromuscular disorders

1.2 Gait Analysis Systems

A typical gait analysis system consists of cameras for observing subject's motion from different perspectives, image storing devices for each camera, active and passive markers

placed on the subject at different locations. The initial objective is to find the 3D trajectories followed by these markers.

Although the 3D coordinates of a marker can be determined when seen by two cameras, the realities of gait analysis require that four, five or six cameras be used. The use of multiple cameras increases the overlap and decreases marker drop out (Shafiq M.S., 1998)

The location of the markers with respect to anatomical landmarks is critical to the overall accuracy of the system. The marker set is also coupled to a biomechanical model. The marker and model combination allows the calculation of angular and linear positions, velocities and accelerations of the body segments.

The ground reaction forces are measured by force plates, which contain several transducers that provide data associated with the three force components of the ground reaction force, the vertical ground reaction torque, and location of the center of pressure.

1.3 Motivation

The Biomechanics Laboratory at the Mechanical Engineering Department of the Middle East Technical University consists of six cameras, two force plates and the associated software called Kiss-GAIT.

No written material about the main software that calculates the joint angles, moments and powers had been available. Therefore, the documentation and re-generation of the joint angle calculation procedure was the first objective of the thesis.

Some shortcomings of the current protocol were demonstrated through a set of experiments performed. Possible solutions for these shortcomings that would harm the quality of the results were searched. As a result, an alternative new protocol described in this study is proposed and tested.

1.4 Scope of the Thesis

After the survey of the related literature, the thesis is composed of three parts. The first part, chapter III, is the documentation of the current protocol in detail, which is believed to be a valuable source for future studies and experiments to be conducted in the biomechanics laboratory.

The second part of the thesis, chapter IV, is the critical investigation of the current protocol to analyze the effects of mislocation of some anatomical landmarks and repeatability of the experiments.

The third part, chapter V, is on the development and documentation of a new protocol proposed for the calculation of

joint angles that would eliminate the problems observed in the current protocol.

CHAPTER II

LITERATURE SURVEY

2.1 General Remarks

According to Andriacchi and Alexander, (2000) the first attempt to quantify human motion dates back to Weber Brothers' (1836) studies on the temporal and distance parameters during human locomotion. Later, the works of Marey and Muybridge around 1870's were among the first to quantify the patterns of human movement using photographic techniques.

The methodology for determination of joint kinematics is an important aspect of motion analysis systems. Several studies exist in the literature for the calculation of kinematical joint parameters from three dimensional marker data. Cappozzo (1984) described the general methodology of gait analysis and pointed out the importance of filling the gap between the clinician and the engineer.

A survey on the available literature revealed the issues affecting the reliability of the gait analysis results, in particular those related to the kinematics of gait.

The underlying guidelines, which are central to a successful determination of kinematics in the gait analysis, can be summarized as follows:

1. Marker sets must have a definite relationship to the underlying anatomy.

2. Three-dimensional techniques must be employed since the motion is three-dimensional.

3. Utmost care should be paid in the application of the marker set on the human anatomy and accuracy of the measurements for a successful gait analysis.

In what follows; the factors affecting the quality of gait experiments, in terms of reliability and repeatability of the results, are discussed in more detail.

2.2 Protocols Employed For Joint Angle Calculations

A gait analysis protocol involves the marker set configuration (i.e. the number of markers and their location) and the way the coordinate systems are constructed using these markers. Prior to calculating segment and joint angles, suitable estimates for the

rotation matrices must be obtained from judiciously positioned and measured landmarks. These landmarks are artificial markers embedded in the bones or affixed to the skin.

Davis, et al. (1991) introduced the protocol that is being used in Newington Children's Hospital, Newington, USA. The most detailed data collection and reduction protocol is described in this work. The system employs nineteen markers attached to the subject. The instantaneous orientation of an orthogonal marker-based-embedded-coordinate system is determined for pelvis, each thigh, shank and foot segments. The marker-based-embedded coordinate systems of thigh, shank and foot are then realigned with the instantaneous-joint center based-embedded-coordinate systems. The joint angles are then calculated. The estimation of the hip joint center location is carried out by employing empirical relations using leg length and the distance between the two anterior superior iliac spines.

Apkarian, et al. (1989) modeled the lower limb as a sequence of four rigid links connected by three universal rotary joints representing the hip, knee and ankle. Also, a method is described to measure the gait variables so that all nine angles can be computed based on the positions of eighteen markers placed on the subject.

Kadaba et al. (1990) also described a technique for determination of joint kinematics from markers on lower extremity.

2.3 Parametrization of Joint Angles

The relative position of two segments at a joint is described by three angles. A model for the joints is needed to find a parametric representation for these angles.

Euler (Cardan) angles are frequently used to determine the relative orientation of segments (Wisman et al. (1980); Grood and Suntay (1983); Apkarian et al. (1989); Kadaba et al. (1990); Davis et al. (1991); Woltring (1991)). Euler angles however have some drawbacks, one of which is their sequence dependency such that different sequences yield different numerical values of the angles for the same orientation. Moreover, if the sequence is not carefully selected, some singularities in inverse kinematics may be encountered, which renders the determination of the angles impossible.

A standardization proposal for the joint angle parameterization has been suggested by Grood and Suntay (1983), which introduces the concept of joint coordinate system. The joint coordinate system is modeled as a four-link open kinematic chain consisting of cylindrical joints where the relative

motion between the links is described using Hartenberg and Denavit convention. The application of the joint coordinate system yields either directly the anatomical angles or the resulting angles are easily convertible to the anatomical convention.

In clinical gait analysis, another method used is the 'projected angles' in three major movement planes in order to parameterize joint and segment rotations. In this method, the rotation angles about each coordinate axes are simply the angles between the initial and final positions of a chosen vector. Although not sequence dependent, as are the Euler angles, projected angles are unreliable in their application to the joint motion. This approach yields kinematically valid results only when the segment angles are relatively small with respect to the reference attitudes (Sutherland et al., 1988; Woltring, 1991)

It is also a common application to use the concept of helical axis (screw axis) to quantify relative segment orientation (Kinzel et al., 1972; Spoor and Veldpaus, 1980; Woltring et al., 1985; Woltring, 1986; 1991; 1994). In this method, any finite movement from a reference position and attitude to a current one can be described in terms of a rotation about and translation along a directed line in space. Helical axis method completely describes any kind of joint motion and is independent of the choice of the

coordinate system. However, it is rather difficult to estimate the helical axis since the method is particularly sensitive to measurement errors. (Lange et al., 1990; Woltring, 1994). Moreover, the difficulty for a clinician to relate the helical axis to anatomical angles prevents extensive use of this method.

2.4 Location of the Hip Joint Center

Estimating the location of the hip joint center from the positions of external markers is important in an accurate calculation of angles and moments at the hip and knee joints (Crowninshield et al., 1977; Cappozzo, 1986; Woltring and Fioretti, 1989; Kadaba et al., 1990; Cappozzo, 1991).

In literature, both invasive and non-invasive methods to estimate hip joint center are described. Invasive methods are out of scope of this study, so only non-invasive methods for determining the location of hip joint center will be considered.

There are a number of non-invasive methods for estimating the hip joint center location:

i. **Leardini's method**: In this method, the subject is made to perform continuously and sequentially a flexion/extension followed by an abduction/adduction of the hip. Later this data is used to estimate hip joint center by regression equations. Although

Leardini's experiment shows that the functional method is the most accurate and can be applied to any size and shape of pelvis, it does not seem to be appropriate for the patient who cannot fulfill the hip rotation trials. This method proves useful when able-bodied persons are examined. (Leardini et al., 1998)

ii. **Davis's method**: This method is currently employed in Kiss-GAIT protocol, which is used in the Biomechanics Laboratory at METU. Davis suggested an algorithm to estimate the hip joint center from the regression of leg length, pelvic width, marker radius and generalized stratified values. The angular constants and other numerical relationships used in the function are estimated through radiographic examination of hip studies (Davis et al., 1991).

iii. **Bell's method**: Bell estimated the hip joint center from the basis of ASIS to ASIS distance (inter-ASIS distance). He reported twice on this topic. In the first report, 3D hip joint center can be located from ASIS by 30% of inter-ASIS distance distal, 14% medial and 22% posterior. In the second report, hip joint center was located from ASIS by 30% of interASIS distance distal, 14% medial and 19% posterior. The difference between two reports came from the different definition of pelvic reference frame. It was reported that this method is able to locate the 3D

hip joint center on the point with approximately 1.5 cm from true location, which is superior to functional method (Bell et al., 1989; 1990). Bell's method, however, has one limitation. It considers only the inter-ASIS distance for hip joint center estimation on the assumption that the 3D configuration of pelvis is determined only by inter-ASIS distance. However, with same length of inter-ASIS distance, a variable length of proximal/distal or anterior/posterior distance can be possible according to the shape of pelvis.

iv. Siedel's method: This method makes use of several parameters to estimate the hip joint center. In addition to the pelvic width (inter-ASIS distance), the pelvic height (perpendicular from pubic center to inter-ASIS line) and the pelvic depth (from ASIS to PSIS) are also measured. The hip joint center is located as 14% of pelvic width medial, 34% of pelvic depth posterior and 79% of pelvic height inferior from ASIS. It is reported that the mean error for each direction is around 0.50 cm, which is more accurate than Bell's method (Seidel et al., 1995). However, this method has some problems because it defines the frontal plane formed by both ASIS and pubic tubercle as the reference frame of pelvis and the pelvic depth is measured obliquely from ASIS to ipsilateral PSIS. If this method is used, markers should be placed

on pubic symphsys and both PSIS, which is an added complication in the protocol.

v. **Vaughan's method**: Vaughan used a method similar to Bell's. The horizontal plane of pelvis is used as reference plane and the relative length of the inter-ASIS distance is measured. The hip joint center marker is estimated by 59.6% of the inter-ASIS distance to anterior direction, 34.4% to lateral direction and 29% to distal direction from the mid-PSIS marker. But, this method also suffers from the fact that the proximal/distal or anterior/posterior distance of pelvis may vary according to the shape of the pelvis (Vaughan *et al*, 1992).

vi. **Güler's method**: In this method, the location of the hip joint center is located using a technical marker on the greater trochanter (GT) and anthropometric properties of femur. The method may be preferred in a protocol where GT marker is used. However, the effectiveness of the method has not been yet investigated (Güler, 1998).

A comparison of different methods for locating the hip joint center is summarized in table 2.1.

Table 2.1: Comparison of hip joint center location estimation methods

Method	Accuracy (distance between true & estimated)	Needed marker	Applicable age group
Davis	not assessed	both ASIS, midPSIS	not specified
Bell, 1989	within 25 mm	both ASIS, PS	adult
Bell, 1990	12- 19 mm	both ASIS, midPSIS	adult
Bell+Andriacchi	10 mm	both ASIS, midPSIS, GT	adult
Siedel	5 mm	both ASIS, PS, both PSIS	adult
Vaughan	not assessed	both ASIS, mid PSIS	not specified
PS is pubic symphysis		GT is greater trochanter	

The errors in estimating the hip joint center location, the center of the femoral head, may lead to errors in the femoral anatomical system of axes, the hip and knee joint coordinate systems thus hip and knee angles. Moreover, the hip joint center is the point with respect to which hip joint moments are calculated (Stagni et al. 2000), so an accurate estimation for the hip joint center is required.

However, the ambiguity still remains since none of the methods in the literature are proven to be superior over others.

2.5 Anatomical Landmark Calibration

An anatomical landmark is defined as a point, or effectively small area, reliably identifiable within a biological structure (bone).

Anatomical landmark position vectors in the relevant bone-embedded technical frame are assumed to be time invariant and determined through an ad hoc experiment referred to as 'anatomical landmark calibration' (Cappozzo, 1984; Cappozzo et al., 1995; Cappello et al., 1997). The purpose of this anatomical calibration is to identify the anatomical landmarks of interest (e.g., hip joint center, knee joint center, ankle joint center) with respect to an easily identifiable group of markers (e.g. greater trochanter, lateral condyle, and lateral malleolus on the femur), which are more convenient to track with the motion analysis system. The trajectories of an adequate number of bony anatomic landmarks allow for the determination of the pose of a bone-embedded anatomical frame versus time. Using the poses of two adjacent bone-embedded anatomical frames, six variables are derived that thoroughly and effectively describe relative joint kinematics.

For this purpose the static shot concept is being used. Cappozzo et al. (1995) describes this technique under the name: 'Calibrated Anatomical System Technique' (CAST).

2.6 Soft Tissue Movement

Currently, one of the primary technical factors limiting the advancement of the study of human movement is the measurement of skeletal movement from markers placed on the skin. The most frequently used method for measuring human movement involves placing markers or fixtures on the skin's surface of the segment being analyzed (Benedetti and Cappozzo, 1994). The movement of the markers is typically used to infer the underlying relative movement between two adjacent segments (e.g. knee joint) with the goal of precisely defining the movement of the joint. Skin movement relative to the underlying bone is one of the primary factors limiting the resolution of detailed joint movement using skin-based systems (Cappozzo et al., 1997; Sati et al., 1996; Reinschmidt et al., 1997; Holden et al., 1997). The effects of skin movement artifact in Kiss-GAIT protocol are discussed and investigated by Afşar H. (2001).

CHAPTER III

KISS-GAIT: THE CURRENT GAIT ANALYSIS PROTOCOL

3.1 Laboratory and System Description

The Biomechanics Laboratory at the Mechanical Engineering Department of the Middle East Technical University has been established using off-the-shelf equipment, original design, locally available production facilities and software development studies (Figure 3.1).

The motion measurement system used in the laboratory employs six CCD (charge coupled device) cameras with special infrared sources mounted around lenses (Figure 3.2). The cameras also use infrared filters to recognize only the reflection of 2.5 cm diameter markers. The view of the markers is obtained at a 50 Hertz sampling frequency and 752 by 291 active elements configured in the interlaced mode of cameras.

A video triggering unit, designed by BİLTEN and produced by ODESA A.Ş., provides synchronized collection and storage of the camera shots.

Data from the two force platforms (BERTEC) and electromyography (EMG) (BORTEC Octopus 8-channel), all synchronized with the camera signals are collected by an analog to digital converter (National Instruments, DT 2801) and sent to a computer for storage.

Two force plates are embedded in a 4.6 meters long walking band, staggered for right and left steps (Figure 3.3).

There are also a linearization table to correct the lens distortion errors in camera images and four camera calibration rods (Figure 3.1) to estimate the calibration parameters to be used in relating 2-D data with its 3-D counterpart.

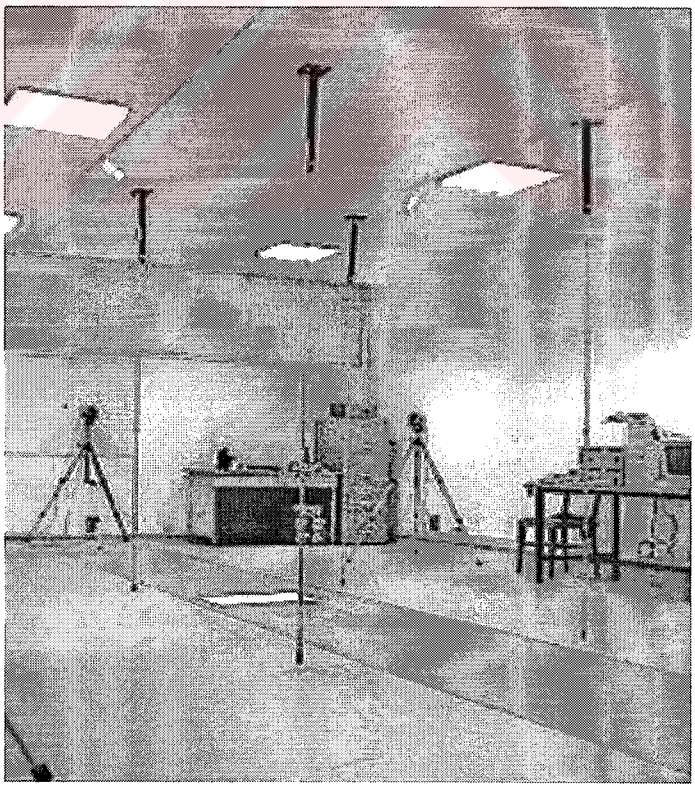

Figure 3.1: General view of the laboratory

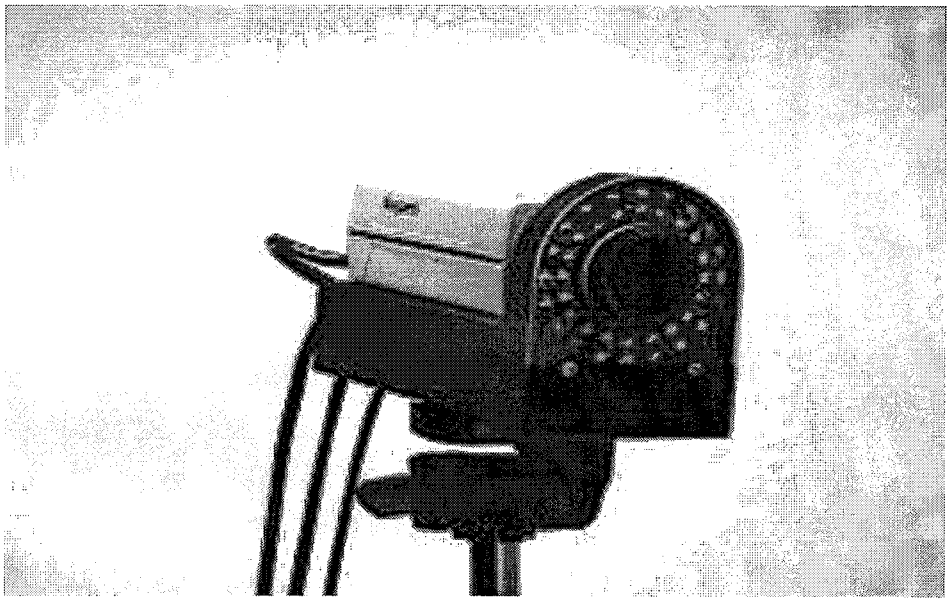

Figure 3.2: CCD cameras

Figure 3.3: Force plates

3.1.1 Markers

Markers are 25 mm diameter spheres, covered with retro-reflective material (3M) sensitive to infrared light. Four types of markers shown in Table 3.1 are used:

Table 3.1: Types of markers

Type 1		Circular base, marker directly on top.
Type 2	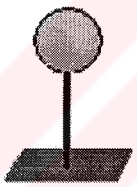	Rectangular base, marker on a 40 mm rod.
Type 3	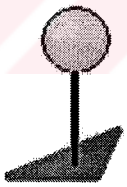	Triangular base, marker on a 40 mm rod.
Type 4	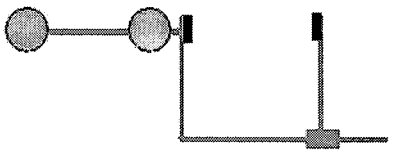	Knee and ankle centering devices (KCD, ACD). Vise-like devices with two markers attached at a distance.

3.1.2 'KISS' Gait Analysis System

In the laboratory, the analysis is performed using a set of software called '**Kiss**' (**K**as **İs**kelet **S**istemi), which is supported by two user-interfaced softwares.

The user interactive data acquisition (**Kiss-DAQ**) software has been developed to perform camera calibration and linearization, to record and store images synchronously with force platform and EMG measurements. This software also processes the image data for pixel grouping and marker identification, and automatically generates 3-D marker trajectories. After online data recording, subsequent off-line processing terminates with the labeling of the marker trajectories by the system operator.

An intermediate software combines the marker trajectories and force plate and EMG data to create a single input file.

The second software called '**Kiss-GAIT**' performs the calculation and presentation of the gait parameters. The Kiss-GAIT accepts the combined file as input and utilizes a biomechanical model to compute the following global gait parameters:

- **Time-Distance Parameters:**

  Step length and time; stride length and time, cadance, etc.

- **Joint Angles:**

Pelvic tilt, rotation, obliquity angles, hip joint extension-flexion, abduction-adduction, internal-external rotation angles, knee joint extension-flexion, varus-valgus, internal-external rotation angles, ankle joint dorsi-plantal flexion internal-external rotation angles and foot angle with respect to the platform.

- **Joint Moments:**

Hip joint extension-flexion, abduction-adduction, internal-external rotation moments, knee joint extension-flexion, varus-valgus, internal-external rotation moments, ankle joint dorsi-plantal flexion internal-external rotation moments.

- **Joint Powers:**

Hip joint extension-flexion, abduction-adduction powers, knee joint extension-flexion power, and ankle joint dorsi-plantal flexion power.

Finally, joint angles, moments and powers are drawn on scaled graphs whose horizontal axis representing the percentage of gait cycle.

3.2 Experimental Protocol

There are two stages in the experiment. First stage is the static shot, in which 19 markers are attached to the body as shown in Figure 3.4.

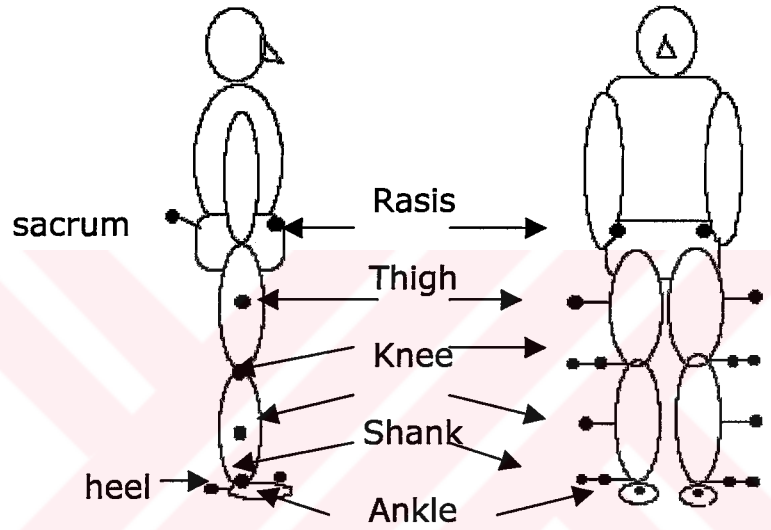

Figure 3.4: Marker placement for the static shot

LABEL	PLACE	MARKER TYPE
RASIS	Right pelvis anterior superior iliac spine	1
LASIS	Left pelvis anterior superior iliac spine	1
SACRUM	Middle of posterior iliac spine	3
RTHIGH	Right thigh (place not important)	2

LTHIGH	Left thigh (place not important)	2
ROKCD	Right outer knee centering device	4
LOKCD	Left outer knee centering device	4
RIKCD	Right inner knee centering device	4
LIKCD	Left inner knee centering device	4
RSHANK	Right shank	2
LSHANK	Left shank	2
ROACD	Right outer ankle centering device	4
LOACD	Left outer ankle centering device	4
RIACD	Right inner ankle centering device	4
LIACD	Left inner ankle centering device	4
RHEEL	Right heel	1
LHEEL	Left heel	1
RMETA2	Right second metatarsal	1
LMETA2	Left second metatarsal	1

The subject is asked to take natural upright position on the right force plate and one or two static shot data are stored for a period of one second. This completes the static part of the experiment.

Gait trials require 13 markers attached on the lower extremity as shown in Figure 3.5.

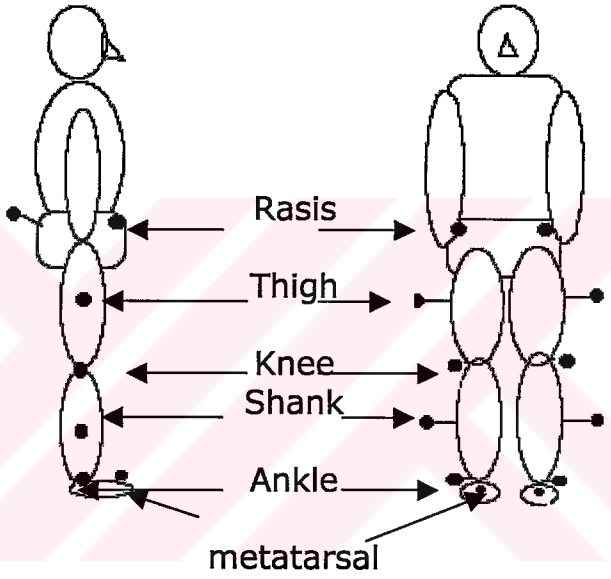

Figure 3.5: Marker placement for gait trials

LABEL	PLACE	MARKER TYPE
RASIS	Right pelvis anterior superior iliac spine	1
LASIS	Left pelvis anterior superior iliac spine	1

SACRUM	Middle of posterior iliac spine	3
RTHIGH	Right thigh (place not important)	2
LTHIGH	Left thigh (place not important)	2
RKNEE	Right knee	1
LKNEE	Left knee	1
RSHANK	Right shank	2
LSHANK	Left shank	2
RANKLE	Right ankle	2
LANKLE	Left ankle	2
RMETA2	Right second metatarsal	1
LMETA2	Left second metatarsal	1

The subject is asked to perform some warming up walking trials in order to find the best starting point to walk. While gait testing, the subject must finish two complete steps within the calibration volume and must step on only one force plate at a time. After all necessary adjustments are completed, the gait data is stored for a period of 5 seconds for a number of gait trials (around 7-10), and those involving proper foot placement on the force plates are chosen for processing by means of KissGAIT.

Lastly, anthropometric measurements are taken for:

Height	
Weight	
DASIS	Distance between two ASIS'
RLEG	Leg length measured through trochantor major-lateral femoral condyl-lateral malleoli
LLEG	
KW	Knee width between two femoral condyles
AW	Ankle width between two malleoli

3.3 Method of Analysis

3.3.1 Reference Coordinate Systems

Data acquisition software, 'Kiss-DAQ' and 'Kiss-GAIT' use different coordinate systems to define 3D marker coordinates.

The Kiss-DAQ estimates the marker coordinates with respect to coordinate system as shown in Figure 3.6(a). Whereas, the Kiss-GAIT uses the reference coordinate system shown in Figure 3.6(b) to define and calculate the required parameters.

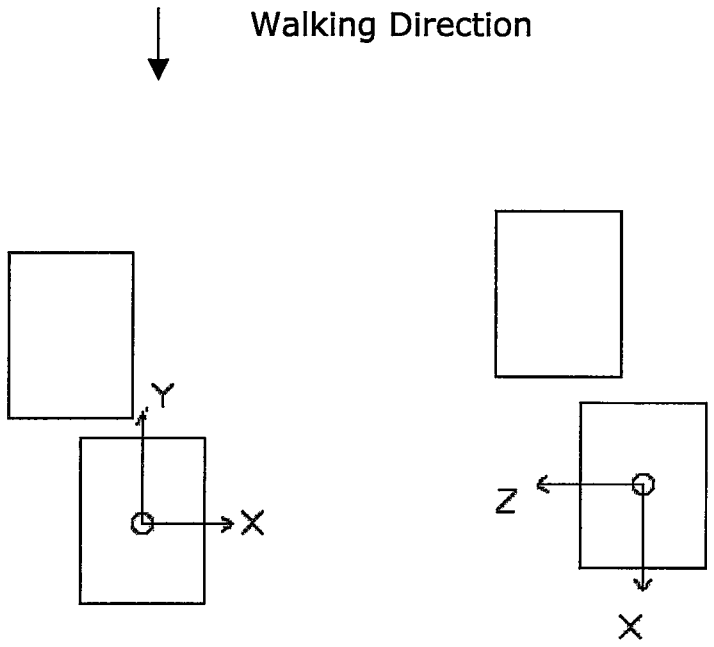

Figure 3.6:(a) Reference coordinate system of Kiss-DAQ

(b) Reference coordinate system of Kiss-GAIT

Motion data obtained from Kiss-DAQ is transformed to the coordinate system of Kiss-GAIT by using the transformation matrix below:

$$\hat{C}^{(A,L)} = \begin{bmatrix} 0 & -1 & 0 \\ 0 & 0 & 1 \\ -1 & 0 & 0 \end{bmatrix} \tag{3.1}$$

and all the marker coordinates are pre-multiplied as:

$$\overline{P}_i = \hat{C}^{(A,L)} * \overline{P}_i(L) \tag{3.2}$$

3.3.2 Digital Filtering

Like all experimental measurements, the measurements of the 3-D coordinates of the markers are contaminated with noise. (Güler, 1998)

One of the techniques to eliminate this noise is to use some sophisticated integration techniques that also smooth the signal to some extent. Another method is to make use of a low pass digital filter with a suitable cut-off frequency.

In Kiss-GAIT, a 4^{th} order Butterworth filter with a cut-off frequency of 6 Hz is used to eliminate noise. The filter is applied separately to the three components of the 3-D coordinates of the marker points. To get a 4^{th} order filtering a 2^{nd} order filter is applied to the data once forward in time and once backward in time to eliminate phase lag. This digital filter is characterized by a recursive equation:

$$X_n^* = c_0 X_n + c_1 X_{n-1} + c_2 X_{n-2} + b_1 X_{n-1}^* + b_2 X_{n-2}^* \qquad (3.3)$$

Where X is the raw and X^* is the filtered data and n denotes the time step. Values of the constants c_0, c_1, c_2, b_1, b_2 are given in Appendix A.

3.3.3 Definition of Link Coordinate Systems

Link coordinate systems are defined using the surface markers attached to the body segments. However, the calculation of anatomically meaningful joint angles requires tracing the motions of the joint centers as well.

Locations of the hip joint center are calculated using regression equations. The knee and ankle joint centers, on the other hand, are determined relative to the positions of the existing markers during the static shot. The main purpose of static shot is to find a constant transformation between surface-marker-defined coordinate system (technical coordinate system) and inside-body-marker-defined coordinate system (anatomical coordinate system).

The markers, anatomical and technical coordinate systems for the segments can be viewed in Figure 3.7.

Using the static shot data, the transformation matrix between technical coordinate system and anatomical coordinate system for each link is found once, and anatomical coordinate systems are obtained from technical coordinate systems by assuming that this transformation matrix remains constant during gait.

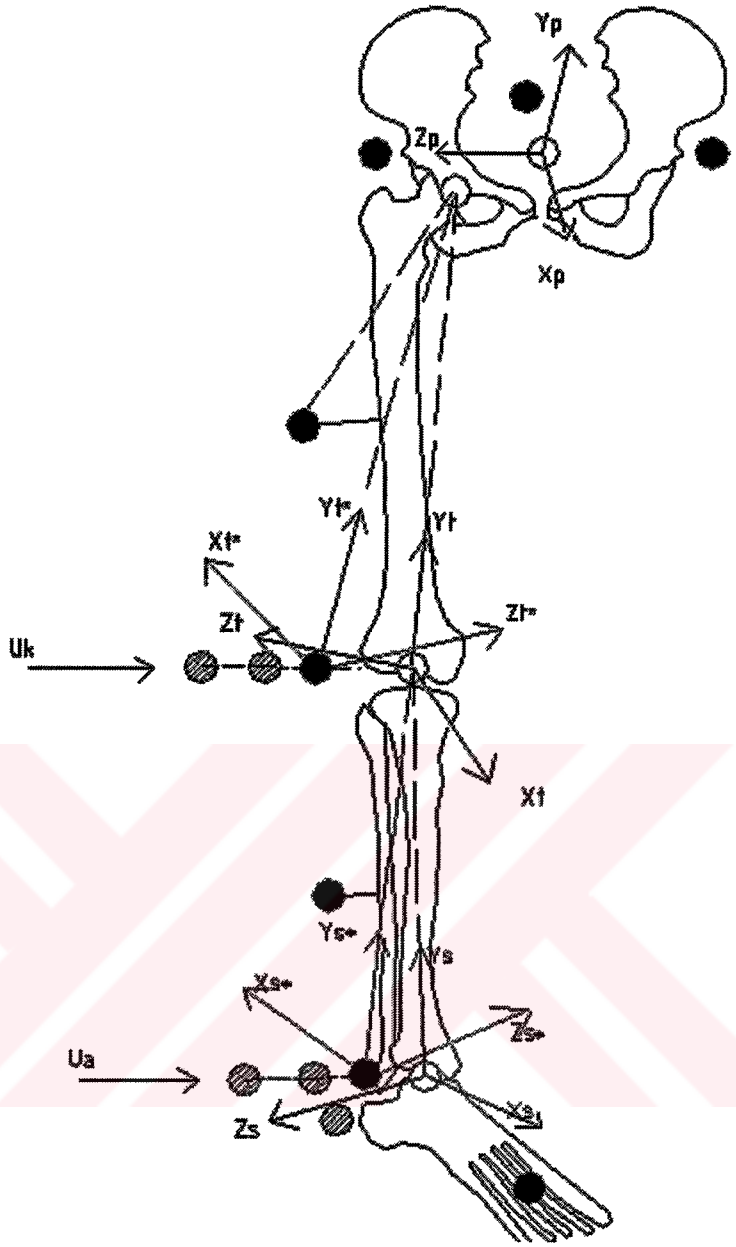

Figure 3.7: Coordinate systems for the segments. (Dark markers are placed in dynamic trial, empty ones show joint centers and hatched markers are placed for static shot only. The coordinate systems with star represent technical coordinate system)

3.3.4 Marker Enumeration

The following numerical symbols will be used for the 17 markers (Figure 3.4 and Figure 3.5) during the calculations:

P1: RASIS

P2: LASIS

P3: SACRUM

P4: THIGH

P5: KNEE

P6: SHANK

P7: ANKLE

P8: HEEL

P9: METATARSAL

P10: PELVIC CENTER

P11: HIP CENTER

P12: KNEE CENTER

P13: ANKLE CENTER

P14: OUTER KNEE

P15: INNER KNEE

P16: OUTER ANKLE

P17: INNER ANKLE

3.4 Calculation Procedure

3.4.1 Pelvis

For pelvis, technical and anatomical planes are coincident, so no transformation is needed to calculate joint angles. Also static and dynamic test calculations are the same for pelvis.

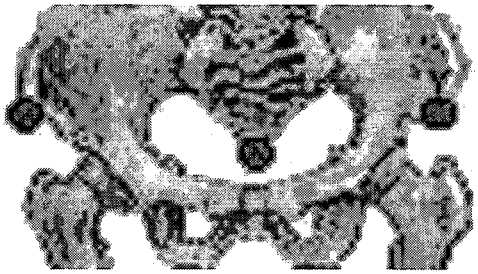

Figure 3.8: Marker placement for pelvis.

Summary of the coordinate system for pelvis:

Center: P10

z_p axis: along P2-P1, towards P1 (right-hand-side)

y_p axis: perpendicular to plane defined by P1, P2, P3, in superior direction

x_p axis: perpendicular to the other two axes

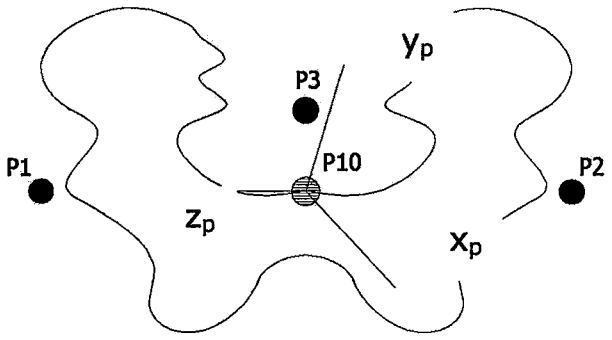

Figure 3.9: Coordinate axes of pelvis

The pelvic center is found as the mid point of left and right ASIS (P1 and P2).

$$\vec{P10} = \frac{\vec{P1} + \vec{P2}}{2} \tag{3.4}$$

The unit vector along z-axis from LASIS (P2) to RASIS (P1):

$$\vec{k}_p = \frac{\vec{P1} - \vec{P2}}{\left\| \vec{P1} - \vec{P2} \right\|} \tag{3.5}$$

The unit vector along y-axis is perpendicular to the plane formed by the two ASIS' (P1 and P2) and sacrum (P3):

$$\vec{j}_p = \frac{(\vec{P1} - \vec{P2}) \times (\vec{P2} - \vec{P3})}{\left\| (\vec{P1} - \vec{P2}) \times (\vec{P2} - \vec{P3}) \right\|} \tag{3.6}$$

The unit vector along x-axis is perpendicular to the plane formed by the vectors above:

$$\vec{i}_p = \vec{j}_p \times \vec{k}_p \tag{3.7}$$

So, the pelvis coordinate system (Figure 3.9) is defined by:

$$\hat{C}^{(A,P)} = \left[\bar{i}_p(A) \quad \bar{j}_p(A) \quad \bar{k}_p(A) \right] \tag{3.8}$$

3.4.2 Thigh

For thigh, two different coordinate systems are found using static test data: the technical coordinate system and the anatomical coordinate system. The transformation between these two coordinate systems is assumed to be constant during gait. The technical coordinate system is found both during static calculations and throughout the gait.

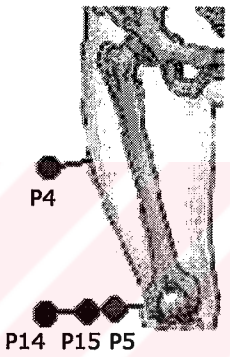

Figure 3.10: Marker placement for thigh

Hip Joint Center

The hip joint center is calculated from the positions of pelvic markers by using a regression equation given by Davis et al., (1991).

$$C=0,115*LEG - 15,3 \text{ (LEG is either RLEG or LLEG)} \quad (3.9)$$

$$x_{dis}= 0,1288* LEG-48,56 \quad (3.10)$$

$$X_H= -(x_{dis}+ r_m) \cos\beta+C \cos\theta \sin\beta \quad (3.11)$$

$$Y_H = -(x_{dis} + r_m)\sin\beta - C\cos\theta\cos\beta \quad (3.12)$$

$$Z_H = -\sigma[C\sin\theta - DASIS/2] \quad (3.13)$$

σ=1 for right side

σ=-1 for left side

Where $\theta = 28.4^0 * \pi/180^0$,

$\beta = 18^0 * \pi/180^0$

r_m is the marker radius (12.5 mm)

DASIS is the distance between two ASIS markers.

The hip joint center using the pelvic axes is then given by:

$$\vec{P}11 = \vec{P}10 + X_H\vec{i}_p + Y_H\vec{j}_p + Z_H\vec{k}_p \quad (3.14)$$

Knee Joint Center

The axis of rotation for knee is found once using the markers in static shot, then transformed for dynamic calculations using the transformation matrix for thigh.

The unit vector along the axis of rotation is defined from OKCD (P14) to IKCD (P15) and is given as:

$$\vec{u}_k = \frac{\vec{P}15 - \vec{P}14}{\left\|\vec{P}15 - \vec{P}14\right\|} \quad (3.15)$$

The motion data for the knee marker (P5) is collected in dynamic tests. For calculation of thigh coordinate axes at static posture, the virtual knee marker (P5) is found as:

$$\vec{P5} = \vec{P15} + KCDO.\vec{u}_k \quad (3.16)$$

where KCDO (knee centering device offset) is the offset of the inner knee marker (P15) in static shot with respect to the knee marker (P5) in dynamic test (Figure 3.11).

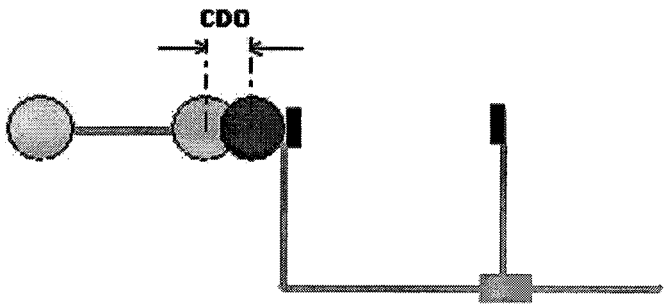

Figure 3.11: Centering device offset

Then, the knee center is calculated as:

$$\vec{P12} = \vec{P5} + (\frac{KW}{2} + r_m).\vec{u}_k \quad (3.17)$$

where KW is the knee width, r_m is the marker radius.

3.4.2.1 TECHNICAL COORDINATE SYSTEM FOR THIGH

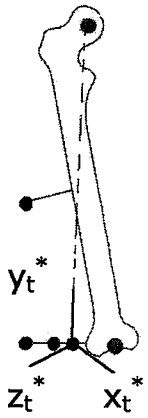

Figure 3.12: Technical coordinate system of thigh

Summary of the technical coordinate system of thigh (Figure 3.12):

Center: P5

y_t^* axis: along P5-P11 towards P11

x_t^* axis: perpendicular to the plane defined by P4, P5, P11, in anterior direction

z_t^* axis: perpendicular to the other two axes

The technical coordinate system for thigh has the origin at the knee marker (P5).

The unit vector from the knee marker (P5) to the hip center (P11) along y-axis:

$$\vec{j}_t^{\,*} = \frac{\overrightarrow{P11} - \overrightarrow{P5}}{\left\| \overrightarrow{P11} - \overrightarrow{P5} \right\|} \tag{3.18}$$

The unit vector perpendicular to the plane formed by the knee marker (P5), the hip joint center (P11) and the thigh marker (P4):

$$\vec{i}_t^{\,*} = \frac{(\overrightarrow{P5} - \overrightarrow{P11}) \times (\overrightarrow{P4} - \overrightarrow{P11})}{\left\| (\overrightarrow{P5} - \overrightarrow{P11}) \times (\overrightarrow{P4} - \overrightarrow{P11}) \right\|} \tag{3.19}$$

The vector perpendicular to the plane formed by these two unit vectors above is the unit vector in z-direction:

$$\vec{k}_t^{\,*} = \vec{i}_t^{\,*} \times \vec{j}_t^{\,*} \tag{3.20}$$

The transformation matrix for the technical coordinate system of thigh is:

$$\hat{C}^{(A,t^*)} = \left[\bar{i}_t^{\,*}(A) \; \bar{j}_t^{\,*}(A) \; \bar{k}_t^{\,*}(A) \right] \tag{3.21}$$

3.4.2.2 ANATOMICAL COORDINATE SYSTEM FOR THIGH

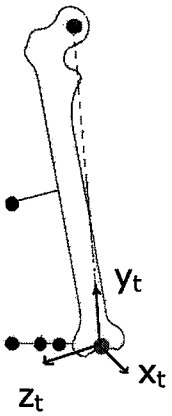

Figure 3.13: Anatomical coordinate system of thigh

Summary of the anatomical coordinate system of thigh (Figure 3.13):

Center: P12

y_t axis: along P12-P11 towards P11

x_t axis: perpendicular to the plane defined by P11, P12 and the knee axis, in anterior direction

z_t axis: perpendicular to other two axes

The origin of the anatomical coordinate system for thigh is the knee center.

The unit vector from the knee center (P12) to the hip center (P11):

$$\vec{j}_t = \frac{\overrightarrow{P11} - \overrightarrow{P12}}{\left\| \overrightarrow{P11} - \overrightarrow{P12} \right\|} \tag{3.22}$$

Unit vector perpendicular to the plane formed by knee center (P12), hip center (P11) and unit vector along the knee axis (u_k):

$$\vec{i}_t = \sigma \frac{(\overrightarrow{P12} - \overrightarrow{P11}) \times \vec{u}_k}{\left\| (\overrightarrow{P12} - \overrightarrow{P11}) \times \vec{u}_k \right\|} \tag{3.23}$$

where,

σ=1 for right side

σ=-1 for left side

Unit vector perpendicular to the plane defined by the vectors above: $\vec{k}_t = \vec{i}_t \times \vec{j}_t$ (3.24)

The transformation matrix for anatomical coordinate system of thigh is:

$$\hat{C}^{(A,t)} = \left[\bar{i}_t(A) \quad \bar{j}_t(A) \quad \bar{k}_t(A) \right] \tag{3.25}$$

3.4.2.3 TRANSFORMATION MATRIX FOR THIGH

After technical and anatomical coordinate system matrices are found in static calculation, the general transformation matrix is calculated as:

$$\hat{C}^{(t^*,t)} = \hat{C}^{(A,t^*)^T} . \hat{C}^{(A,t)} \tag{3.26}$$

All technical coordinate system matrices and unit vector along the knee axis are pre-multiplied with this transformation matrix to obtain anatomical coordinates during dynamic test calculations.

3.4.3 Shank

For shank, like thigh, two coordinate systems are found using static test data: the technical coordinate system and the anatomical coordinate system. The transformation between the two coordinate systems is found and assumed to be constant during gait.

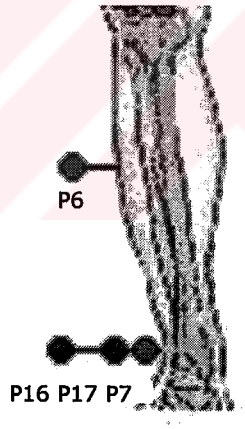

Figure 3.14: Marker placement for shank

Ankle Center

The unit vector along the axis of rotation is defined from OACD (P16) to IACD (P17) and is given as:

$$\vec{u}_a = \frac{\overrightarrow{P17} - \overrightarrow{P16}}{\left\| \overrightarrow{P17} - \overrightarrow{P16} \right\|} \tag{3.27}$$

The data for the ankle marker (P7) is collected during gait trials. For the calculation of shank anatomical coordinate axes at static posture, the position of the virtual ankle marker (P7) is found as:

$$\vec{P7} = \vec{P17} + ACDO.\vec{u}_a \tag{3.28}$$

Where ACDO is the offset of the inner ankle marker with respect to the ankle marker during gait trials (Figure 3.11).

Then, the ankle center (P13) is calculated;

$$\vec{P13} = \vec{P7} + (\frac{AW}{2} + r_m).\vec{u}_a \tag{3.29}$$

where AW is the ankle width and r_m is the marker radius.

3.4.3.1 TECHNICAL COORDINATE SYSTEM FOR SHANK

The origin of the technical coordinate system of shank is the ankle marker (P7) (Figure 3.15).

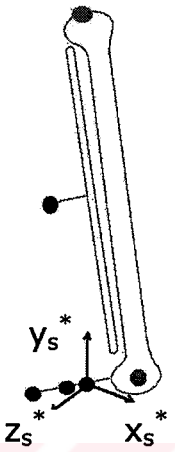

Figure 3.15: technical coordinate system of shank

Summary of the technical coordinate system of shank:

Center: P7

y_s^* axis: along P7-P12 towards P12

x_s^* axis: perpendicular to the plane defined by P7, P12, P6, in anterior direction

z_s^* axis: perpendicular to other two axes

The unit vector along y-axis:

$$\vec{j}_S^{\,*} = \frac{\overrightarrow{P12} - \overrightarrow{P7}}{\left\| \overrightarrow{P12} - \overrightarrow{P7} \right\|} \tag{3.30}$$

It is from ankle marker (P7) to knee center (P12).

The unit vector perpendicular to the plane formed by the ankle marker (P7), the knee center (P12), and the shank marker (P6):

$$\vec{i}_S^{\,*} = \frac{(\overrightarrow{P7} - \overrightarrow{P12}) \times (\overrightarrow{P6} - \overrightarrow{P12})}{\left\| (\overrightarrow{P7} - \overrightarrow{P12}) \times (\overrightarrow{P6} - \overrightarrow{P12}) \right\|} \tag{3.31}$$

The unit vector in z-direction: $\vec{k}_S^{\,*} = \vec{i}_S^{\,*} \times \vec{j}_S^{\,*}$ (3.32)

The matrix for the technical coordinate system of shank is:

$$\hat{C}^{(A,s^*)} = \left[\bar{i}_s^{\,*}(A) \; \bar{j}_s^{\,*}(A) \; \bar{k}_s^{\,*}(A) \right] \tag{3.33}$$

3.4.3.2 ANATOMICAL COORDINATE SYSTEM FOR SHANK

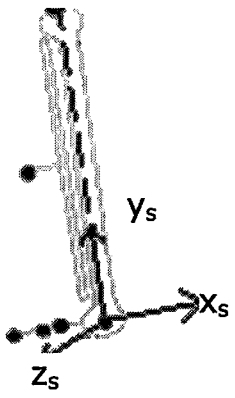

Figure 3.16:Anatomical coordinate system of shank

Summary of the anatomical coordinate system of shank (Figure 3.16):

Center: P13

y_s axis: along P13-P12 towards P12

x_s axis: perpendicular to the plane defined by P12, P13 and ankle axis, in anterior direction

z_s axis: perpendicular to other two axes

The origin of the anatomical coordinate system for shank is the ankle center (P13).

The unit vector from the ankle center (P13) to the knee center (P12):

$$\vec{j}_S = \frac{\overrightarrow{P12} - \overrightarrow{P13}}{\left\| \overrightarrow{P12} - \overrightarrow{P13} \right\|} \tag{3.34}$$

The unit vector perpendicular to the plane formed by the knee center (P12), the ankle center (P13) and the unit vector along the ankle axis (u_a):

$$\vec{i}_S = \sigma \frac{(\overrightarrow{P13} - \overrightarrow{P12}) \times \vec{u}_a}{\left\| (\overrightarrow{P13} - \overrightarrow{P12}) \times \vec{u}_a \right\|} \tag{3.35}$$

where,

σ=1 for right side

σ=-1 for left side

The unit vector perpendicular to the plane defined by the vectors above: $\vec{k}_S = \vec{i}_S \times \vec{j}_S$ (3.36)

The transformation matrix for anatomical coordinate system of shank is:

$$\hat{C}^{(A,s)} = \left[\bar{i}_s(A) \quad \bar{j}_s(A) \quad \bar{k}_s(A) \right] \tag{3.37}$$

3.4.3.3 TRANSFORMATION MATRIX FOR SHANK

The transformation matrix to be used in obtaining anatomical coordinates from technical coordinates is:

$$\hat{C}^{(s^*,s)} = \hat{C}^{(A,s^*)^T} . \hat{C}^{(A,s)} \tag{3.38}$$

All technical coordinate system matrices and unit vector along ankle axis are pre-multiplied with this transformation matrix during dynamic test calculations.

3.5 Kinematic Model and Joint Angles

3.5.1 Biomechanical Model

The experimental study of joint kinematics in three dimensions requires the description and measurement of six motion components. This description is required to be in terms of clinically meaningful joint angle definitions.

In clinical movement analysis, there is an interest to depict 3-D joint and segment angulations in terms of three independent

quantifiers that denote flexion/extension, abduction/adduction and endorotation/exorotation (internal/external rotation).

The biomechanical model developed by E.S. Grood and W. J. Suntay (1983) proposes a *joint coordinate system*, which involves angles independent of sequence and can easily be correlated with the clinically meaningful joint definitions. In this proposal, the rotations about and the translations along the defined coordinate axes form a set of independent generalized coordinates, which can be described using commonly employed clinical terminology. A desirable characteristic of this coordinate system is that joint displacements within the system are independent of the order in which the component translations and rotations occur. This eliminates the requirement of specifying the order of the rotations, a necessary procedure when Euler angles are used.

As a concept, the model used in the software considers a joint as a 3-degree-of-freedom kinematic structure between the proximal (near to the body) and distal (far from body) links. Kinematic modeling of the structure is obtained using the 'Hartenberg-Denavit' convention as shown in Figure 3.17.

According to Hartenberg-Denavit convention, Table 3.2 is obtained where, θ is the angle of rotation, α is the twist angle, 'a' is the link length, d is the offset.

After the rotation angles are found, the correlation with the clinically meaningful angles is needed.

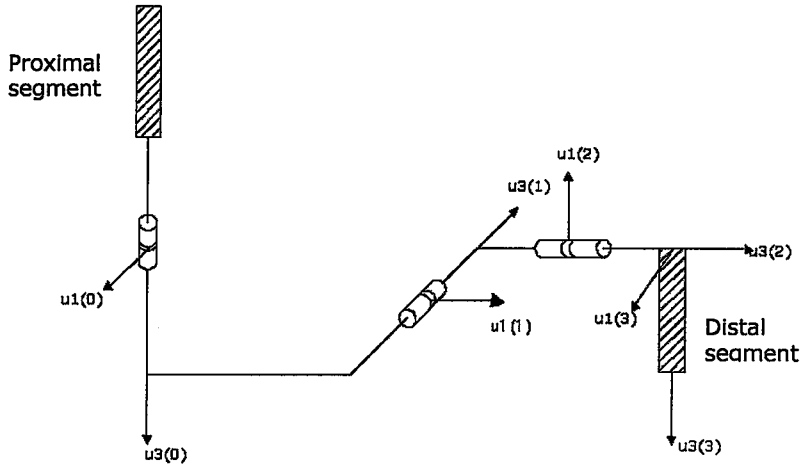

Figure 3.17: Schematic view of the biomechanical model

Table 3.2: Hartenberg-Denavit parameters

link	Joint angle θ_i at the reference position	α	d	a
1	θ_1=90°	-90°	0	0
2	θ_2=90°	-90°	0	0
3	θ_3=90°	-90°	$-l_d$	0

3.5.2 Calculating Joint Angles

In order to find anatomical joint angles via Cardan angles (θ_1, θ_2, θ_3) the transformation matrix between proximal and distal segments are found.

$$\hat{C}^{(P,D)} = \begin{bmatrix} c_{11} & c_{12} & c_{13} \\ c_{21} & c_{22} & c_{23} \\ c_{31} & c_{32} & c_{33} \end{bmatrix} \tag{3.39}$$

After the transformation matrix is obtained, to calculate angles θ_1, θ_2, θ_3 the inverse kinematics method in robotics applications is used. In this method, the transformation matrix should be obtained parametrically, as in the following:

$$\hat{C}^{(P,D)} = \hat{R}_3(\theta_1).\hat{R}_1(\frac{-\pi}{2}).\hat{R}_3(\theta_2).\hat{R}_1(\frac{-\pi}{2}).\hat{R}_3(\theta_3).\hat{R}_1(\frac{-\pi}{2}) \tag{3.40}$$

where, R_1 and R_3 represent elementary rotation matrices from which we obtain:

$$\hat{C}^{(P,D)} = \begin{bmatrix} c\theta_1 c\theta_2 c\theta_3 + s\theta_1 s\theta_3 & c\theta_1 s\theta_2 & -c\theta_1 c\theta_2 s\theta_3 + s\theta_1 c\theta_3 \\ c\theta_1 c\theta_2 s\theta_3 - s\theta_3 c\theta_1 & s\theta_1 s\theta_2 & -s\theta_1 c\theta_2 s\theta_3 - c\theta_1 c\theta_3 \\ -s\theta_2 c\theta_3 & c\theta_2 & s\theta_2 s\theta_3 \end{bmatrix} \tag{3.41}$$

In equation (3.41) $c\theta$ is the cosine of the angle and $s\theta$ is the sine of the angle.

From the matrix above the following angles are found parametrically as:

$\theta_2 = \text{acos}(c_{32})$ $\quad 0<\theta_2<\pi/2 \text{ if } c_{32}>0$ $\quad (3.42)$

$\pi/2<\theta_2<\pi \text{ if } c_{32}<0$

$\sigma = \text{sgn}(\sin\theta_2)$ $\quad (3.43)$

$\theta_1 = \text{angle}(\sigma . c_{12}, \sigma . c_{22})$ $\quad (3.44)$

$\theta_3 = \text{angle}(-\sigma . c_{31}, \sigma . c_{33})$ $\quad (3.45)$

Definitions of anatomical angles are given in Figure 3.18.

- **Pelvis Angles**

For pelvis, the orientation matrix is directly used to calculate the angles:

$\text{Pelvic tilt} = 90-\theta_1$ $\quad (3.46)$

$\text{Pelvic obliquity} = 90-\theta_2$ $\quad (3.47)$

$\text{Pelvic rotation} = 90-\theta_3$ $\quad (3.48)$

- **Hip Joint Angles**

The relative transformation matrix between pelvis and thigh is calculated as:

$$\hat{C}^{(A,t)} = \hat{C}^{(A,t^*)} * \hat{C}^{(t^*,t)} \quad (3.49)$$

$$\hat{C}^{(p,t)} = \hat{C}^{(A,p)^T} * \hat{C}^{(A,t)} \quad (3.50)$$

Definitions : A : Anterior; P : Posterior; L : Lateral; M : Medial
Subscripts "r" and "l" show to which side the angles belong
i.e. β_r : angle β for the right side; β_l : angle β for the left side.

HIP JOINT :

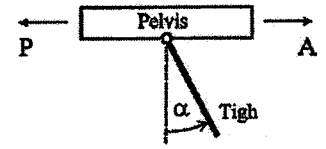

α>0 : Hip flexion
α<0 : Hip extension

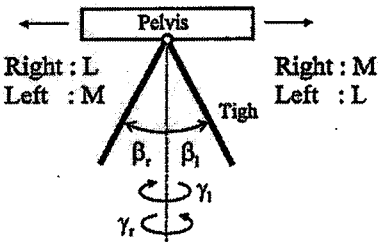

β>0 : Hip abduction
β<0 : Hip adduction

γ>0 : Hip internal rotation
γ<0 : Hip external rotation

KNEE JOINT :

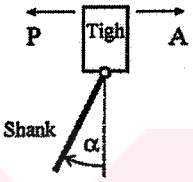

α>0 : Hip flexion
α<0 : Hip extension

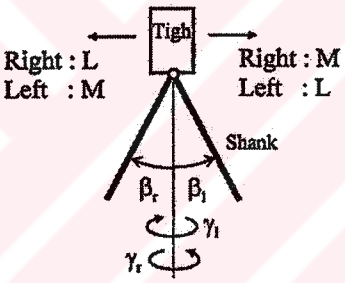

β>0 : Valgus
β<0 : Varus

γ>0 : Knee internal rotation
γ<0 : Knee external rotation

ANKLE JOINT :

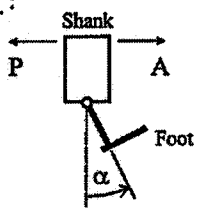

α>0 : Dorsiflexion
α<0 : Plantarflexion

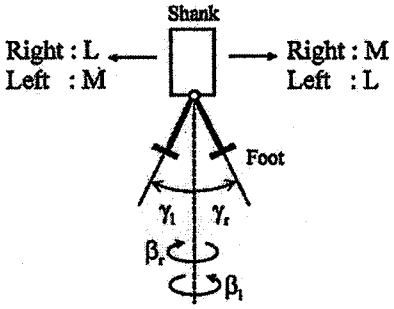

β>0 : Foot external rotation
β<0 : Foot internal rotation

γ>0 : Inversion
γ<0 : Eversion

Figure 3.18: Definitions of anatomical joint angles

Using the equations given in 3.49 and 3.50, the angles are found and the anatomical angles are:

Hip flexion= θ_1-90 (3.51)

Hip ab/adduction=δ (θ_2 –90) (3.52)

Hip rotation= δ (90- θ_3) (3.53)

where,

δ=1 for right leg

δ=-1 for left leg

- **Knee Joint Angles**

Applying the same procedure, the relative transformation matrix between the thigh and shank is found as:

$$\hat{C}^{(A,s)} = \hat{C}^{(A,s^*)} * \hat{C}^{(s^*,s)} \quad (3.54)$$

$$\hat{C}^{(t,s)} = \hat{C}^{(A,t)^T} * \hat{C}^{(A,s)} \quad (3.55)$$

The anatomical joint angles for knee are:

Knee flexion= 90-θ_1 (3.56)

Knee rotation= δ (θ_3-90) (3.57)

Knee valgus= δ (θ_2-90) (3.58)

where,

δ=-1 for left leg

δ=1 for right leg

3.6 Foot

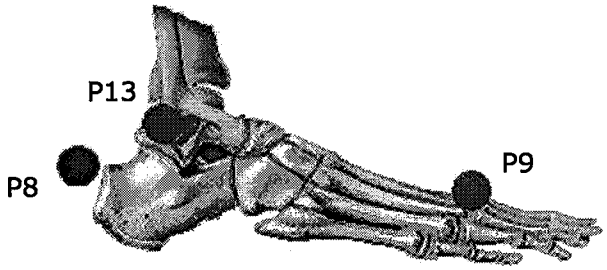

Figure 3.19: Marker placement for foot

The marker placement of foot is shown in Figure 3.19.

The angle between the vector from the second metatarsal (P9) to the heel (P8) and the vector from the second metatarsal (P9) to the ankle center (P13) (Figure 3.20) is calculated from static shot data.

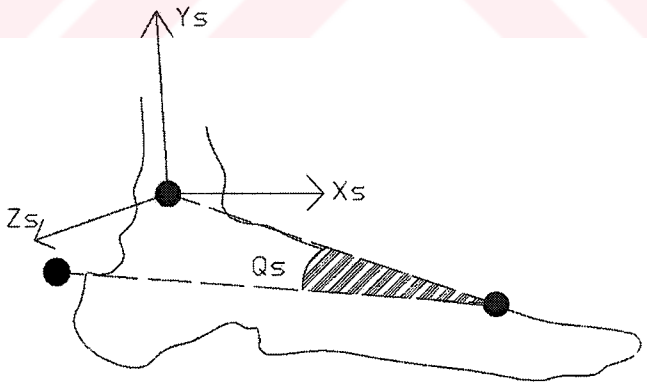

Figure 3.20: Static dorsiflexion angle

$$\theta_s = \arccos\left[\frac{\left(\vec{P13} - \vec{P9}\right)\cdot\left(\vec{P8} - \vec{P9}\right)}{\left|\vec{P13} - \vec{P9}\right| * \left|\vec{P8} - \vec{P9}\right|}\right] \tag{3.59}$$

Then, using the data from gait trials the following foot angles are calculated.

- **Foot Dorsiflexion Angle:**

The dorsiflexion angle of foot is the change in angle calculated in the static posture. It is the rotation of foot around z-axis of the shank coordinate system.

$$dorsflx = \arctan\left[\frac{\bar{u}_2{}^t \cdot \hat{C}^{(s,A)} \cdot \left\{(\vec{P9} - \vec{P13})\right\}^{(A)}}{\bar{u}_1{}^t \cdot \hat{C}^{(s,A)} \cdot \left\{(\vec{P9} - \vec{P13})\right\}^{(A)}}\right] - \theta_s \tag{3.60}$$

- **Foot Rotation Angle:**

The foot rotation angle is the rotation of the foot around y-axis of the shank coordinate system.

$$footrot = \arctan\left[\frac{\bar{u}_3{}^t \cdot \hat{C}^{(s,A)} \cdot \left\{(\vec{P9} - \vec{P13})\right\}^{(A)}}{\bar{u}_1{}^t \cdot \hat{C}^{(s,A)} \cdot \left\{(\vec{P9} - \vec{P13})\right\}^{(A)}}\right] \tag{3.61}$$

- **Foot Alignment:**

The foot alignment is the rotation of the foot around global y-axis.

$$footalignment = \arctan\left[\frac{\vec{u}_3 \cdot (\overrightarrow{P9} - \overrightarrow{P13})}{\vec{u}_3 \cdot (\overrightarrow{P9} - \overrightarrow{P13})}\right] \quad (3.62)$$

CHAPTER IV

EVALUATION OF THE CURRENT SYSTEM

4.1 Introduction

There are a number of factors affecting the performance of a gait analysis system. Some factors are inevitable and common for all systems, however some others are system specific and it is very important to estimate the errors involved due to these factors.

The performance of the instrumentation and software with which the marker coordinates are reconstructed in the laboratory frame is an important criterion for evaluation. The Kiss system has been exhaustively evaluated based on this criterion by Karpat Y., (2000).

Another factor affecting the performance of a gait analysis system is the soft tissue movement due to relative movement between the marker and the underlying bone. Afşar H., has evaluated Kiss system for skin movement artifact (2001).

There are inevitable errors in a gait analysis system due to assumptions involved in biomechanical models; since modeling a complex structure like human body can never be perfect. Furthermore, the true motion of the human body cannot be measured without these errors.

Another important factor for gait analysis systems is the estimation of anatomical landmarks especially joint centers from marker positions. In this part of the thesis, a set of experiments performed with the purpose of evaluating the effects of errors involved in the hip joint center estimation and the placement of knee centering device (KCD) and ankle centering device (ACD) will be presented.

4.2 Hip Joint Center Location

As discussed in the second chapter, an accurate estimation of the hip joint center using external markers is important in the calculation of the hip and knee joint angles, moments and powers.

In the Kiss-GAIT protocol, the hip joint center is calculated using the method introduced by Davis et al. (1991). The formulae for this method are given in Chapter III.

Figure 4.1 shows how the error in the hip joint center estimation propagates during the joint angle calculation procedure of the Kiss system.

PROPOGATION OF ERROR IN ESTIMATION OF HJC

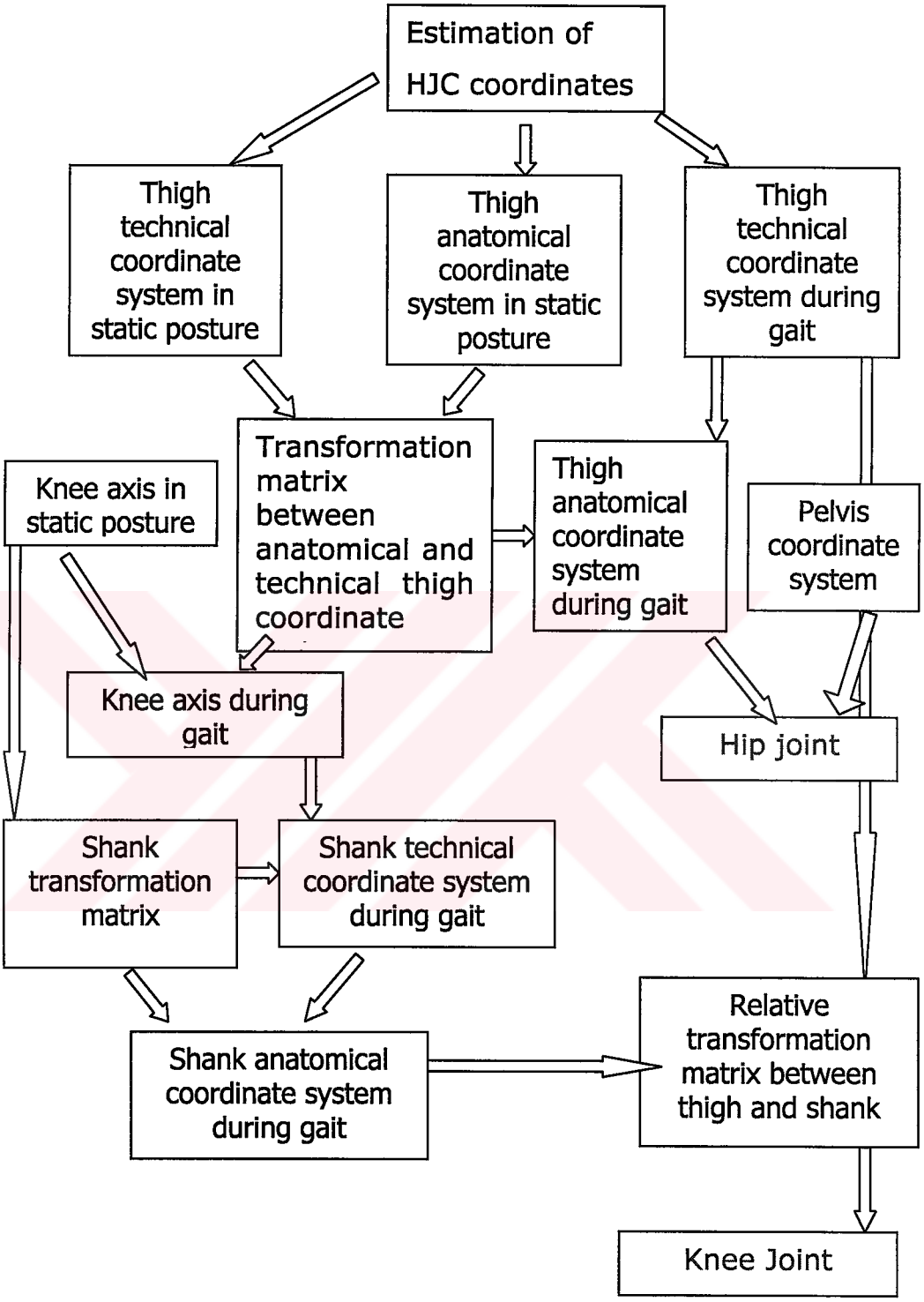

Figure 4.1: Propagation of error in estimation of hip joint center

For the purpose of investigating the effect of the hip joint center mislocation on the gait analysis results, the hip joint center is perturbated ± 30 mm in all three directions, separately. With these artificially imposed errors, knee and hip joint angles are calculated and variations are presented on the resulting 18 graphs to observe the effects of errors in hip joint center location.

The directions are the coordinates of the pelvic coordinate system as shown in Figure 3.9., where x-coordinate lies in anterior(+)/posterior(-) direction, y-coordinate lies in superior(+)/inferior(-) direction and z-coordinate lies on medial(-) /lateral(+) direction.

Figure 4.2 illustrates the joint angles when ±30 mm error is imposed in x-direction. It is seen that the percent changes in the flexion/extension angles of both hip and knee joint is negligible.

The error in x-coordinate of the hip joint center affects the abduction/adduction angle of hip joint and varus/valgus, internal/external rotation angle of the knee joint considerably. The knee varus/valgus angle is the most affected angle from the error imposed in this direction. The changes in these angles seem to be small, but when expressed as a percentage of the nominal value, they are hardly negligible.

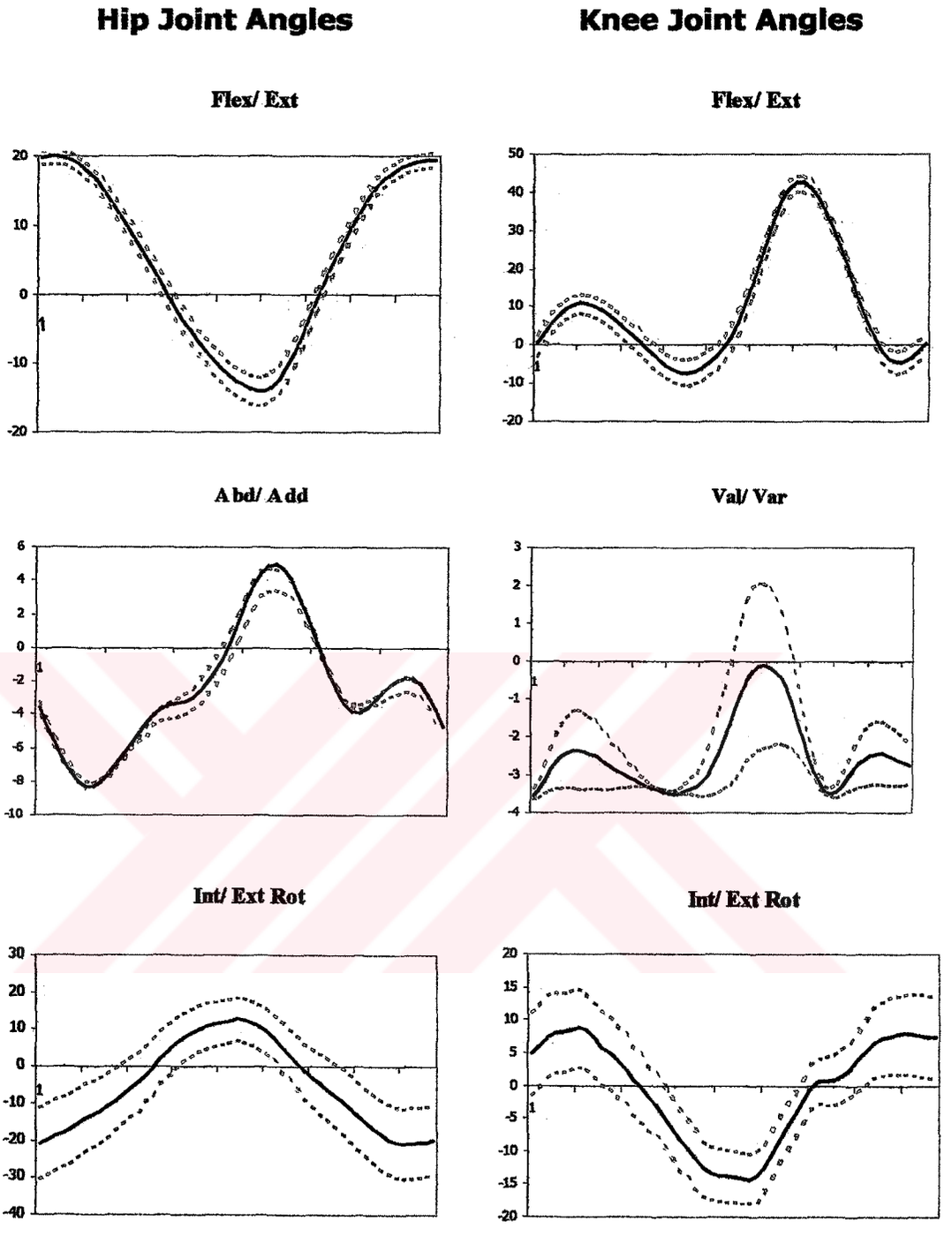

Figure 4.2: Graphs for Δx=±30mm mislocation in HJC

(red lines are obtained by (+)30mm perturabation,
blue lines are obtained by (-)30 mm perturbation,
black lines are the nominal values)

Figure 4.3 illustrates the joint angles when an error of ±30 mm in y-direction is imposed to the location of hip joint center. This error only occurs as a shift with small amplitude in all angles. Again knee varus/valgus and hip abduction/adduction angles seem to be affected more than the other angles in terms of percentage of the nominal values.

Lastly Figure 4.4 shows the results when an error of ± 30mm is imposed in z-direction. This error only affects the angles in frontal plane. All angles other than hip abduction/adduction angle and knee varus/valgus angle nearly remain the same. The error shows itself as a monotonic shift in the named angles. It should also be noted that when hip center is shifted along +z-direction medio-lateral rotation range of hip angles shift towards medial and medio-lateral rotation range knee angles shift towards lateral, which is as expected.

As the variations of angles with respect to percentage of gait cycle do not provide a sufficient base for comparison on their own, a statistical parameter, called the *coefficient of variation,* is calculated for evaluation purposes.

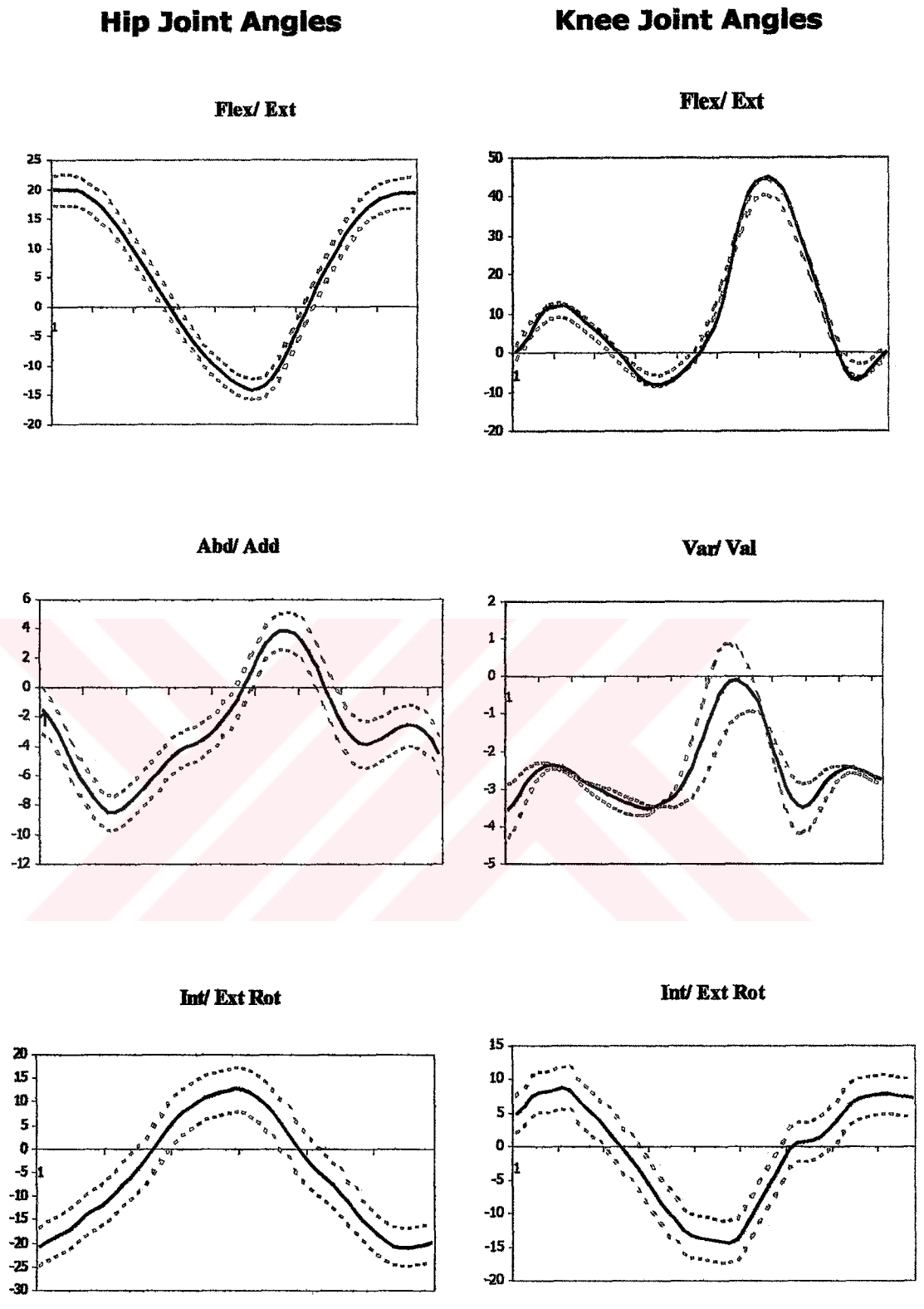

Figure 4.3: Graphs for Δy=±30mm mislocation in HJC

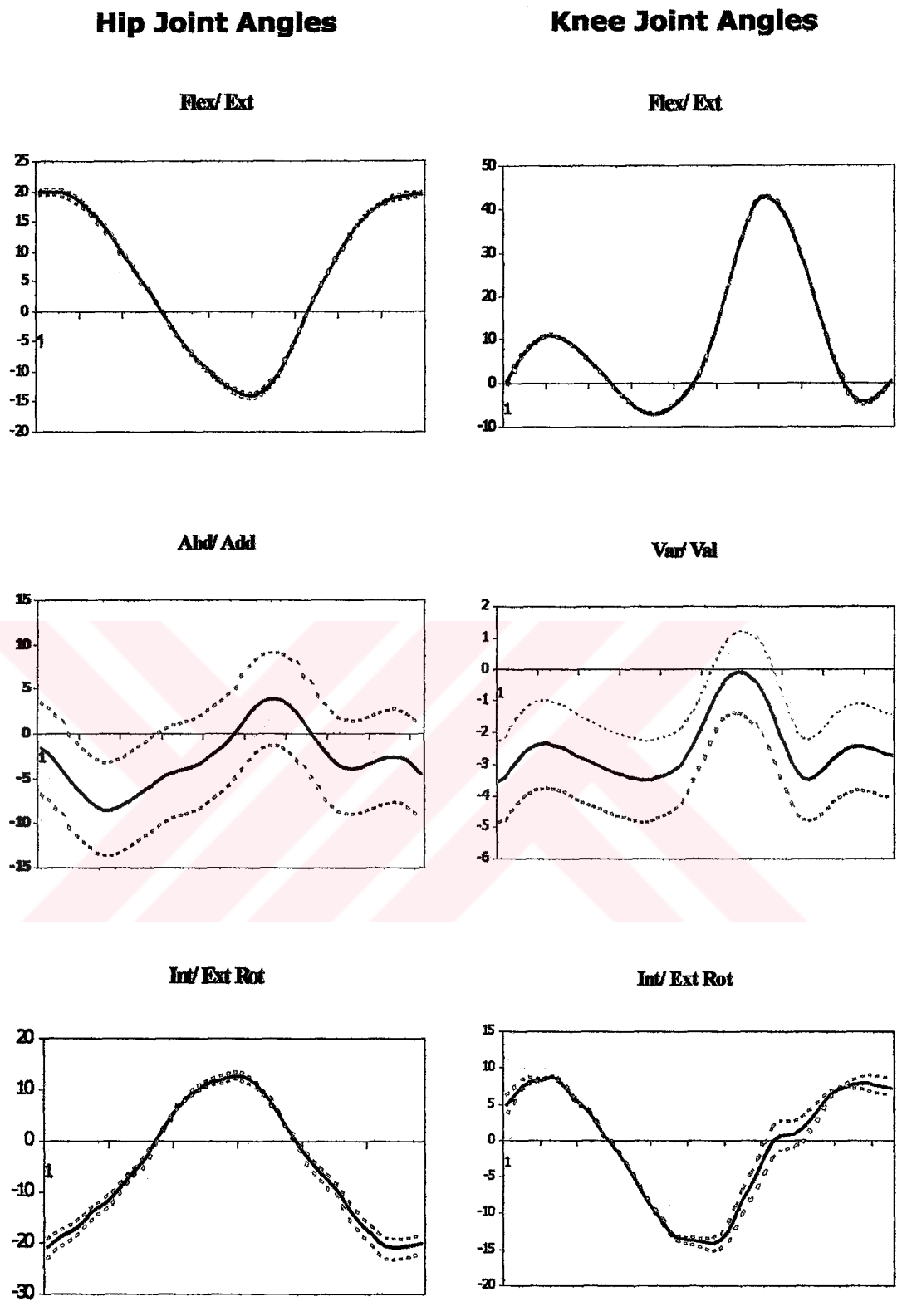

Figure 4.4: Graphs for Δz=±30mm mislocation in HJC

The *coefficient of variation* is the average standard deviation for the value over the whole gait cycle divided by the average mean as defined by Winter (1991), for joint angles during gait:

$$CV = \frac{\sqrt{1/N \sum_{i=1}^{N} \sigma_i^{\,2}}}{1/N \sum_{i=1}^{N} \left| X_i \right|} \qquad (4.1)$$

where, N is the number of data point in a gait cycle (100), σ is the standard deviation at an instant (the measurement of how widely the values are dispersed from the average when hip joint center location is perturabated), X_i is the mean value of the angle at that instant.

When the percent coefficient of variation is between 0 and 50 the quantity is considered to be reasonably consistent, between 50 and 100 the coefficient of variation does not supply any information, when the percent coefficient of variation is more than 100 the quantity can be classified to be inconsistent.

Table 4.1 illustrates the coefficients of variation for hip and knee joint angles when hip joint center location is located ± 30 mm.

Table 4.1: Coefficients of variation for hip and knee joint angles

	Hip Joint Angles			Knee Joint Angles		
	Flex-Ext	**Abd-Add**	**Int-Ext Rot**	**Flex-Ext**	**Var-Val**	**Int-Ext Rot**
$\Delta x=\pm 30$	14%	13%	78%	9%	27%	32%
$\Delta y=\pm 30$	13%	30%	19%	12%	27%	25%
$\Delta z=\pm 30$	5%	60%	12%	10%	47%	13%

The coefficients of variation are very consistent with the observations made on the graphs. As seen in table 4.1, the angles in frontal and transverse planes are the most sensitive angles to mislocation of hip joint center location. However none of the values calculated, indicate an imminent loss of reliability of the system.

As discussed in the literature survey chapter there is no generally excepted method for estimation of hip joint center location. Invasive methods are more accurate for finding hip joint center. However these methods are very expensive and the discussion on the ethics of these methods is inevitable (e.g. X-Ray). For the gait system currently being used in the Biomechanics Laboratory in the Mechanical Engineering department at the Middle East Technical University, namely Kiss-GAIT, hip joint abduction/adduction, internal/external rotation and knee joint varus/valgus, internal/external rotation angles are affected by the hip joint center mislocation.

4.3 Knee and Ankle Centering Device Placement

As suggested in the 'Future Work' section of Dr. H. Cenk Güler's Ph.D. thesis, investigation of the effects of knee centering device (KCD) and ankle centering device (ACD) placement in static shot of the experiment is necessary for assuring the repeatability of the system.

The diagram showing the propagation of error in placing KCD is shown in Figure 4.5. and the diagram showing the effect of ACD device is given in Figure 4.6.

There are two factors affecting the proper placement of the KCD and ACD. The first factor is related to the experience of the person who performs the gait experiment (performer) on placing the centering device correctly and consistently on a particular subject. The second factor is related to the suitability of the standard centering devices for different anthropometric properties of different subjects.

A set of experiments has been performed with 3 subjects (M.E., U.S., B.S.) and 4 performers. For each subject a gait trial is recorded together with the 12 static shot records performed by four performers. The classification of performers according to their experience in conducting gait analysis experiments are shown in Table 4.2.

Table 4.2: Performer classification

Performer number:	Experience level:
Performer 1	*Acquainted*
Performer 2	*Expert*
Performer 3	*Unaware*
Performer 4	*Knowledgeable*

Kiss-GAIT has been used for analysis of each combination. Hip, knee and ankle joint angles have been used as indicators of the above two factors.

Standard deviations and mean values of the angles for each subject have been calculated. Then, the results are plotted for hip joint, knee and ankle joint angles. The graphs plotted for the subjects M.E, U.S, B.S by four performers are given in Appendix B together with the analysis for each subject when different performers perform the experiments.

As an additional tool, the coefficients of variation for hip, knee and ankle joint angles are calculated. Table 4.3 illustrates the values for each subject.

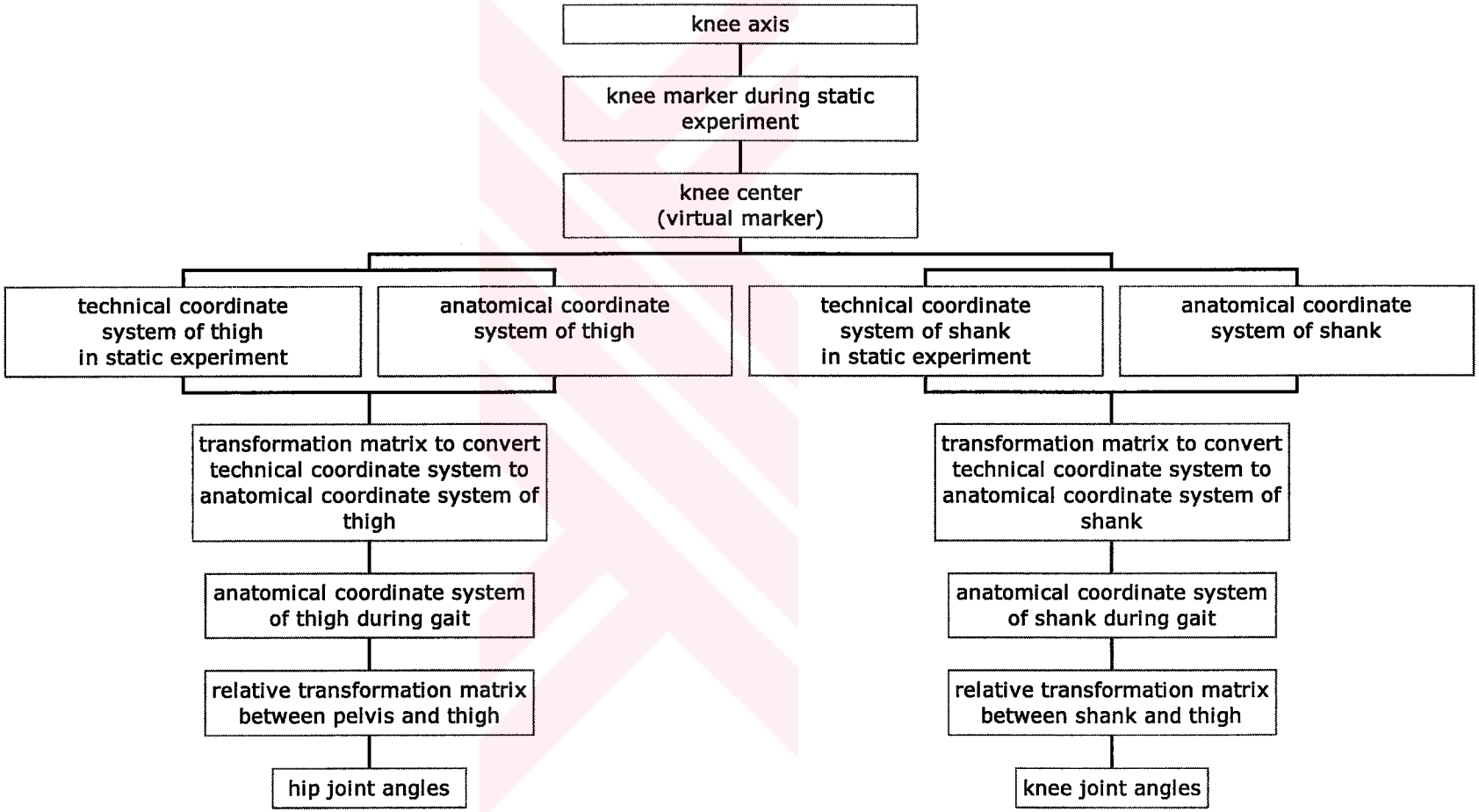

Figure 4.5: Effect of knee centering device on gait results

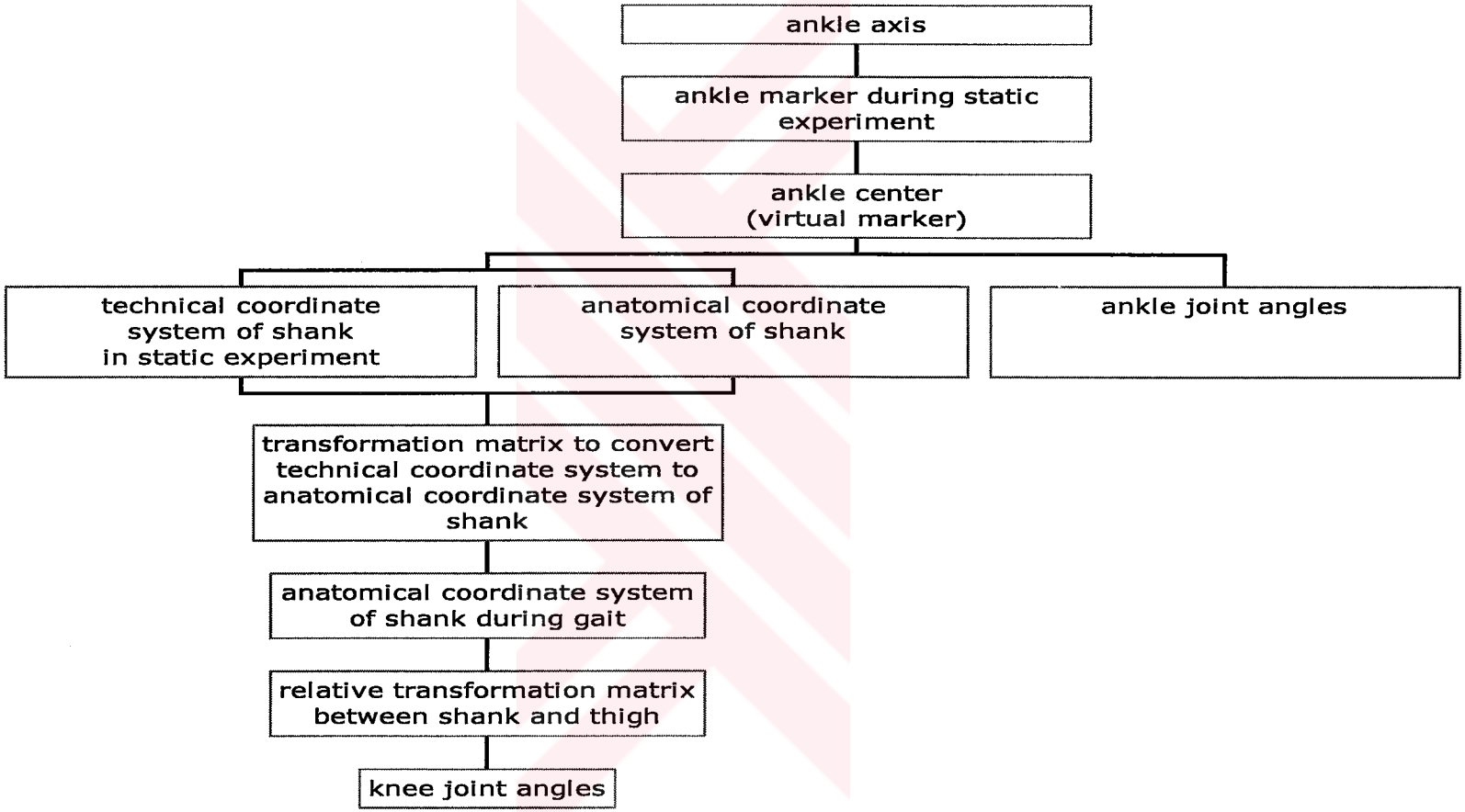

Figure 4.6: Effect of ankle centering device on gait result

Table 4.3: Coefficient of variations for three subjects

M.E	hip flex	hip abd	hip rot	knee flx	knee val.	knee rot.	dorsiflx
Exp.	5%	8%	54%	5%	53%	22%	22%
Know.	7%	12%	42%	18%	41%	28%	28%
Acq.	14%	69%	**136%**	13%	**132%**	10%	28%
Unaw.	17%	48%	**110%**	38%	93%	59%	59%

U.S	hip flex	hip abd	hip rot	knee flex	knee val.	Knee rot.	dorsiflx
Exp.	20%	69%	**139%**	16%	**156%**	33%	92%
Know.	4%	24%	**112%**	4%	72%	**294%**	54%
Acq.	14%	82%	66%	8%	88%	27%	62%
Unaw.	26%	**124%**	59%	32%	68%	**120%**	95%

B.S	hip flex	hip abd	hip rot	knee flex	knee val.	knee rot.	dorsiflx
Exp.	4%	2%	40%	12%	22%	22%	42%
Know.	7%	5%	**380%**	17%	54%	59%	42%
Acq.	11%	29%	**312%**	34%	94%	**111%**	90%
Unaw.	2%	3%	**117%**	8%	17%	64%	55%

To evaluate the results, the average values of the three experiments performed by the same performer on a subject are graphically presented in Figure 4.7 a, b, c and d.

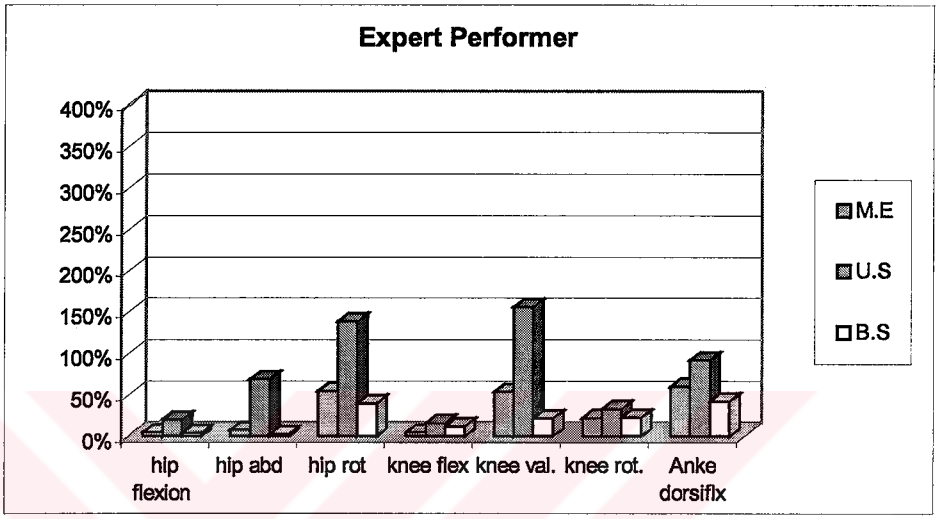

Figure 4.7a: Experiments performed by the expert performer.

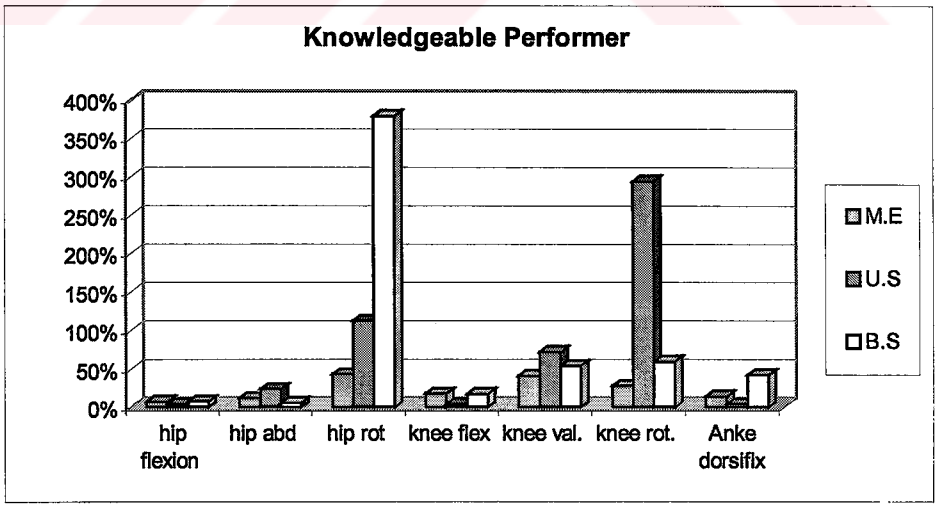

Figure 4.7b: Experiments performed by the knowledgeable performer.

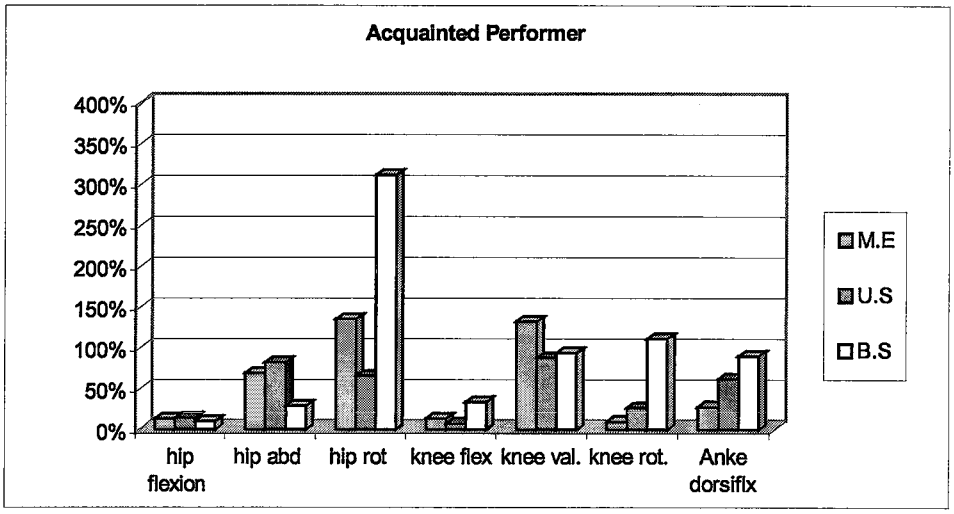

Figure 4.7c: Experiments performed by the acquainted performer.

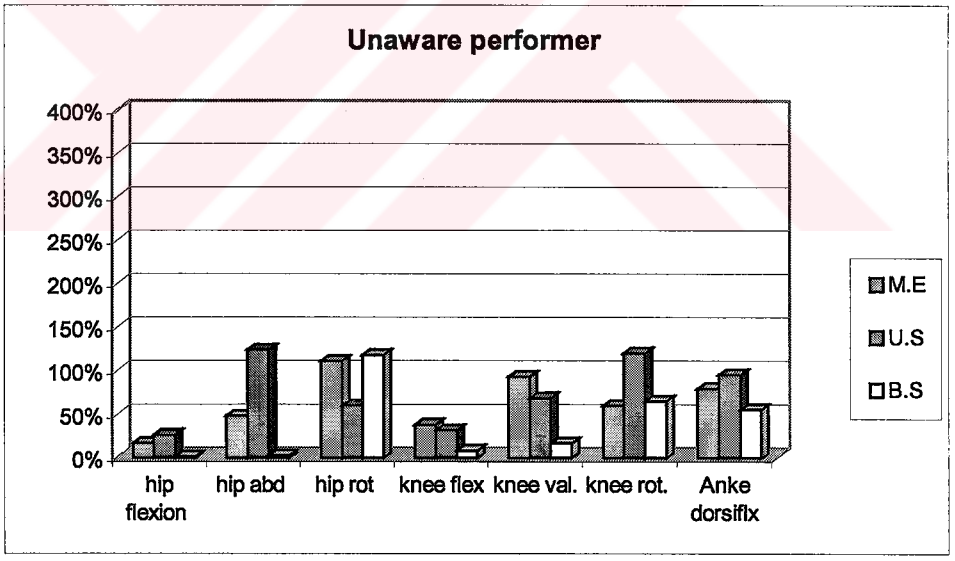

Figure 4.7d: Experiments performed by the unaware performer.

When all of the tools to investigate the effect of centering device placement for the static shot are considered, it can be concluded that:

1. Hip rotation, knee valgus/varus, knee rotation angles are the most sensitive angles to the centering device placement,
2. Experience is an important factor for centering device placement. The results of the most experienced performer, the expert, are more consistent than the others.
3. The standard deviation for most of the angles is considerable when expressed as a percentage of the nominal value.

4.4 General Remarks on the Current Protocol

When the whole evaluation is considered the following conclusions are reached:

1. Hip joint center mislocation is not a major problem affecting the repeatability of the system. However some offsets can be seen while evaluating the results.
2. Hip joint center mislocation calculations need not be refined since no method described in the literature is proven to be superior to the one adapted in this protocol. Also, the search for new methods for hip joint center location requires a lot of expensive invasive studies as well as cadaver studies for accuracy and precision.

3. Knee and ankle centering device placements in the static shot cause a lot of ambiguity about the repeatability of the system. The placement varies from one experiment to another for a performer and it varies from one performer to another.
4. A new approach for estimating joint angles without centering devices should be searched, in order to eliminate the influence of the centering devices and the performer on the results of gait analysis.

CHAPTER V

A NEW PROTOCOL FOR THE METU GAIT ANALYSIS SYSTEM

5.1 The Need

In the current protocol used in the Biomechanics Laboratory at the Mechanical Engineering Department, the knee and ankle rotation axes are found during static shot by utilizing centering devices (ACD: ankle centering device and KCD: knee centering device). The relation of these axes to the surface markers is assumed to remain constant throughout the gait cycle.

The accuracy of the knee and ankle centers estimated from the static shot was shown to be highly dependent on the person conducting the experiment. Moreover, the effectiveness of the ACD and KCD used in the static shot change for different subjects, and the use of subject-tailored centering devices would not be practical. Therefore a new approach for gait protocol is needed which avoids the use of centering devices during static shot.

5.2 Description of the New Protocol

The knee axis is defined as the axis of rotation between thigh and shank. The new protocol is based on the assumption that between two successive frames (1/50 sec), there is a single axis about which the relative rotation between shank and thigh takes place. In the same manner, ankle axis is the axis of rotation between shank and foot.

In the new protocol, it is proposed to use a cluster of three markers on rigidly attached rods (Figure 5.1) defining an orthogonal coordinate system for each body segment. These clusters attached on the body segments are kept during the gait trials. In this method, static shot and the use of centering devices are eliminated with the aid of additional calculations for the rotation axes.

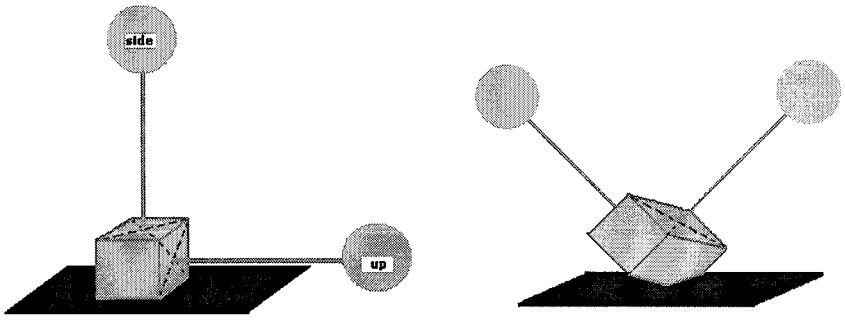

(a) (b)

Figure 5.1: (a) Marker clusters for thigh and shank

(b) Marker clusters for foot

After the marker data are stored for gait trials, marker identification and labeling are performed in Kiss-DAQ. The trajectory data for the markers are filtered using 4th order Butterworth filtering as in the current KissGAIT protocol described in Chapter III. The joint angles are then calculated and the graphs are presented whose details are explained later in this chapter.

5.3 Experimental Procedure

There is no static shot involved in this protocol. Once the markers are placed as shown in Figure 5.2, the subject is asked to walk along the walking band 5 or 6 times and the gait data is recorded for a period of 5 seconds.

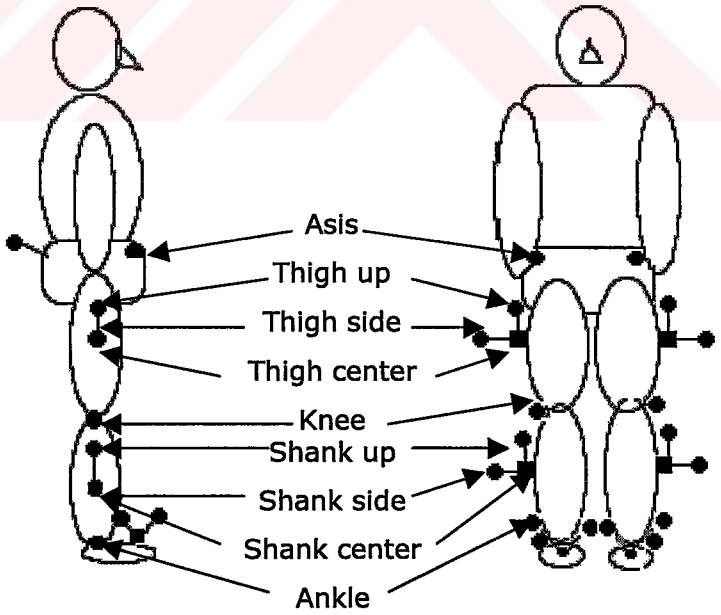

Figure 5.2: Marker placement

Anthropometric measurements are taken for:

DASIS	Distance between two ASIS's
RLEG	Leg length measured through trochantor
LLEG	major-lateral femoral condyl-lateral malleoli
KW	Knee Width
AW	Ankle Width

5.3.1 Marker Enumeration

The following numerical symbols will be used for the 18 markers (Figure 5.2) during the calculations:

P1: RASIS
P2: LASIS
P3: SACRUM
P4: THIGH CENTER
P5: KNEE
P6: SHANK CENTER
P7: ANKLE
P8: THIGH SIDE
P9: THIGH UP
P10: SHANK SIDE
P11: SHANK UP
P12: FOOT CENTER
P13: FOOT 1
P14: FOOT 2
P15: PELVIC CENTER
P16: HIP CENTER
P17: KNEE CENTER
P18: ANKLE CENTER

5.4 Calculation Procedure

5.4.1 Pelvis

Pelvis calculations are same as in the previous protocol, which are repeated here for the sake of completeness.

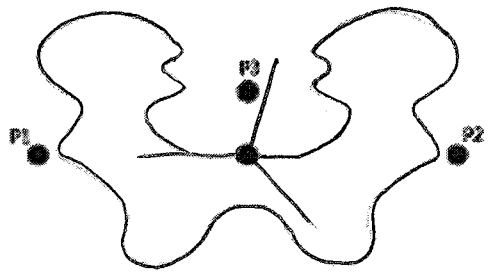

Figure 5.3: Coordinate system for pelvis

The following procedure is applied:

1. The pelvic center is found as the mid point of left and right ASIS (P1 and P2).

$$\vec{P15} = \frac{\vec{P1} + \vec{P2}}{2} \tag{5.1}$$

2. The pelvic coordinate system, the pelvic center (P15) being the origin, is obtained as:

   Unit vector along z-axis from LASIS (P2) to RASIS (P1):

$$\vec{k}_p = \frac{\vec{P1} - \vec{P2}}{\left\| \vec{P1} - \vec{P2} \right\|} \tag{5.2}$$

The unit vector along y-axis is perpendicular to the plane formed by the two ASIS' (P1 and P2) and sacrum (P3):

$$\vec{j}_p = \frac{(\vec{P1} - \vec{P2}) \times (\vec{P2} - \vec{P3})}{\left\| (\vec{P1} - \vec{P2}) \times (\vec{P2} - \vec{P3}) \right\|} \tag{5.3}$$

The unit vector along x-axis is perpendicular to the plane formed by the vectors above:

$$\vec{i}_p = \vec{j}_p \times \vec{k}_p \tag{5.4}$$

So, the pelvis coordinate system (Figure5.3) is:

$$\hat{C}^{(A,P)} = \left[\bar{i}_p(A) \quad \bar{j}_p(A) \quad \bar{k}_p(A) \right] \tag{5.5}$$

5.4.2 Thigh Technical Coordinate System

The following unit vectors are calculated to construct the thigh technical coordinate system relative to global reference frame (Figure 5.4).

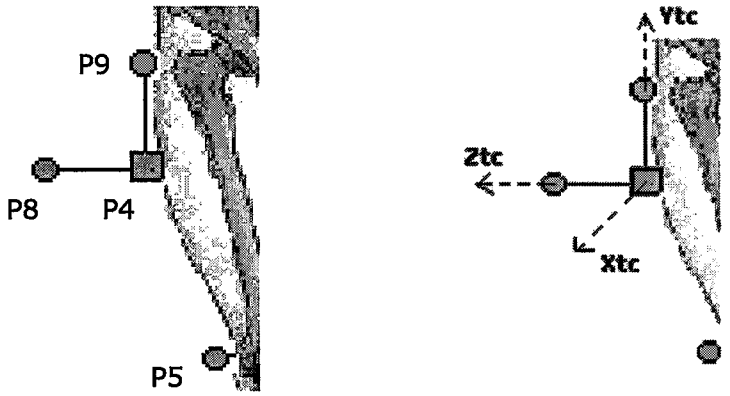

Figure 5.4: Marker placement and technical coordinate axes for thigh

$$\vec{y}_{tc} = \frac{\vec{P}9 - \vec{P}4}{\left|\vec{P}9 - \vec{P}4\right|} \tag{5.6}$$

$$\vec{z}_{tc} = \frac{\vec{P}8 - \vec{P}4}{\left|\vec{P}8 - \vec{P}4\right|} \tag{5.7}$$

$$\vec{x}_{tc} = \vec{y}_{tc} \times \vec{z}_{tc} \tag{5.8}$$

$$\hat{C}^{(A,t_C)} = \left[\bar{x}_{tc}(A) \quad \bar{y}_{tc}(A) \quad \bar{z}_{tc}(A)\right] \tag{5.9}$$

The transformation matrix for thigh should be orthogonal, but due to noise and errors in data collection, the angle between the calculated two direction vectors (y and z axes) although constructed to be perpendicular, came out to be around 88-89 degrees. In order to avoid any further amplified error in calculations, these three vectors are orthogonalized using *Gram-Schmidth Orthogonalization Procedure*.

Gram-Schmidth Orthogonalization Procedure:

From the set of vectors x_{tc}, y_{tc}, z_{tc}, the set of orthonormal vectors q_1, q_2, q_3 are obtained as follows:

1. Since the vectors along z and y directions are already normalized one of them is chosen to be the first vector.

$$\vec{q}_1 = \vec{y}_{tc} \tag{5.10}$$

2. The second vector is orthogonalized as:

$$\vec{q}_2 = \vec{z}_{tc} - (\vec{z}_{tc} \cdot \vec{q}_1)\vec{q}_1 \tag{5.11}$$

3. Then the second vector q_2 is normalized as: $\hat{q}_2 = \frac{\vec{q}_2}{|\vec{q}_2|}$ (5.12)

4. The third vector is then orthogonolized as follows:

$$\vec{q}_3 = \vec{x}_{tc} - (\vec{x}_{tc} \cdot \vec{q}_1)\vec{q}_1 - (\vec{x}_{tc} \cdot \vec{q}_2)\vec{q}_2$$

5. Then the third vector q_3 is normalized as: $\vec{q}_3 = \frac{\vec{q}_3}{|\vec{q}_3|}$ (5.13)

So, an orthogonal orientation matrix is obtained for further calculations.

5.4.3 Shank Technical Coordinate System

The following unit vectors are calculated and shank technical coordinate system relative to global reference frame is constructed (Figure 5.5).

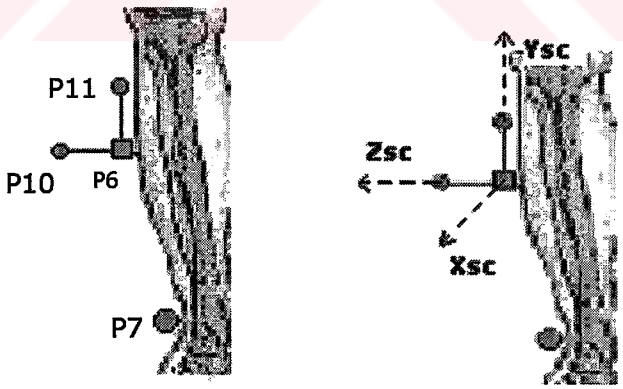

Figure 5.5: Marker placement and technical coordinate axes for shank

$$\vec{y}_{sc} = \frac{\vec{P}11 - \vec{P}6}{\left|\vec{P}11 - \vec{P}6\right|} \tag{5.14}$$

$$\vec{z}_{sc} = \frac{\vec{P}10 - \vec{P}6}{\left|\vec{P}10 - \vec{P}6\right|} \tag{5.15}$$

$$\vec{x}_{sc} = \vec{y}_{sc} \times \vec{z}_{sc} \tag{5.16}$$

$$\hat{C}^{(A,s_C)} = \left[\bar{x}_{sc}(A) \quad \bar{y}_{sc}(A) \quad \bar{z}_{sc}(A)\right] \tag{5.17}$$

Again, the relative transformation matrix is orthogonalized using Gram-Schmidth procedure described in section 5.4.2.

5.4.4 Foot Technical Coordinate System

Figure 5.6: Marker placement and technical coordinate system for foot

Following unit vectors are found and foot coordinate system relative to global reference frame is constructed (Figure 5.7).

$$\vec{y}_{fc} = \frac{\vec{P}14 - \vec{P}12}{\left|\vec{P}14 - \vec{P}12\right|} \tag{5.18}$$

$$\vec{z}_{sc} = \frac{\vec{P}13 - \vec{P}12}{\left|\vec{P}13 - \vec{P}12\right|} \tag{5.19}$$

$$\vec{x}_{fc} = \vec{y}_{fc} \times \vec{z}_{fc} \tag{5.20}$$

$$\hat{C}^{(A,f_c)} = \left[\bar{x}_{fc}^{(A)} \quad \bar{y}_{fc}^{(A)} \quad \bar{z}_{fc}^{(A)}\right] \tag{5.21}$$

The position matrix for foot is also orthogonalized using the Gram-Schmidht Orthogonolization procedure described above.

5.4.5 Joint Centers

Hip Joint Center:

The hip joint center is calculated as in the previous method, but again, repeated here for the sake of completeness.

The hip joint center is calculated from the positions of pelvic markers by using a regression equation given by Davis et al., (1991).

$C=0,115*LEG - 15,3$ (LEG is either RLEG or LLEG) (5.22)

$x_{dis}= 0,1288* LEG-48,56$ (5.23)

$X_H= -(x_{dis}+ r_m) \cos\beta+C \cos\theta \sin\beta$ (5.24)

$Y_H= - (x_{dis}+ r_m) \sin\beta -C \cos\theta \cos\beta$ (5.25)

$Z_H= -\sigma[C \sin\theta - DASIS/2]$ (5.26)

where,

$\sigma=1$ for right side

$\sigma=-1$ for left side

where $\theta=28.4^0 * \pi/180^0$,

$\beta=18^0 * \pi/180^0$

r_m is the marker radius (12.5 mm)

DASIS is the distance between two asis markers.

The hip joint center using the pelvic axes is then given by:

$$\vec{P}16 = \vec{P}15 + X_H \vec{i}_p + Y_H \vec{j}_p + Z_H \vec{k}_p \quad (5.26)$$

Knee Joint Center:

Estimation of Knee Axis:

Two different methods have been used to calculate knee axis dynamically. The comparison and evaluation of these methods are presented at the end of the chapter.

Method 1

The first method for calculation of knee axis is the estimation of the instantaneous axis of rotation. In this method, the relative angular velocity vector is found from which the axis is estimated.

The relative angular velocity vector can be obtained as:

$$\vec{\omega}_{t/s}(A) = \vec{\omega}_{t/A}(A) - \vec{\omega}_{s/A}(A) \quad (5.27)$$

The angular velocities of thigh and shank with respect to global reference frame can be calculated as follows:

$$\tilde{\omega}_{t/A}^{(A)} = \dot{\hat{C}}^{(A,t)} * \hat{C}^{(t,A)} \quad (5.28)$$

$$\tilde{\omega}_{s/A}^{(A)} = \dot{\hat{C}}^{(A,s)} * \hat{C}^{(s,A)} \tag{5.29}$$

where $\tilde{\omega}_{t/A}^{(A)}$ and $\tilde{\omega}_{s/A}^{(A)}$ are skew-symmetric matrices generated from the columns $\bar{\omega}_{t/A}^{(A)}$ and $\bar{\omega}_{s/A}^{(A)}$, which are angular velocities of thigh and shank with respect to global frame.

In these equations, the differentiation of the relative transformation matrices is performed numerically using first order central difference scheme, and the relative transformation matrices are calculated as the average of the two consecutive transformation matrices.

$$\dot{\hat{C}}^{(A,t)} = \frac{\hat{C}^{(A,t_1)} - \hat{C}^{(A,t_2)}}{\Delta t} \tag{5.30}$$

$$\dot{\hat{C}}^{(A,s)} = \frac{\hat{C}^{(A,s_1)} - \hat{C}^{(A,s_2)}}{\Delta t} \tag{5.31}$$

$$\hat{C}^{(t,A)} = \frac{\hat{C}^{(t_1,A)} + \hat{C}^{(t_2,A)}}{2} \tag{5.32}$$

$$\hat{C}^{(s,A)} = \frac{\hat{C}^{(s_1,A)} + \hat{C}^{(s_2,A)}}{2} \tag{5.33}$$

The time interval in the difference equation, Δt, is 1/50 seconds, which is the frequency of data collection and matrix $C^{(t,A)}$

is the transpose of the transformation matrix $C^{(A,t)}$ because of the orthagonality of the two matrices.

Since the angular velocities of the segments are calculated separately, the relative angular velocity represented in global frame can be obtained by using equation 5.27 as:

$$\overline{\omega}_{t/s}^{(A)} = \overline{\omega}_{t/A}^{(A)} - \overline{\omega}_{s/A}^{(A)} = \begin{bmatrix} \omega_1 \\ \omega_2 \\ \omega_3 \end{bmatrix} = \begin{bmatrix} \dot{\theta} \cdot u_1 \\ \dot{\theta} \cdot u_2 \\ \dot{\theta} \cdot u_3 \end{bmatrix} = \dot{\theta} \cdot \overline{u}_k^{(A)} \qquad (5.34)$$

$$\overline{u}_k^{(A)} = \begin{bmatrix} u_1 \\ u_2 \\ u_3 \end{bmatrix} = \frac{1}{\dot{\theta}} \cdot \overline{\omega}_{t/s}^{(A)} \qquad (5.35)$$

where $\overline{u}_k^{(A)}$ is the knee axis about which relative rotation between thigh and shank takes place. Here, $u_1^2 + u_2^2 + u_3^2 = 1$ and so $\dot{\theta} = \sigma\sqrt{\omega_1^2 + \omega_2^2 + \omega_3^2}$, where σ=+1 for right leg, σ=-1 for left leg.

Using the equations above knee axis can be calculated all through the gait cycle.

Method 2

The second method for estimating the knee axis makes use of the Rodrigues' formula for finite rotations. Rodrigues' formula represents a transformation between two positions of a body around an axis.

In this method, the reference position is taken as the position at which shank and thigh coordinate systems are coincident. The knee axis is then defined as the axis around which rotation takes place between the reference and current positions. It should also be noted that this axis is not the instantaneous axis of rotation.

The rotation matrix expressed in a selected frame according to Rodrigues' formula is:

$$\hat{C} = \hat{I}\cos(\theta) + \tilde{u}_k \sin(\theta) + \bar{u}_k \bar{u}_k^T (1 - \cos(\theta)) \tag{5.36}$$

This equation can be re-written in the form:

$$\hat{C} = \begin{bmatrix} 1 & 0 & 0 \\ 0 & 1 & 0 \\ 0 & 0 & 1 \end{bmatrix} \cos(\theta) + \begin{bmatrix} 0 & -u_3 & u_2 \\ u_3 & 0 & -u_1 \\ -u_2 & u_1 & 0 \end{bmatrix} \sin(\theta) + \begin{bmatrix} u_1^2 & u_1u_2 & u_1u_3 \\ u_1u_2 & u_2^2 & u_2u_3 \\ u_1u_3 & u_2u_3 & u_3^2 \end{bmatrix} (1 - \cos(\theta)) \tag{5.37}$$

For the present application, matrix C is the relative transformation matrix between thigh and shank; which is:

$$\hat{C}^{(t,s)} = \hat{C}^{(t,A)} \cdot \hat{C}^{(A,s)} = \begin{bmatrix} r_{11} & r_{12} & r_{13} \\ r_{21} & r_{22} & r_{23} \\ r_{31} & r_{32} & r_{33} \end{bmatrix} \tag{5.38}$$

Using the diagonal elements, cosine of the rotation angle is found, and then sine of the angle is computed;

$$\cos(\theta) = \frac{r_{11} + r_{22} + r_{33} - 1}{2} = \gamma \tag{5.39}$$

$$\sin(\theta) = \sigma\sqrt{1 - \gamma^2} \tag{5.40}$$

where, σ=+1 for right leg

σ=-1 for left leg

Then, using the off-diagonal elements, the knee axis is estimated.

$$u_1 = \frac{r_{32} - r_{23}}{2\sin(\theta)} \quad (5.41)$$

$$u_2 = \frac{r_{13} - r_{31}}{2\sin(\theta)} \quad (5.42)$$

$$u_3 = \frac{r_{21} - r_{12}}{2\sin(\theta)} \quad (5.43)$$

$$u_k^{(A)} = \begin{bmatrix} u_1 \\ u_2 \\ u_3 \end{bmatrix} \quad (5.44)$$

Knee Joint Center Calculation:

After the knee axis is found as a vector represented in global frame, the knee center is calculated as in the previous protocol.

$$\vec{P}17 = \vec{P}5 + \frac{KW}{2} \cdot \vec{u}_k \quad (5.45)$$

Where KW is the knee width and P5 is the knee marker attached to the subject. But for the first method, in which two successive frames are used, knee marker is calculated as the average of the two consecutive knee marker positions.

Knee axis and knee center are calculated throughout the gait cycle.

Ankle Joint Center:

Like knee axis, the column representation of the ankle axis represented with respect to global frame can be found using the methods mentioned above.

The ankle axis is calculated for the whole range of motion.

$$\underset{u_a}{\overset{\frown}{}}(A) = \begin{bmatrix} u_x \\ u_y \\ u_z \end{bmatrix} \tag{5.46}$$

Then, the ankle center (P31) is calculated as in the previous protocol:

$$\vec{P}31 = \vec{P}7 + \frac{AW}{2} \cdot \vec{u}_a \tag{5.47}$$

where AW is the ankle width and P7 is the ankle marker attached to the subject. The ankle marker is the average of the two consecutive positions for the marker in the calculation for the first method.

5.4.6 Thigh Anatomical Coordinate System

The anatomical coordinate system for thigh is constructed as in the Kiss-GAIT (Figure 5.7). The origin of the anatomical coordinate system for thigh is the knee center.

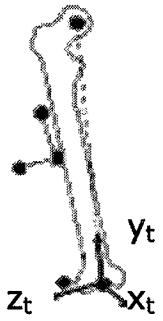

Figure 5.7: Anatomical coordinate system of thigh

The unit vector from the knee center (P17) to the hip center (P16):

$$\vec{j}_t = \frac{\overrightarrow{P16} - \overrightarrow{P17}}{\left\| \overrightarrow{P16} - \overrightarrow{P17} \right\|} \tag{5.48}$$

The unit vector perpendicular to the plane formed by knee center (P17), hip center (P16) and unit vector along the knee axis (u_k):

$$\vec{i}_t = \sigma \frac{(\vec{P}17 - \vec{P}16) \times \vec{u}_k}{\left\| (\vec{P}17 - \vec{P}16) \times \vec{u}_k \right\|} \tag{5.49}$$

where,

σ=1 for right side

σ=-1 for left side

Unit vector perpendicular to the plane defined by the vectors above: $\vec{k}_t = \vec{i}_t \times \vec{j}_t$ (5.50)

The matrix for anatomical coordinate system of thigh is:

$$\hat{C}^{(A,t)} = \left[\bar{i}_t(A) \quad \bar{j}_t(A) \quad \bar{k}_t(A) \right] \tag{5.51}$$

5.4.7 Shank Anatomical Coordinate System

The origin of the anatomical coordinate system for shank is the ankle center (P18) (Figure 5.8).

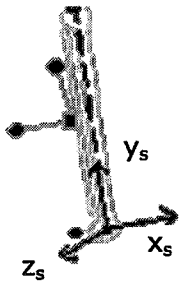

Figure 5.8:Anatomical coordinate system of shank

The unit vector from the ankle center (P18) to the knee center (P17):

$$\vec{j}_S = \frac{\overrightarrow{P17} - \overrightarrow{P18}}{\left\| \overrightarrow{P17} - \overrightarrow{P18} \right\|} \tag{5.52}$$

Unit vector perpendicular to the plane formed by knee center (P17), ankle center (P18) and unit vector along the ankle axis (u_a):

$$\vec{i}_s = \sigma \frac{(\overrightarrow{P18} - \overrightarrow{P17}) \times \vec{u}_a}{\left\| (\overrightarrow{P18} - \overrightarrow{P17}) \times \vec{u}_a \right\|} \tag{5.53}$$

where,

σ=1 for right side

σ=-1 for left side

Unit vector perpendicular to the plane defined by the vectors above: $\vec{k}_S = \vec{i}_S \times \vec{j}_S$ (5.54)

The transformation matrix for anatomical coordinate system of shank is: $\hat{C}^{(A,s)} = \left[\bar{i}_S(A) \quad \bar{j}_S(A) \quad \bar{k}_S(A)\right]$ (5.55)

5.5 Kinematic Model and Joint Angles

5.5.1 Biomechanical Model and Joint Angle Calculations

The biomechanical model and the angular definitions are the same as in the current protocol, KissGAIT (Chapter III). The biomechanical model developed by E.S. Grood and W. J. Suntay (1983), 'Joint coordinate system', is used to define the joint angles.

In order to find anatomical joint angles via technical angles (θ_1, θ_2, θ_3) the transformation matrix between the proximal and distal segments are found in the same way as in the KissGAIT protocol.

$$\hat{C}^{(P,D)} = \begin{bmatrix} c_{11} & c_{12} & c_{13} \\ c_{21} & c_{22} & c_{23} \\ c_{31} & c_{32} & c_{33} \end{bmatrix} \quad (5.56)$$

After the transformation matrix is obtained, to calculate angles θ_1, θ_2, and θ_3 a method known as inverse kinematics method in robotics applications is used. In this method, the transformation

matrix should be obtained parametrically, for this purpose Hartenberg-Denavit principle is used and the same parametric matrix in Chapter III is obtained.

From the matrix the following angles are found parametrically as:

$\theta_2 = \text{acos}(c_{32})$ (5.57)

$\sigma = \text{sgn}(\sin\theta_2)$ (5.58)

$\theta_1 = \text{angle}(\sigma . c_{12}, \sigma . c_{22})$ (5.59)

$\theta_3 = \text{angle}(-\sigma . c_{31}, \sigma . c_{33})$ (5.60)

- **Pelvis Angles**

For pelvis, the position matrix is directly used to calculate the angles:

Pelvic tilt=$90-\theta_1$ (5.61)

Pelvic obliquity=$90-\theta_2$ (5.62)

Pelvic rotation= $90-\theta_3$ (5.63)

- **Hip Joint Angles**

The relative transformation matrix between pelvis and thigh is calculated as:

$$\hat{C}^{(p,t)} = \hat{C}^{(A,p)^T} * \hat{C}^{(A,t)} \quad (5.64)$$

Using the matrix above the angles are found and the anatomical angles are:

Hip flexion= θ_1-90 (5.65)

Hip rotation=δ(90- θ_3) (5.66) where,

Hip abd/add=$\delta(\theta_2 - 90)$ (5.67) δ=-1 for left leg

δ=1 for right leg

- **Knee Joint Angles**

Applying the same procedure the relative transformation matrix between thigh and shank is found.

$$\hat{C}^{(t,s)} = \hat{C}^{(A,t)^T} * \hat{C}^{(A,s)} \quad (5.68)$$

Anatomical joint angles for knee are:

Knee flexion= 90-θ1 (5.69)

Knee rotation= δ (θ3-90) (5.70) where,

Knee valgus= δ (θ2-90) (5.80) δ=-1 for left leg

δ=1 for right leg

- **Ankle Joint Angles**

Foot Dorsiflexion Angle:

Dorsiflexion angle of foot is the change in the angle between the second and the first components of the vector from foot center (P12) to ankle center (P18) represented in shank coordinate system. It is the rotation of foot around z-axis of the shank coordinate system. The expression for dorsiflexion angle is given in the equation 5.81.

$$dorsflx = \arctan\left[\frac{\bar{u}_2{}^t \cdot \hat{C}^{(s,A)} \cdot \{(\vec{P}12 - \vec{P}18)\}^{(A)}}{\bar{u}_1{}^t \cdot \hat{C}^{(s,A)} \cdot \{(\vec{P}12 - \vec{P}18)\}^{(A)}}\right] \quad (5.81)$$

Foot Rotation Angle:

Foot rotation angle is the rotation of the foot around y-axis of the shank coordinate system.

$$footrot = \arctan\left[\frac{\bar{u}_3{}^t \cdot \hat{C}^{(s,A)} \cdot \{(\vec{P}12 - \vec{P}18)\}^{(A)}}{\bar{u}_1{}^t \cdot \hat{C}^{(s,A)} \cdot \{(\vec{P}12 - \vec{P}18)\}^{(A)}}\right] \quad (5.82)$$

The graphs of joint angles that have clinical meaning are plotted over the gait cycle. The graphs are constructed from first heel strike to the second heel strike. Sixth order polynomial is chosen for a curve fit in this application after investigating the correlation coefficients of various order polynomials. It is observed that the correlation coefficient for regression analysis increase dramatically up to the polynomial fit of order six, however higher order polynomials do not change the correlation coefficient that much. So, the angle values in the cycle are fit in a sixth order polynomial by regression. Then hundred points are evaluated and plotted to obtain a percent gait cycle scale.

5.6 Analysis of the Results

Gait experiments were performed on five subjects using the proposed protocol, and two best experiments for each subject were analyzed and compared with those of alternative systems and protocols.

The joint angles obtained by using the proposed methods are presented in Appendix C for all the subjects. The corresponding results from the KissGAIT for the same subject and also corresponding graphs from literature (Apkarian *et al.*, 1989) and a commercial system (VICON) are also given for comparison.

The plots of the anatomical joint angles were compared to the results from KissGAIT for the same subject and general patterns for the angle plots from literature and VICON. The bases for comparison was chosen to be the most characteristic curves that are the angles measured in the sagittal plane (flexion angles), for which the range of motion was comparatively higher than the frontal and transverse planes.

It was originally perceived that more elegant two-frame solution, namely the instant axis of rotation, would give better results. However as seen in the Appendix C, the Rodrigues' method gave results that are in good agreement, both qualitatively and quantitatively, with KissGAIT and other sources.

The reason for this rather unexpected result of the method utilizing data from two successive frames may be attributed to the noise involved in the experimental data. The differences in marker coordinates between two successive frames are nearly in the order of the noise levels. This can be observed by comparing the resultant differences for data points with the estimated errors for KissDAQ, the data acquisition system. The error involved in the system was calculated by Karpat Y. (2000) as 1.06 mm for mean error and 3.09/7.45 mm for maximum and minimum errors respectively with a standard deviation of 1.31 mm. As an example, the mean difference with the standard deviations of coordinates of thigh marker between two successive frames is calculated as in Table 5.1:

Table 5.1: Difference between the coordinates of a marker in two successive frames

Δx	Δy	Δz	total
0.88±1.17mm	8.24±9.73mm	1.66±2.21mm	7.93±9.25mm

As seen from the table above, the differences can sometimes be in the order of data acquisition errors, which affect the reliability of the method based on data from two successive frames.

The effects of such variations are observed especially in knee flexion angle, rather than hip flexion angle, since knee angles are affected from both knee axis and ankle axis.

As a result, when all angles are considered, Rodrigues' formulation gave more satisfactory results. So, in the computer algorithm of DynaGAIT, the software for the proposed protocol, this method is used to calculate joint angles.

5.7 Implementation of The New Protocol: DynaGAIT

All the algorithms and mathematical formulations presented in this chapter were implemented as computer code in Visual Basic 6.0 © language (Figure 5.9).

Figure 5.9: DynaGAIT© opening page

The code consists of three forms. The first form is the main form (Figure 5.10); here the data file is retrieved as an input from the user as a text file (Figure 5.11). The anthropometric data is entered, and then choosing the **'CYCLE'** button the user jumps to the second form. The second form (Figure 5.12) is the simulation of gait so that the user can choose the gait cycle (heel strike's and toe off's).

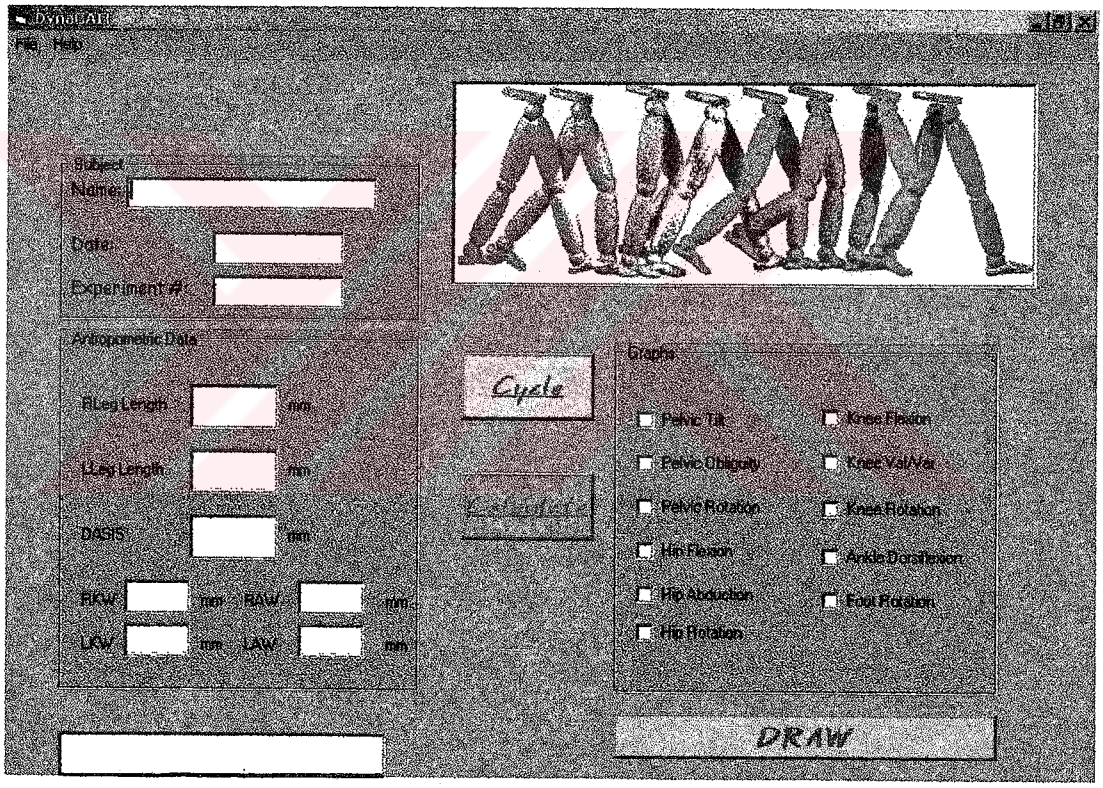

Figure 5.10: DynaGAIT© main frame

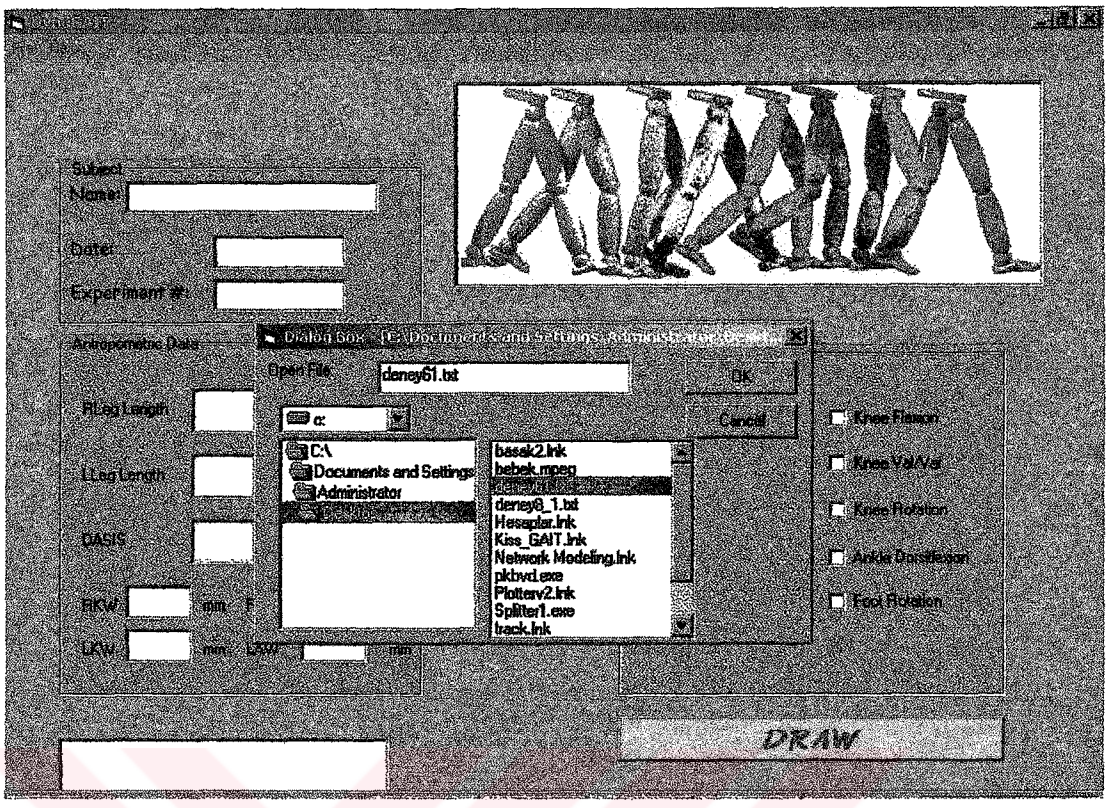

Figure 5.11: DynaGAIT© file-open menu

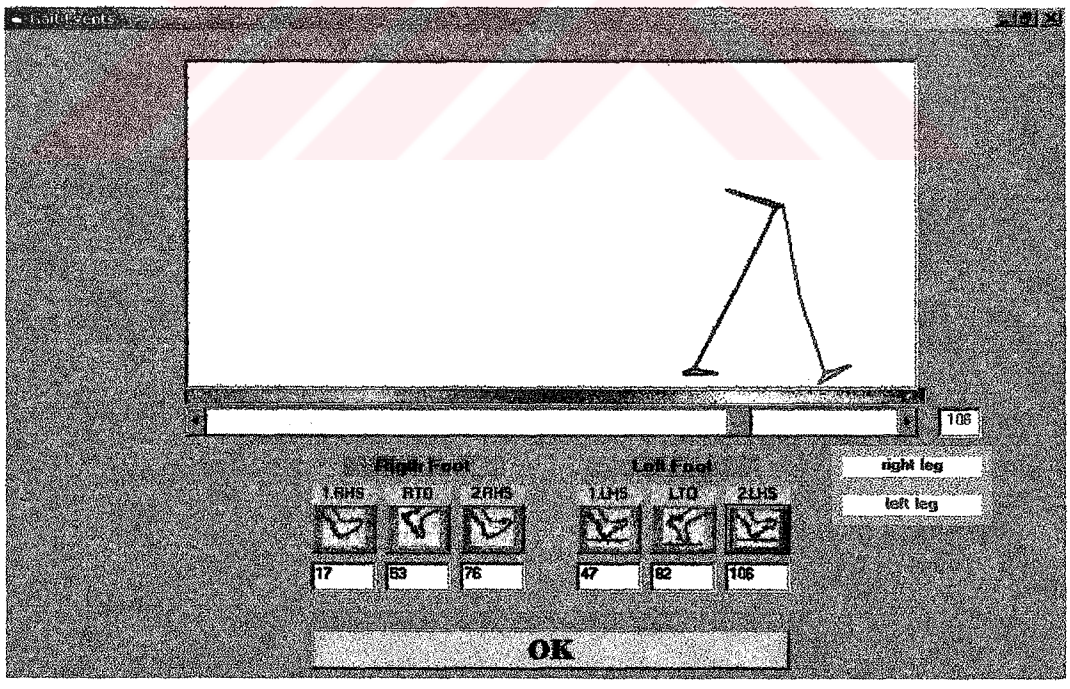

Figure 5.12: DynaGAIT© gait events page

After gait cycle is identified, the user presses '**CALCULATE**' button in order to perform the calculations. The calculation subroutine calculates the joint angles as described in this chapter.

The desired graphs are presented when '**DRAW**' button is pressed. This subroutine performs the curve fitting operations and presents the graphs requested by the user. The graphs may be chosen at different combinations, which is a feature not available in KissGAIT. If only one graph is required then it fills the screen (Figure 5.13), however if more graphs are required then they are scaled so as to fit into one screen (Figure 5.14). Then the graphs can be printed on a paper if the user presses '**PRINT**' button. The user can also return to main page to select different graphs.

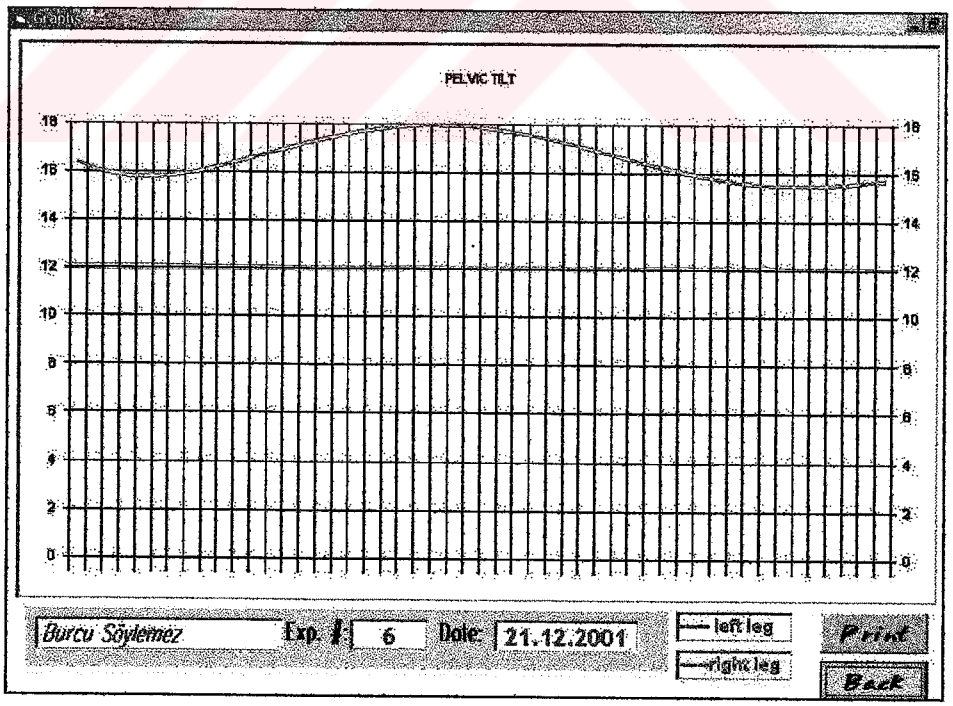

Figure 5.13: DynaGAIT© single graph

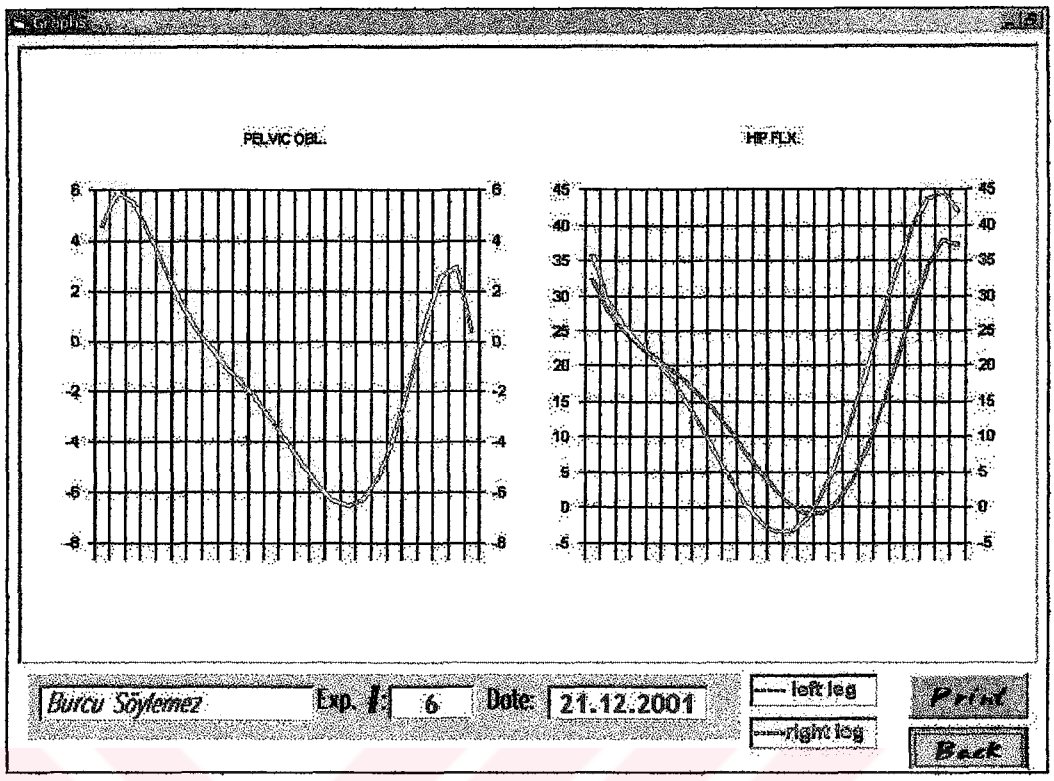

Figure 5.14: DynaGAIT© two graphs

CHAPTER VI

SUMMARY AND CONCLUSIONS

This work is concerned with the evaluation and refinement of the gait analysis protocol at the Mechanical Engineering Department of METU.

Gait Analysis Laboratory at Mechanical Engineering Department in the METU was established for providing clinicians a tool for diagnosis and treatment. It is very important to assure the reliability and repeatability of an experimental setup, especially when human health is concerned.

In this work, the current method of gait analysis is described in detail for future use and to give the reader the idea of gait analysis and methodology of estimating joint angles. This part of the work is based on the software developed by H.Cenk Güler as part of his Ph.D. thesis.

The reliability and repeatability of the system is evaluated through a number of experiments. The effects of hip joint center location estimation were analyzed by perturbating the hip joint center ± 30 mm in three directions. It was shown that errors in

estimating hip joint center location would not affect the reliability and repeatability of the system considerably. Also, the effects of centering device placement were investigated. The analyses were based on experiments conducted on three subjects performed by four performers with different levels of experience. The results demonstrated that centering device placement is an important factor affecting the reliability of the system.

Motivated by the preliminary results obtained, a new dynamic gait analysis protocol (DynaGAIT©) has been proposed and new software has been developed. The protocol offers two different methods for estimating knee and ankle joint axes all through the gait analysis without a static shot.

The protocol was tested on five subjects with ten experiments. The results of the proposed two methods were compared to those found by KissGAIT, a commercial system (Vicon) and the literature (Appendix C). The joint angles calculated through Rodrigues' formula was observed to exhibit a good agreement with the compared ones.

When the current protocol KissGAIT and the proposed protocol DynaGAIT are compared in terms of their easiness and repeatability, it is observed that:

- The time for conducting an experiment using KissGAIT protocol takes about 75-90 minutes since two sets of markers (for static shot and dynamic shot) are used; however, it takes about 30-40 minutes to conduct an experiment employing DynaGAIT protocol.
- KissGAIT calculates knee and ankle axes once then estimates them during gait using assumption-based-matrix multiplications; whereas DynaGAIT calculates these axes at each instant, without assuming that the rotation axes are rigidly attached to a segment, which is a more realistic approach.
- In the new protocol, the person conducting the experiment need not to be experienced since the marker locations are almost arbitrary. The results indicated that the reliability of centering devices depend upon the experience of the person conducting the experiment. In DynaGAIT, there is neither need for consuming application of centering devices nor the experienced performer.

There are, however, some shortcomings of the new protocol when compared to the current one. One such shortcoming is due to the amplified skin vibration since markers at the end of rod vibrate more than skin markers. Therefore, a separate investigation is needed to assess the effects of this potential source of error.

Another point to be investigated is the use of single frame solution for rotation axes calculation. Although the reason for two-frame solution not being precise enough is correlated to the noise involved in the data, single frame solution may be a very approximate estimation. This effect should also be investigated.

REFERENCES

Afşar H. (2001) Evaluation and compensation of soft tissue movement for the Kiss gait analysis system. MSc. Thesis, Middle East Technical University, Mechanical Engineering Department, Ankara, Turkey.

Andriacchi T.P., Alexander E.J. (2000) Studies of human locomotion: past, present and future. *J. of Biomechanics* **33**, 217-224.

Apkarian J., Naumann S., Cairns B. (1989) A three-dimensional kinematic and dynamic model of the lower limb. *J. of Biomechanics* **22**, 143-155.

Bell A.L., Brand R.A., Pedersen D.R. (1989) Prediction of hip joint center location from external landmarks. *Human Movement Science* **8**, 3-16.

Capello A., Cappozzo A., Palombara P.F., Lucchetti L., Leardini A. (1997) Multiple anatomical landmark calibration for optimal bone pose estimation. *Human Movement Science* **16**, 259-274.

Cappozzo A. (1984) Gait analysis methodology. *Human Movement Science* **3**, 27-50.

Cappozzo A., Catani F., Croce U.D., Leardini A. (1995) Position and orientation in space of bones during movement: anatomical frame definition and determination. *Clinical Biomechanics* **10**, 171-178.

Cappozzo A., F. Gazzani (1986) Joint Functional assessment during physical exercise: Methodological considerations. Proceedings of the 5th Meeting of the European Society of Biomechanics p.87.

Cappozzo A., Catani F., Leardini A, Benedetti M.G., Croce U.D. (1996) Position and orientation in space of bones during movement: experimental artefacts. *Clinical Biomechanics* **11**, 90-100.

Cheng P.L., Nicol A.C., Paul J.P. (2000) Determination of axial rotation angles of limb segments — anew method. *J. of Biomechanics* **33**, 837-843.

Crawford N.R., Yamaguchi G.T., Dickman C.A. (1999) Anew technique for determining 3-D joint angles: the tilt/twist method. *Clinical Biomechanics* **14**, 153-165.

Crowninshield R.D., Johnston R.C., Andrews J.G., Brand R.A. (1977) The effect of joint center on hip kinetics. Proceedings of the 23rd Annual ORS Convention.

Davis III R.B., Ounpuu S., Tyburski D., Gage J.R. (1991) A gait analysis data collection and reduction technique. *Human Movement Science* **10**, 575-587.

Ehara Y, Fujimoto H., Miyazaki S., Mochimaru M., Tanaka S. Yamamoto S. (1997) Comparison of the performance of 3D camera systems II. *Gait and Posture* **5**, 251-255.

Grood E.S., Suntay W.J. (1983) A joint coordinate system for the clinical description of three dimensional motions: application to the knee. *J. of Biomech. Engineering* **105** 136-144.

Güler H.C. (1998) Biomechanical modeling of lower extremity and simulation of foot during gait. PhD. Thesis, Middle East Technical University, Mechanical Engineering Department, Ankara, Turkey.

Holden J.P., Orsini J.A., Siegel K.L., Kepple T.M., Gerber L.H., Stanhope S.J. (1997) Surface movements errors in shank kinematics and knee kinetics during gait. *Gait and Posture* **3**, 217-227.

Kadaba M.P., Ramakrishnan H.K., Wooten M.E. (1990) Measurement of lower extremity kinematics during level walking. *J. of Orthopaedic Research* **8,** 383-392.

Karpat Y. (2000) Development and testing of kinematic data acquisition tools for a gait analysis system. MSc. Thesis, Middle East Technical University, Mechanical Engineering Department, Ankara, Turkey.

Kinzel G.L., Hall A.S., Hillberry B.M. (1972) Measurement of total motion between two bod segments – I analytical development. *J. of Biomechanics* **5**, 93-105.

Kirkwood R.N., Culham E.G., Costigan P. (1999) Radiographic and non-invasive determination of the hip joint center location: effect on hip joint moments. *Clinical Biomechanics* **14**, 227-235.

Leardini A, Benedetti M.G., Catani F., Simoncini L., Giannini S. (1999) An anatomically based protocol for description of foot segment kinematics during gait. *Clinical Biomechanics* **14**, 528-536.

Leardini A, Cappozzo A., Catani F., Toksvig-Larsen S., Petitto A., Sforza V., Cassanelli G., Giannini S. (1999) Validation of a

functional method for the estimation of hip joint center location. *J. of Biomechanics* **32**, 99-103.

Lucchetti L., Cappozzo A., Capeelo A., Croce U.D. (1998) Skin movement atefact assessment and compensation in the estimation of knee-joint kinematics. *J. of Biomechanics* **31**, 977-984.

Lundberg A. (1996) On use of bone and skin markers in kinematics research. *Human Movement Science* **15**, 411-422.

Reinschmidt C., Borgert A.J., Nigg B.M., Lundberg A., Murhpy N. (1997) Effect of skin movement on the analysis of skeletal knee joint motion during running. *J. of Biomechanics* **30**, 729-732.

Sati A., Guise J.A., Larouche S., Drouin G. (1996) Quantitative assessment of skin-bane movement at the knee. *The Knee* **3**, 121-138.

Seidel G.K., Marchinda D.M., Dijkers M., Soutas-Little R.W. (1995) Hip joint center location from palpable bony landmarks – a cadaver study. *J. of Biomechanics* **26**, 1091-1104.

Shafiq M.S., Tümer T., Güler H.C. (2001) Marker detection and trajectory generation algorithms for a multicamera based gait analysis system. *Mechatronics* **11**, 409-437.

Shafiq M.S. (1998) Motion tracking in gait analysis. MSc. Thesis, Middle East Technical University, Mechanical Engineering Department, Ankara, Turkey.

Spoor C.W., Veldpaus F.E. (1980) Rigid body motion calculated from spatial coordinates of markers. *J. of Biomechanics* **13**, 391-393.

Stagni R., Leardini A., Cappozzo A., Benedetti M.G., Capello A. (2000) Effects of hip joint center mislocation on gait analysis results. *J. of Biomechanics* **33**, 1479-1487.

Sutherland D.H., R.A. Olsen, E.N. Binden, M.P. Wyatt (1988) The development of mature walking. *Oxford: Blackwell & Philadelphia, PA, USA*.

Vaughan C.L (1992) Dynamics of Human Gait. *Champaign: Human Kinetics Publishers.*

Winter D.A. (1991) The biomechanics and motor control of human gait: normal, elderly and pathological. (2nd Edition) *University of Waterloo Press, Waterloo, Ont., USA.*

Winter D.A. (1990) The biomechanics and motor control of human movement. *John Wiley & Sons Inc.,New York, USA.*

Woltring H.J. (1994) 3-D representation of human joints: A standatization proposal. *J. of Biomechanics* **27,** 1399-1414.

Woltring H.J. (1991) Representation and calculation of 3-D joint movement. *Human Movement Science* **10**, 603-616.

Woltring H.J., S. Fioretti (1989) Representation and Photogrammetric calculation of 3D joint movement. Proceedings of the first IOC World Congress on Sport Science.

Woltring H.J., Huiskes R., De Lange A. (1985) Finite centroid and helical axis estimation from noisy landmark measurements in the study of human joint kinematics. *J. of Biomechanics* **18,** 379-389.

APPENDIX A

DIGITAL FILTER

The recursive equation for digital filter is given by

$$X_n^* = c_0 X_n + c_1 X_{n-1} + c_2 X_{n-2} + b_1 X_{n-1}^* + b_2 X_{n-2}^* \quad \text{(A.1)}$$

The constants in this equation can be calculated using the following relations (Winter, 1990):

$$\omega_c = \tan\left(\frac{\pi f_c}{f_s}\right) \quad \text{(A.2)}$$

$$K_1 = \sqrt{2}\omega_c \qquad K_2 = \omega_c^2 \quad \text{(A.3)}$$

$$c_0 = \frac{K_2}{1 + K_1 + K_2} \qquad c_1 = 2c_0 \qquad c_2 = c_0 \quad \text{(A.4)}$$

$$K_3 = \frac{2c_0}{K_2} \quad \text{(A.5)}$$

$$b_1 = -2c_0 + K_3 \qquad b_2 = 1 - 2c_0 - K_3 \quad \text{(A.6)}$$

Where, f_s is the sampling frequency (50 Hz) and f_c is the cut-off frequency of the filter. To eliminate the phase lag introduced by the filter the data is filtered fed to the filter twice; once forward in time and once backward in time. When data is run through the filter more than once the effective cut-off frequency of the filter is

reduced. Therefore the cut-off should be first adjusted to get the desired frequency (f_d) using the following relation (Robertson *et. al.*, 1992):

$$f_c = \frac{f_d}{\left(\sqrt{2}-1\right)^{1/2}} \qquad \text{(A.7)}$$

Using f_d = 6 Hz the numerical constants come out to be:

$c_0=c_2=0.389651$

$c_1=0.779303$

$b_1=-0.363569$

$b_2=-0.195035$

APPENDIX B

RESULTS OF CENTERING DEVICE PLACEMENT EXPERIMENTS

The results of centering device placement experiments obtained for three subjects and four performers are given below:

1 Graphs for Subject B.S

1.1 Expert Performer

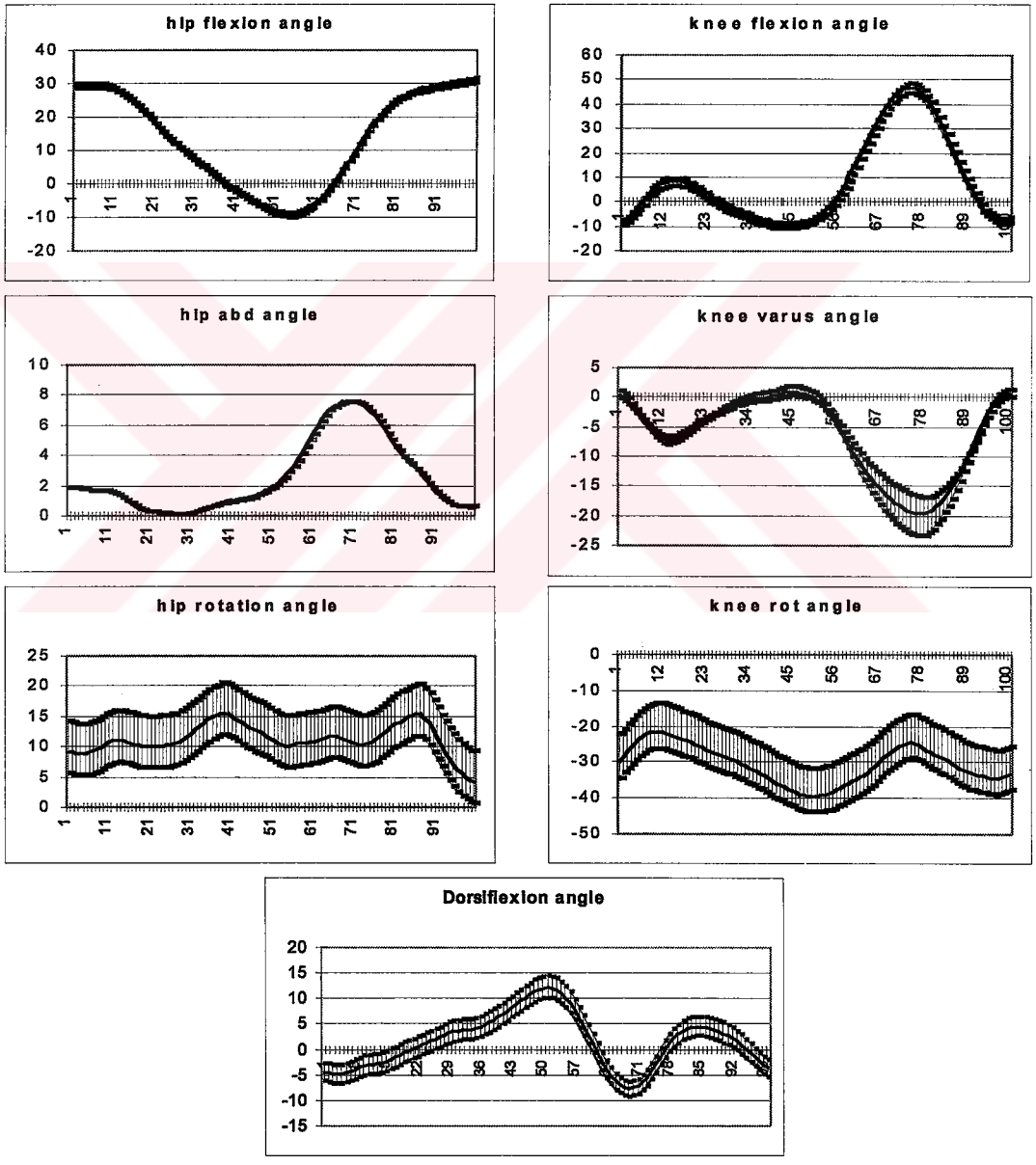

Figure B- 1: Graphs for B.S by expert performer

1.2 Knowledgeable Performer

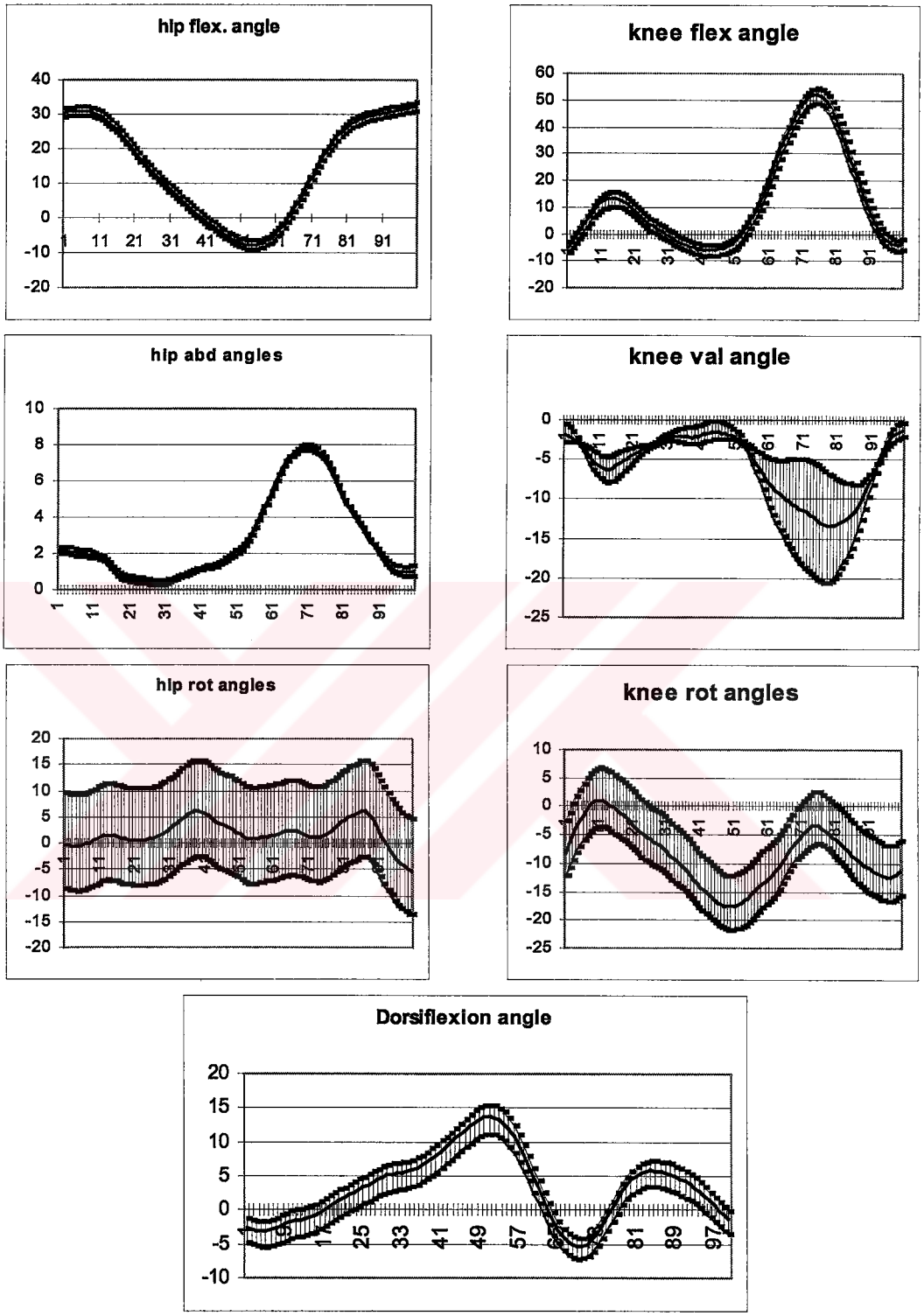

Figure B- 2: Graphs for B.S by knowledgeable performer

1.3 Acquainted Performer

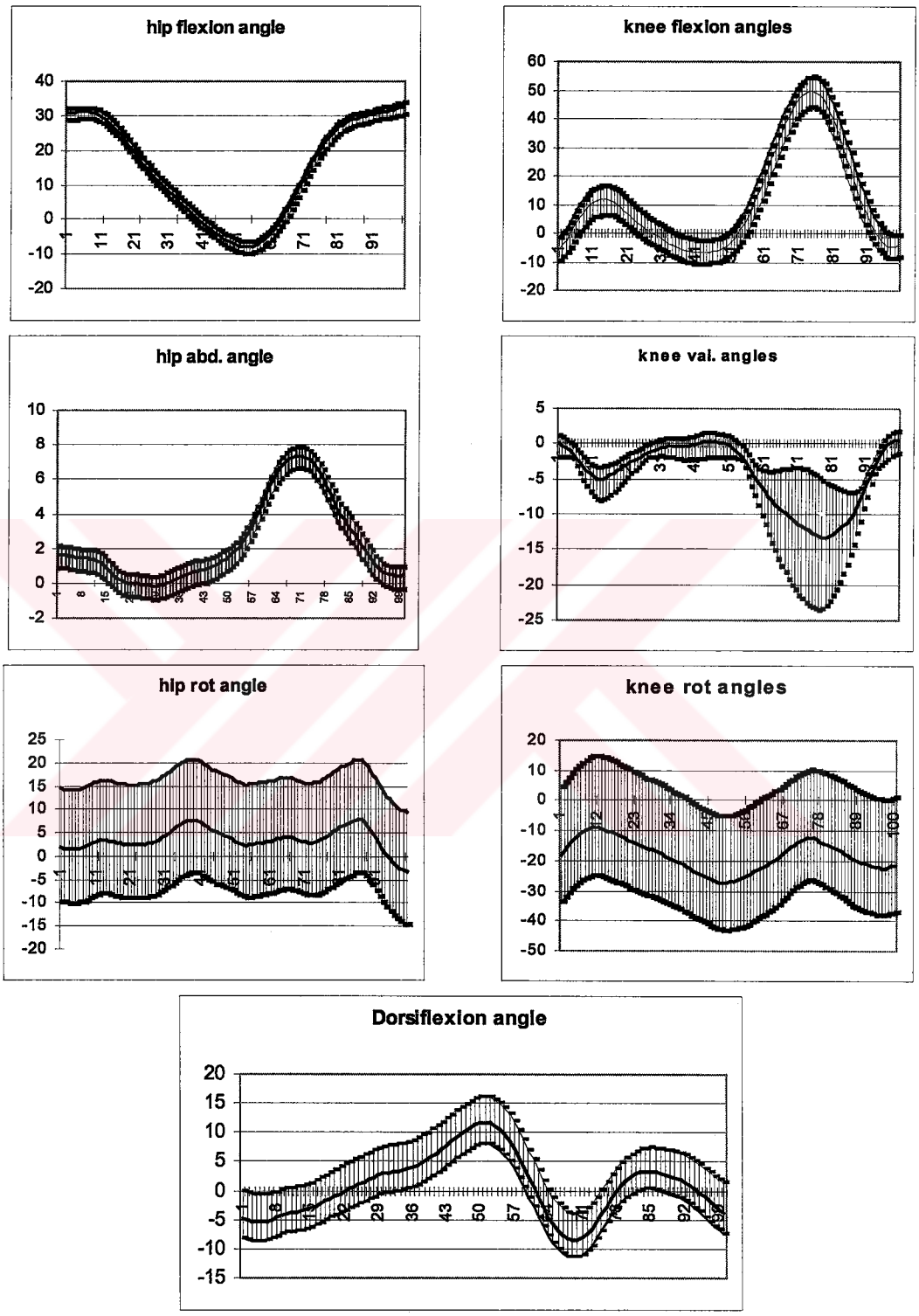

Figure B- 3: Graphs for B.S by acquainted performer.

1.4 Unaware Performer

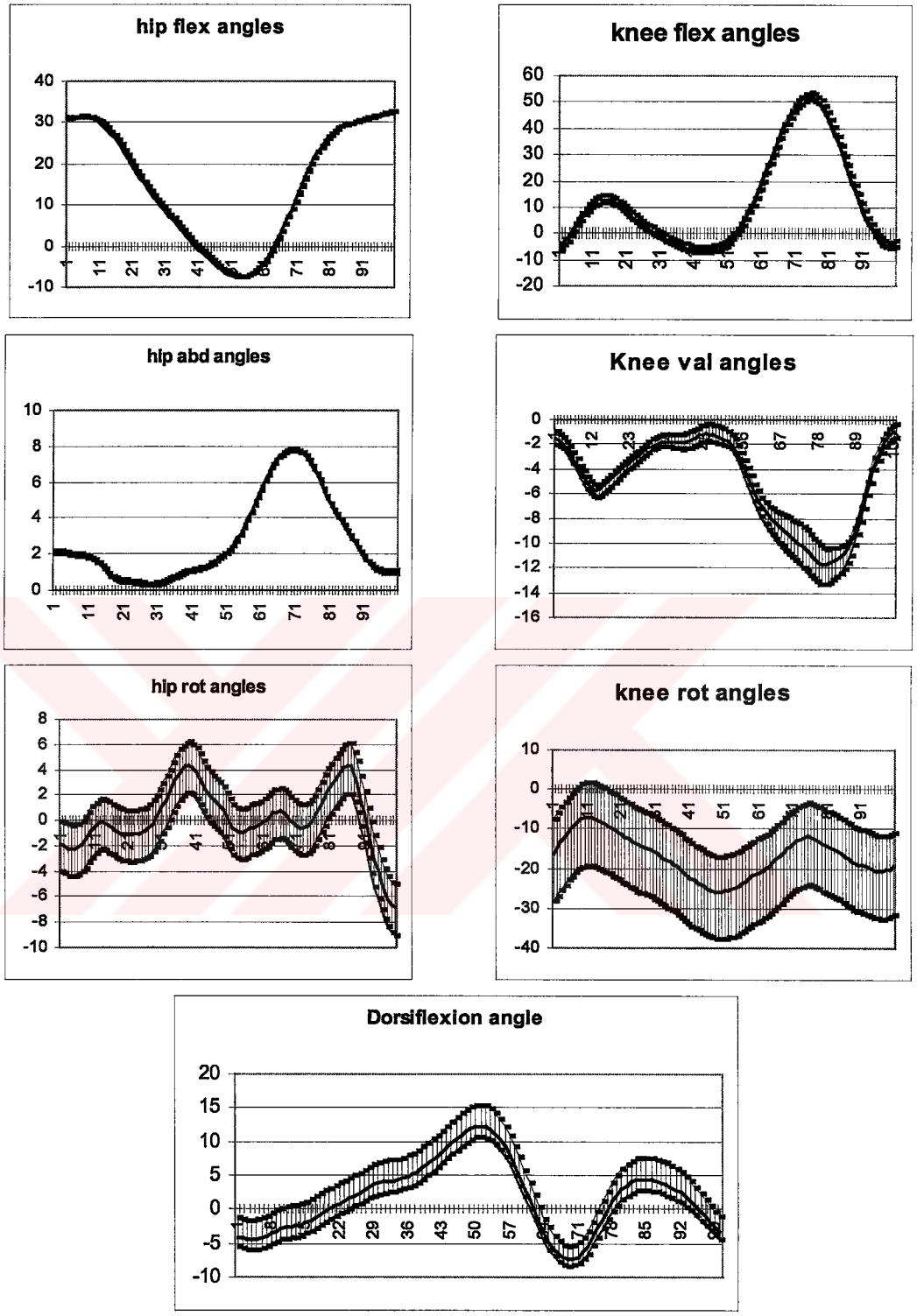

Figure B- 4: Graphs for B.S by unaware performer

1.5 Mean Values for Subject B.S.

The plots below are the mean values for an angle for four performers performing three experiments.

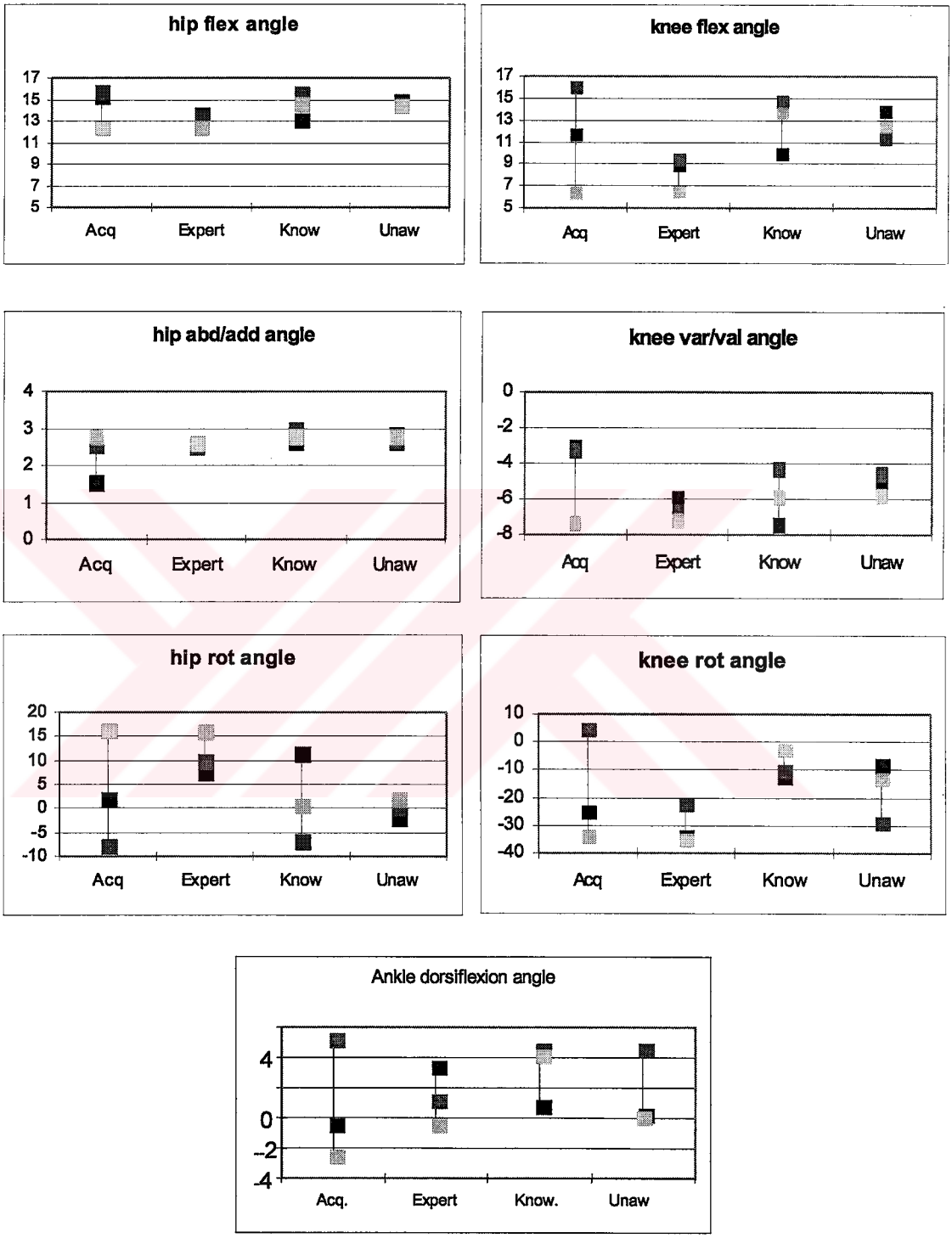

Figure B- 5:Mean values of three experiments for B.S.

2 Graphs For Subject M.E.

2.1 Expert Performer

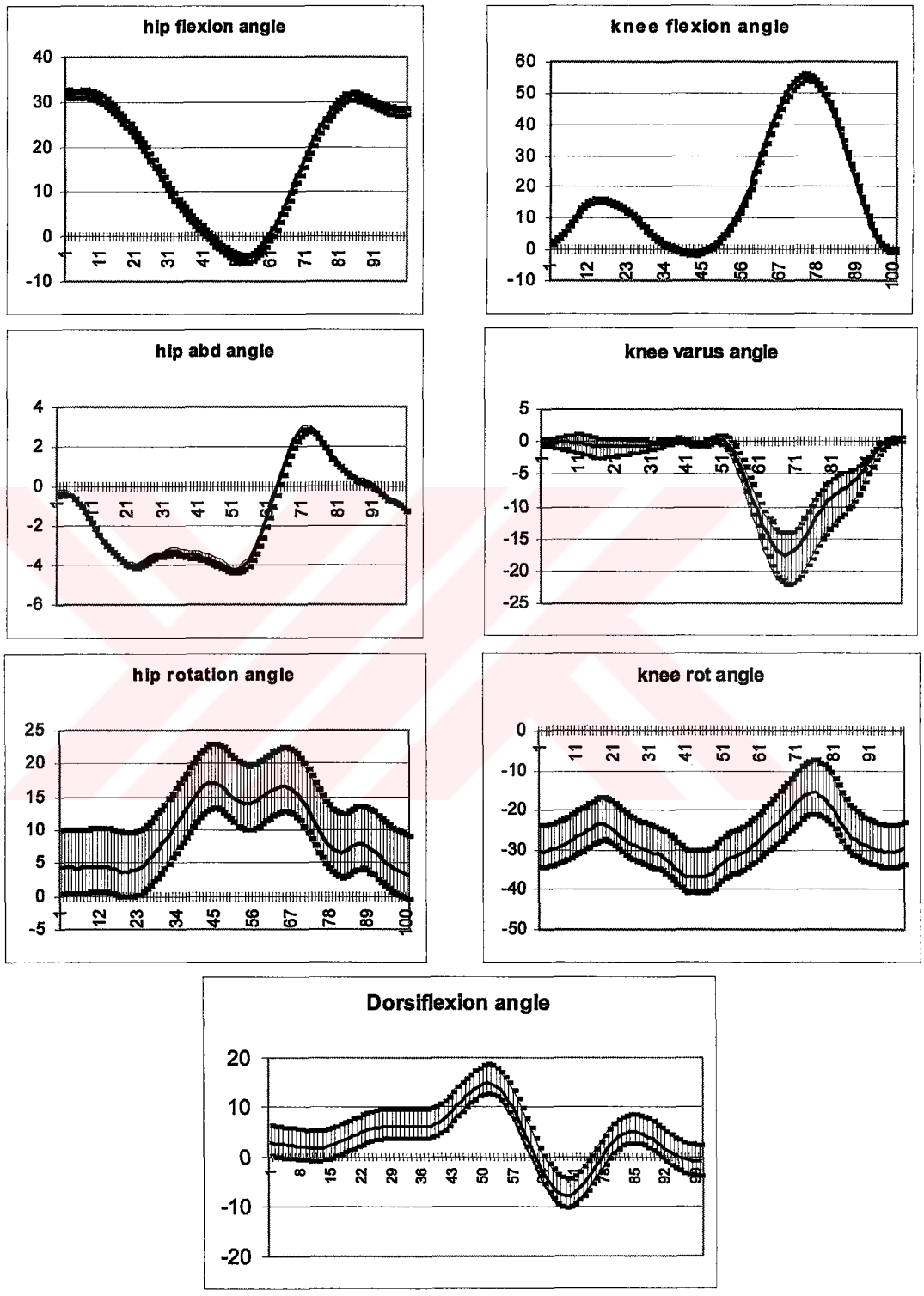

Figure B- 6: Graphs for M.E. by expert performer

2.2 Knowledgeable Performer

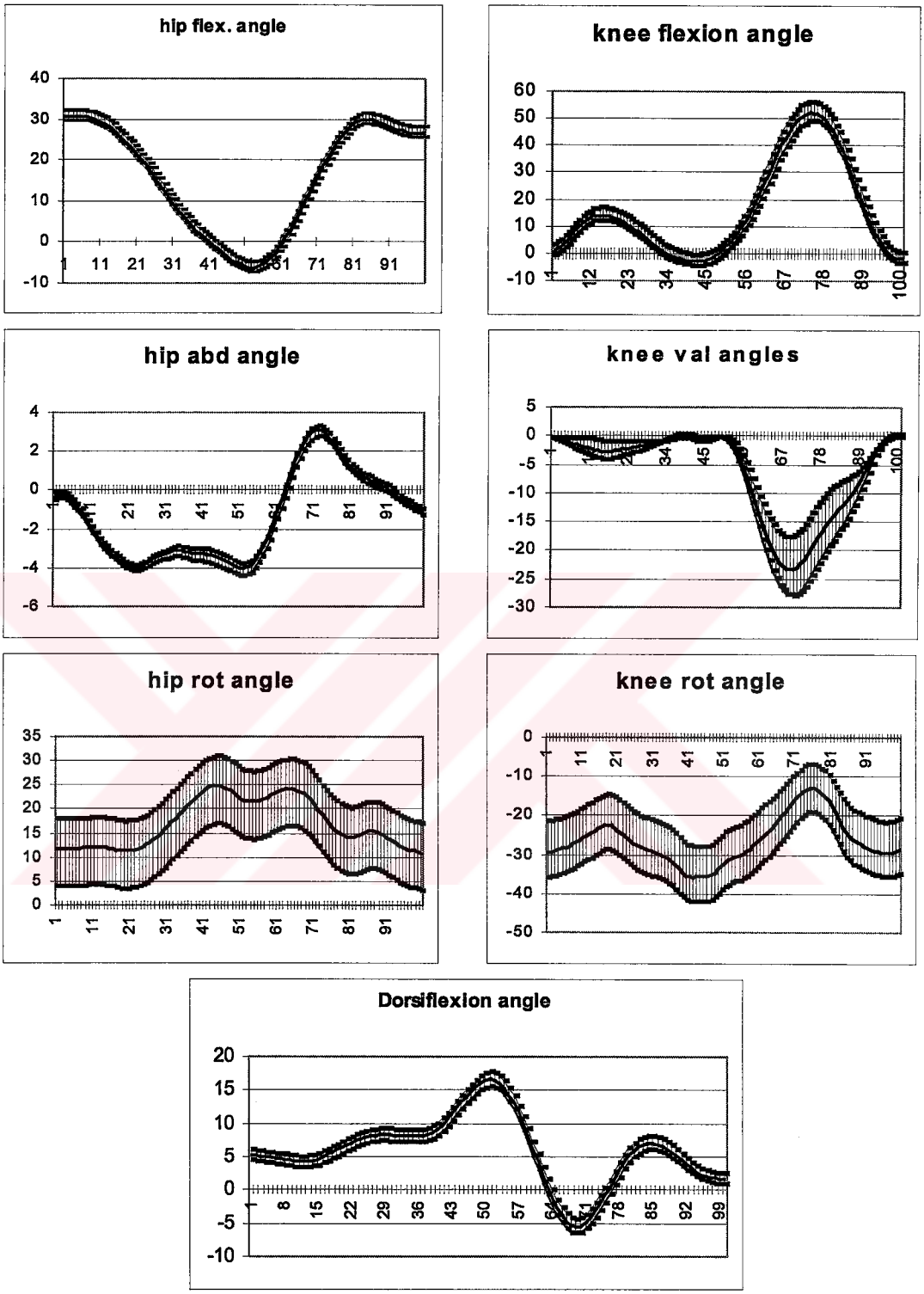

Figure B- 7: Graphs for M.E. by knowledgeable performer

2.3 Acquainted Performer

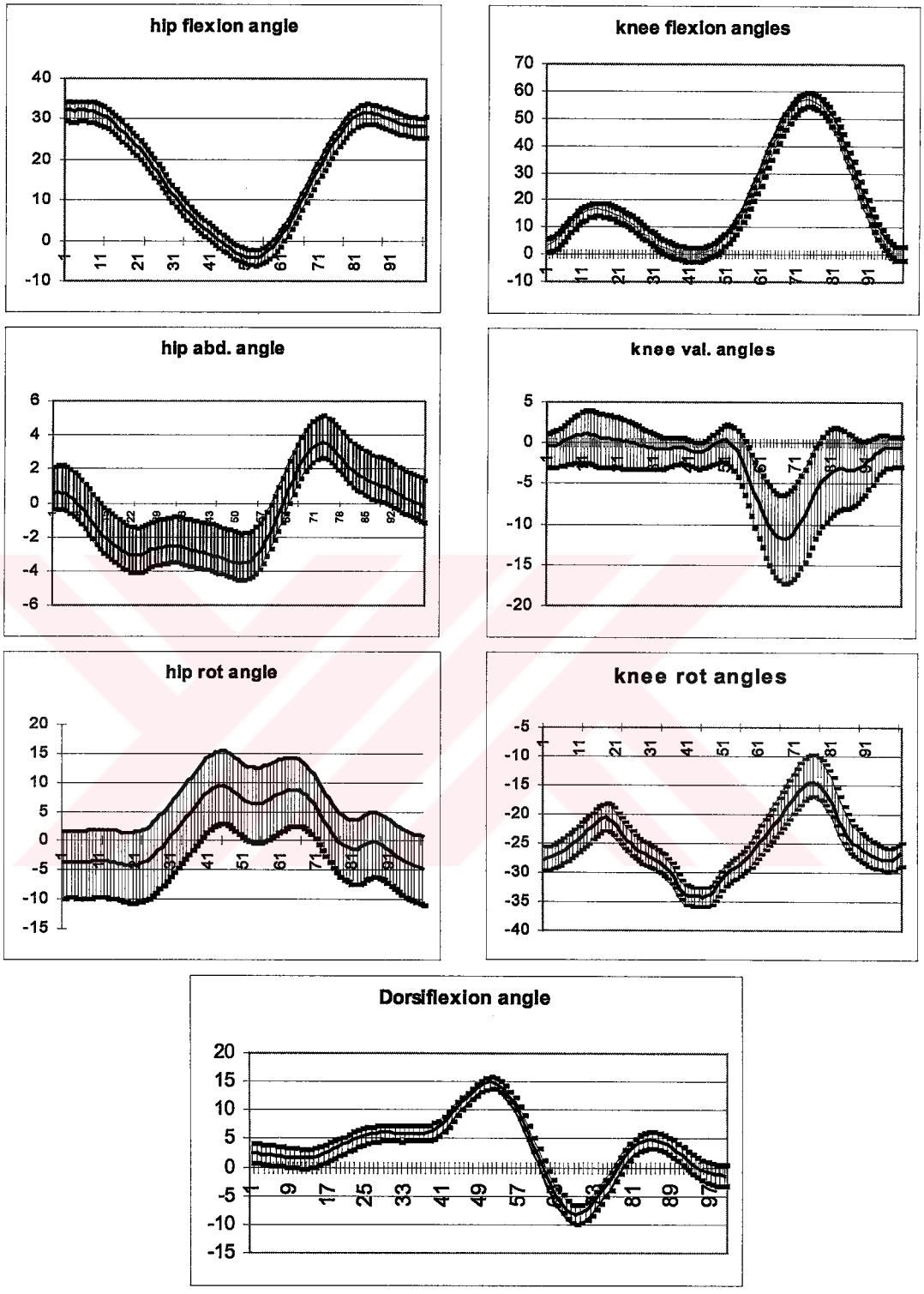

Figure B- 8: Graphs for M.E. by acquainted performer

2.4 Unaware Performer

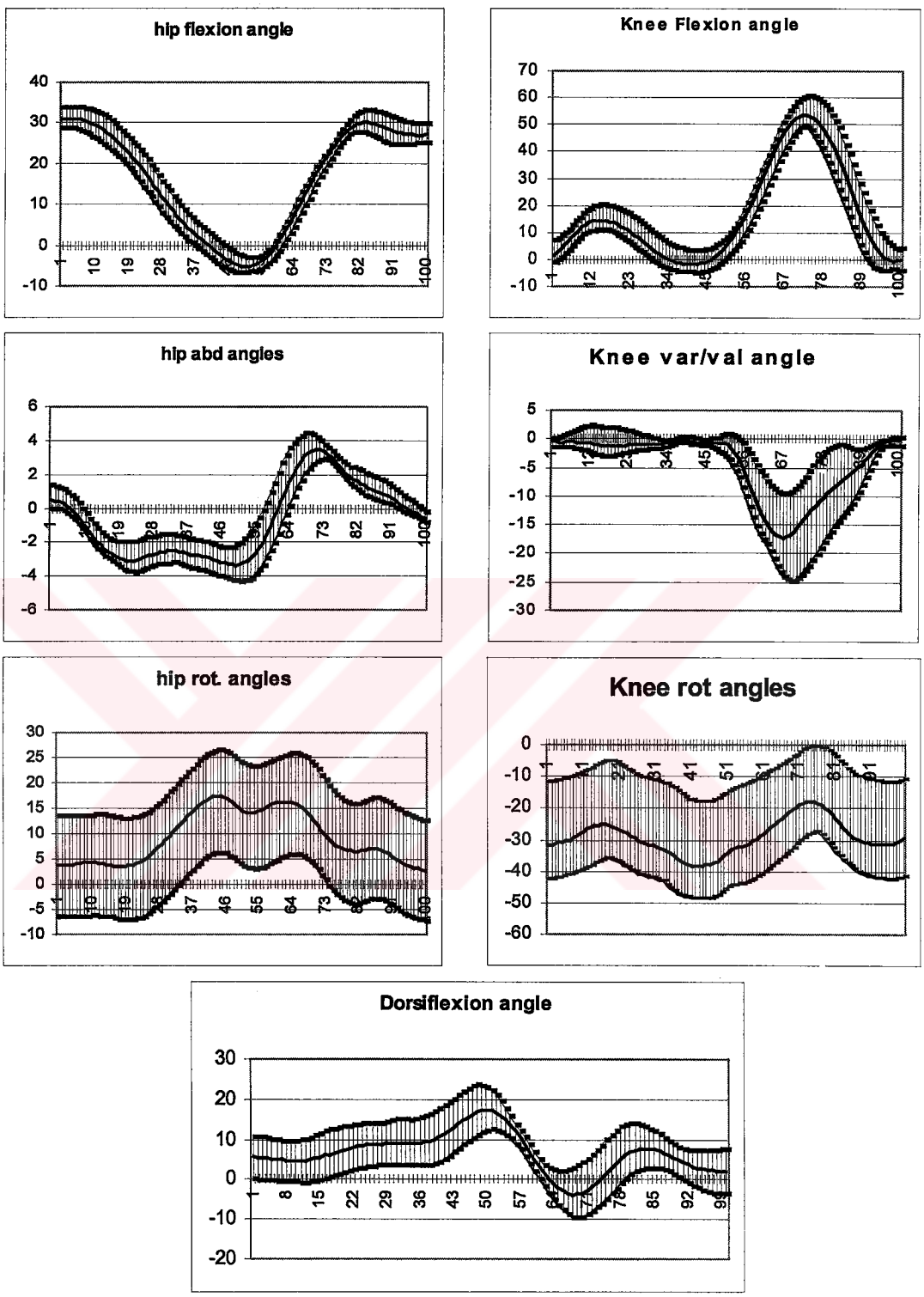

Figure B- 9: Graphs for M.E. by unaware performer

2.5 Mean Values for Subject M.E.

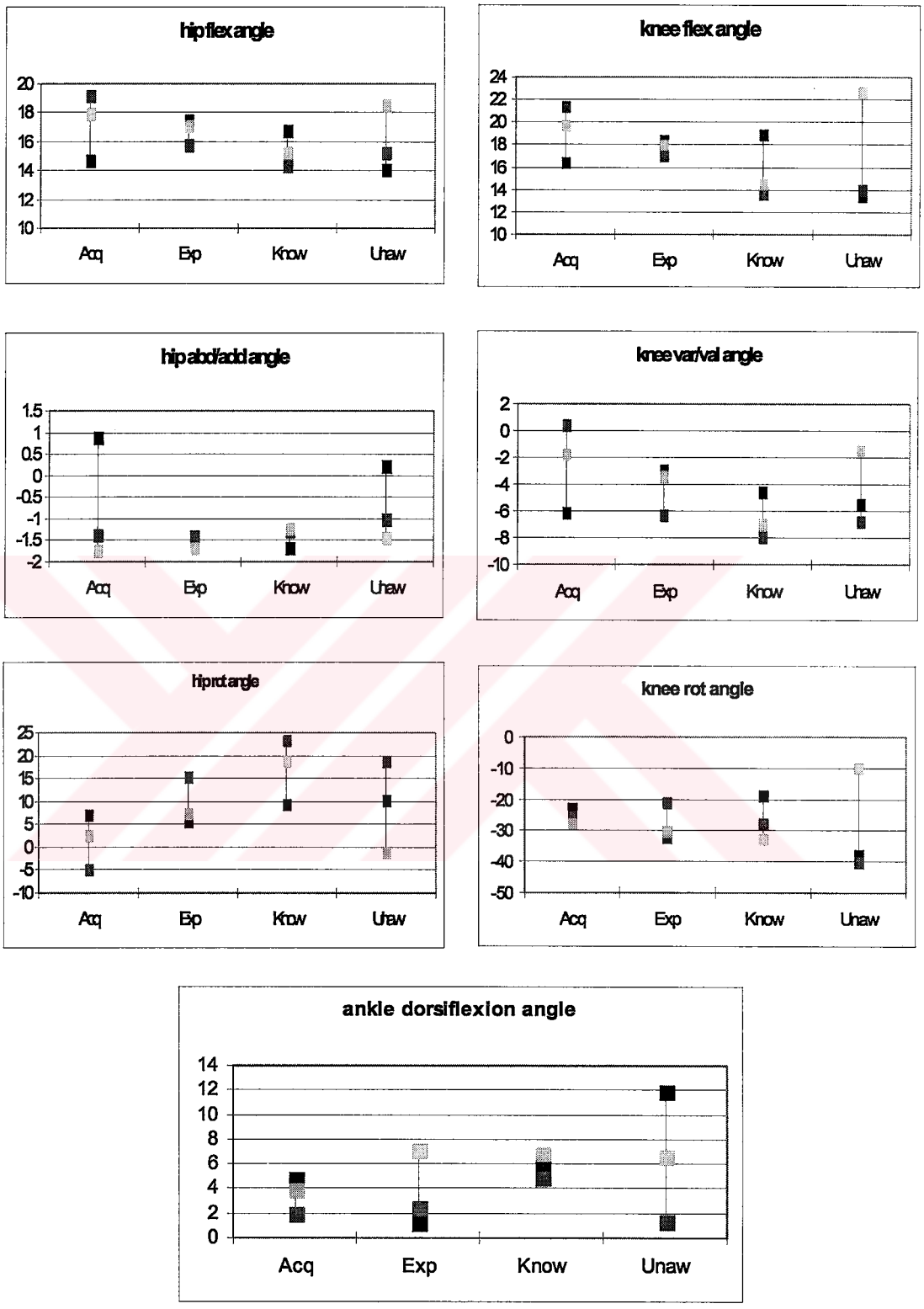

Figure B- 10: Mean values of three experiments for M.E.

3 Graphs For Subject U.S.

3.1 Expert Performer

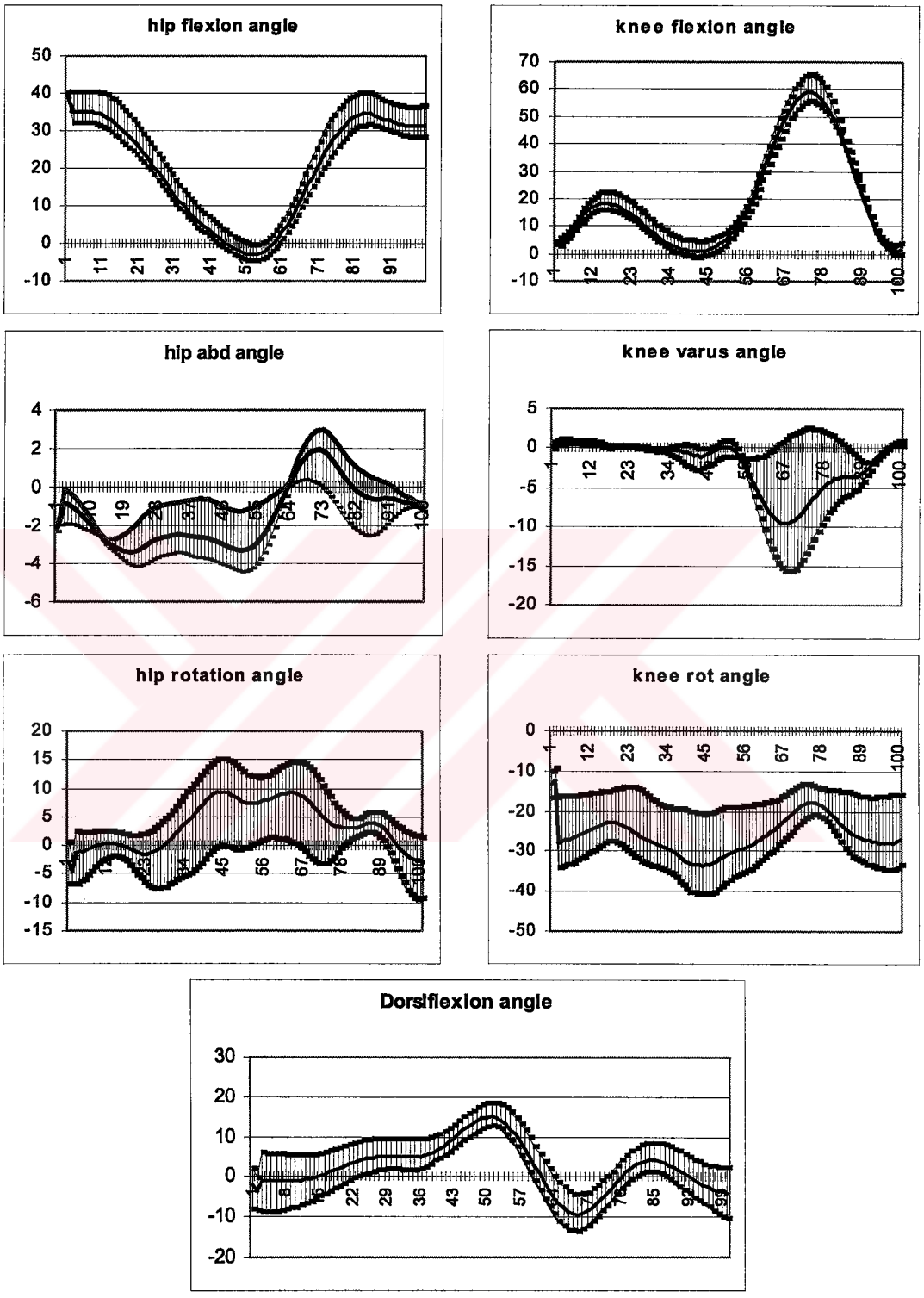

Figure B- 11: Graphs for U.S. by expert performer

3.2 Acquainted Performer

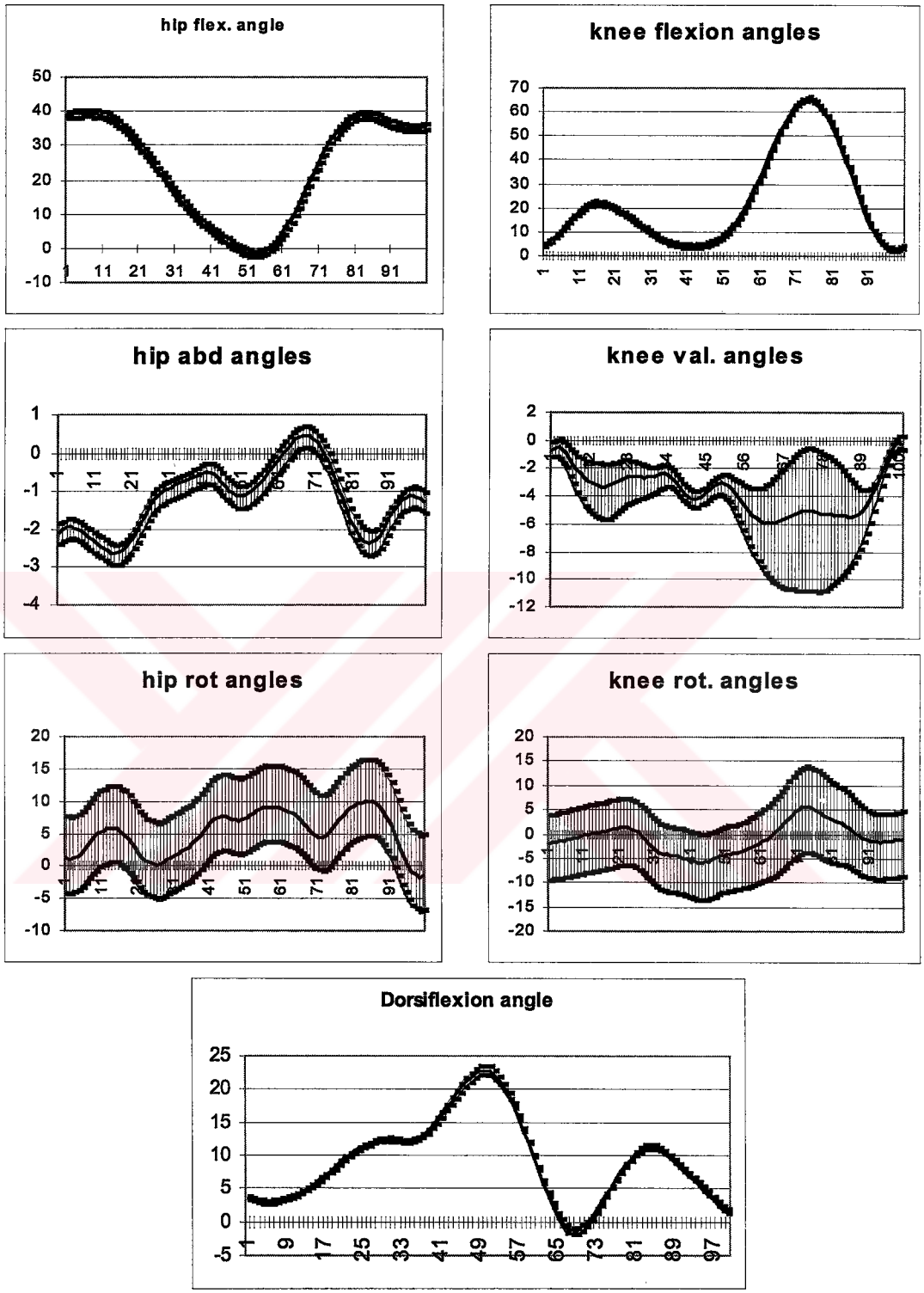

Figure B- 12: Graphs for U.S. by acquainted performer

3.3 Knowledgeable Performer

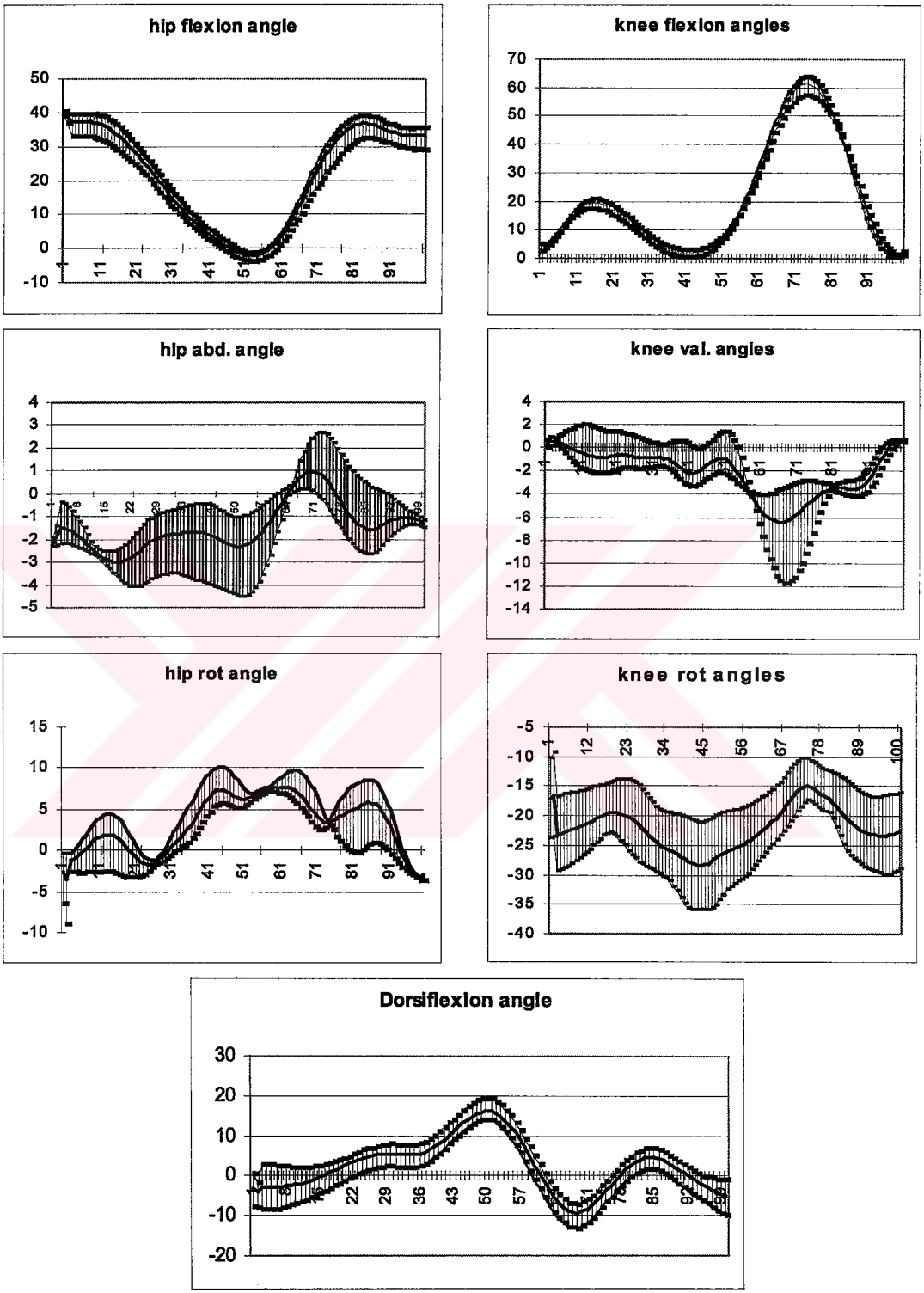

Figure B- 13: Graphs for U.S. by knowledgeable performer

3.4 Unaware Performer

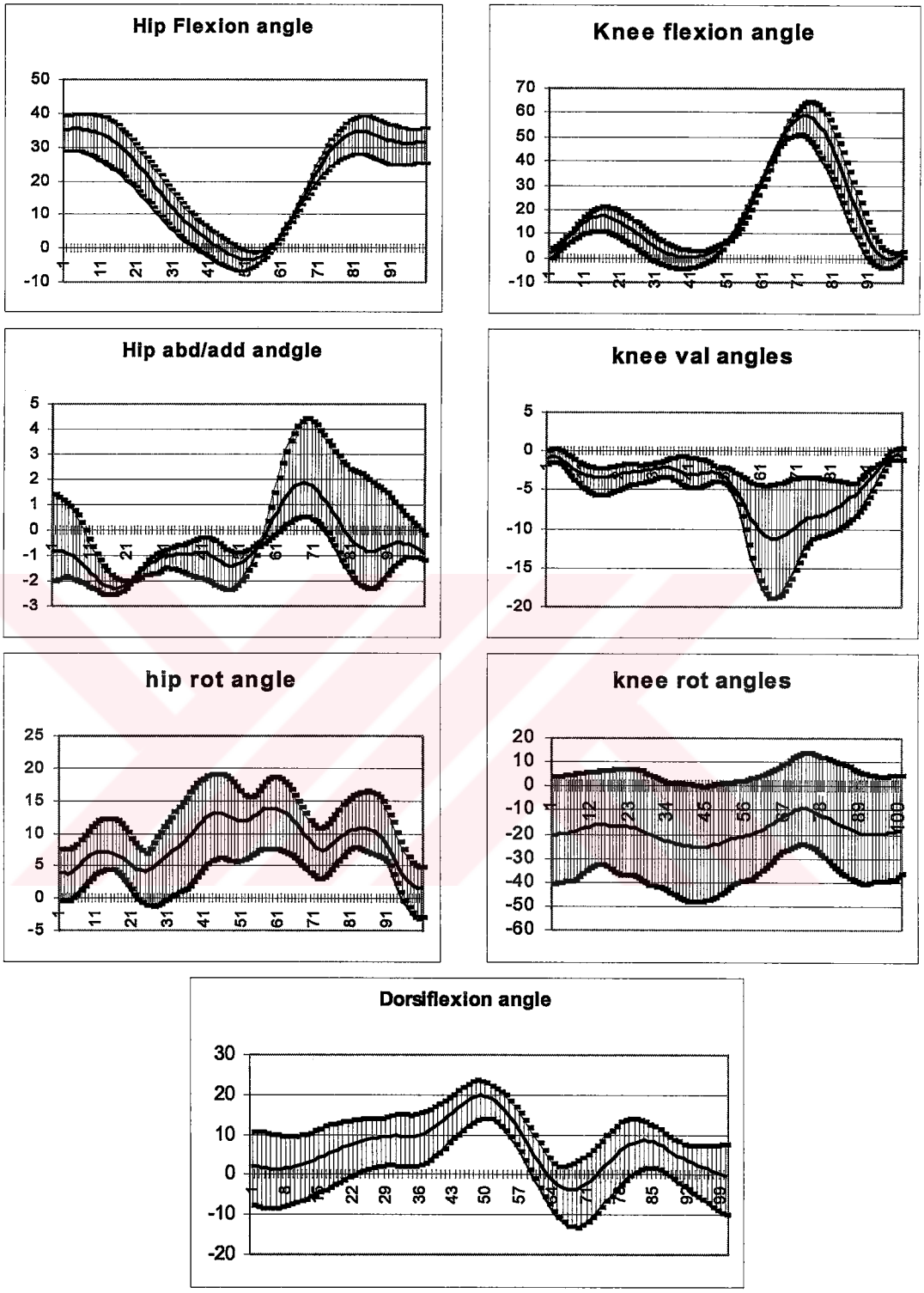

Figure B- 14: Graphs for U.S. by unaware performer

3.5 Mean Values for Subject U.S.

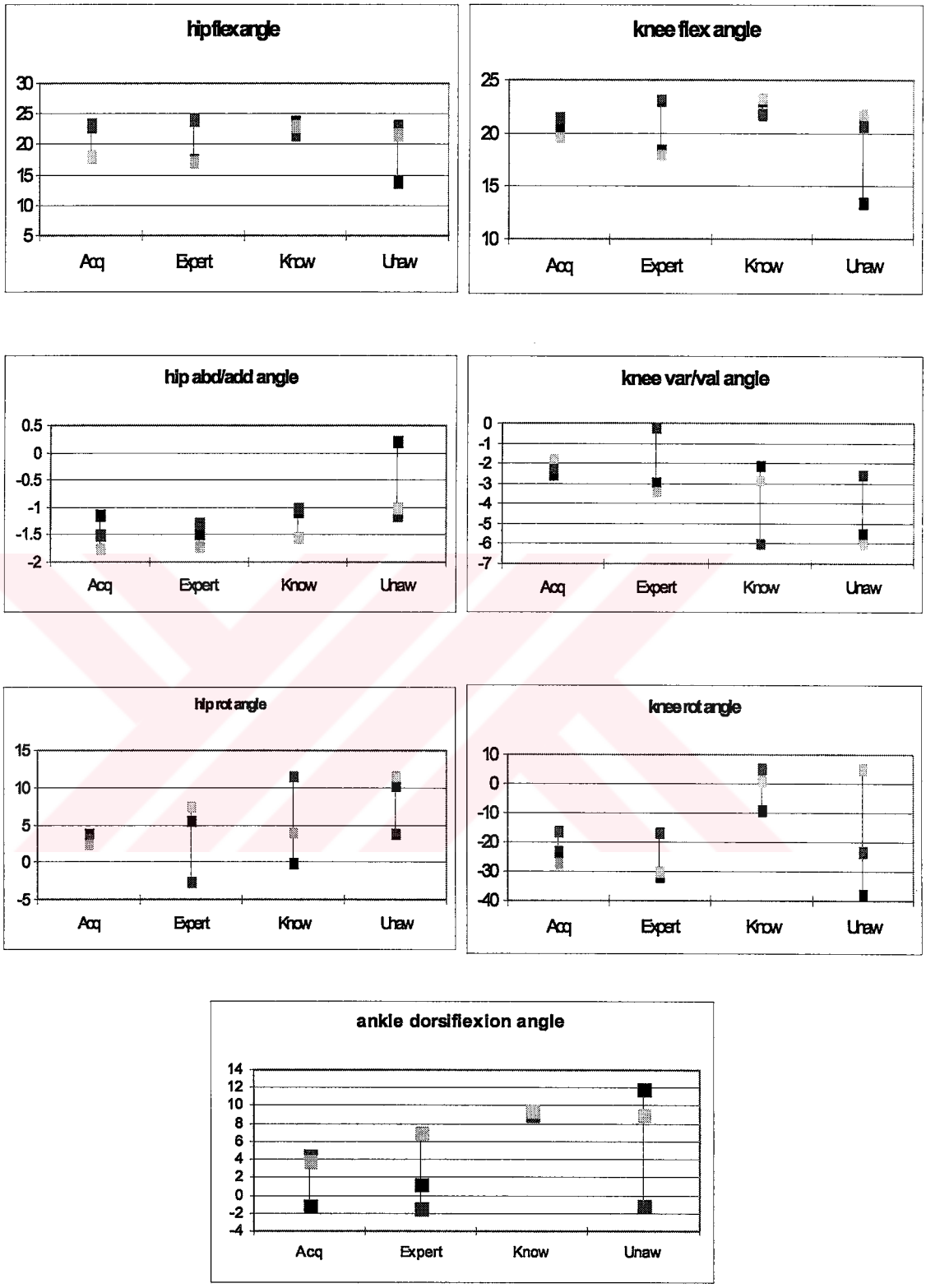

Figure B- 15: Mean values of three experiments for U.S.

APPENDIX C

RESULTS OF PROPOSED PROTOCOL

1 First Subject

1.1 First Experiment

1.1.1 INSTANTANEOUS AXIS OF ROTATION METHOD

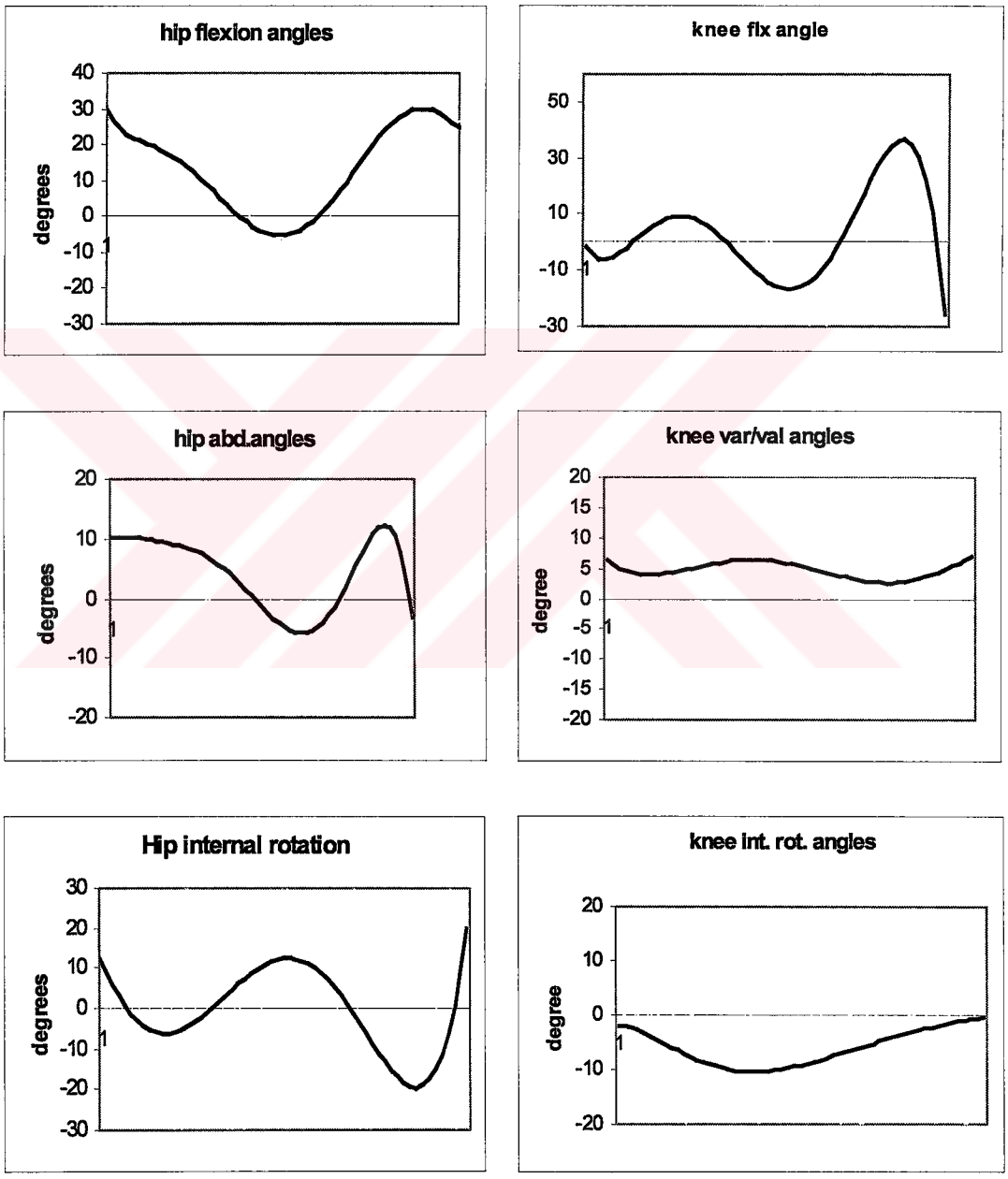

Figure C- 1: Joint angles using instantaneous axis of rotation method

1.1.2 RODRIGUES' FORMULA FOR FINITE ROTATIONS

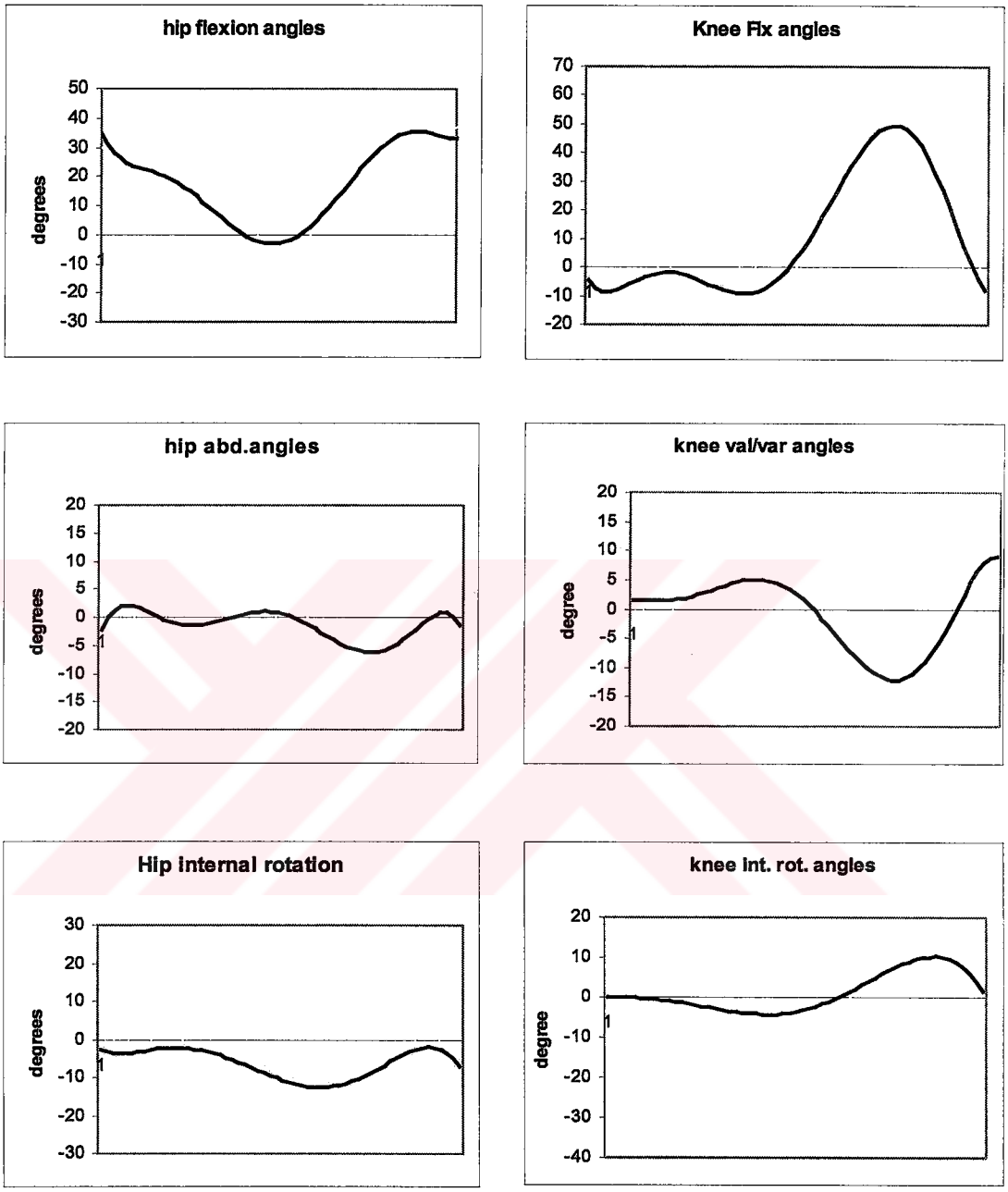

Figure C- 2: Joint angles using Rodrigues' formula

1.2 Second Experiment

1.2.1 INSTANTANEOUS AXIS OF ROTATION METHOD

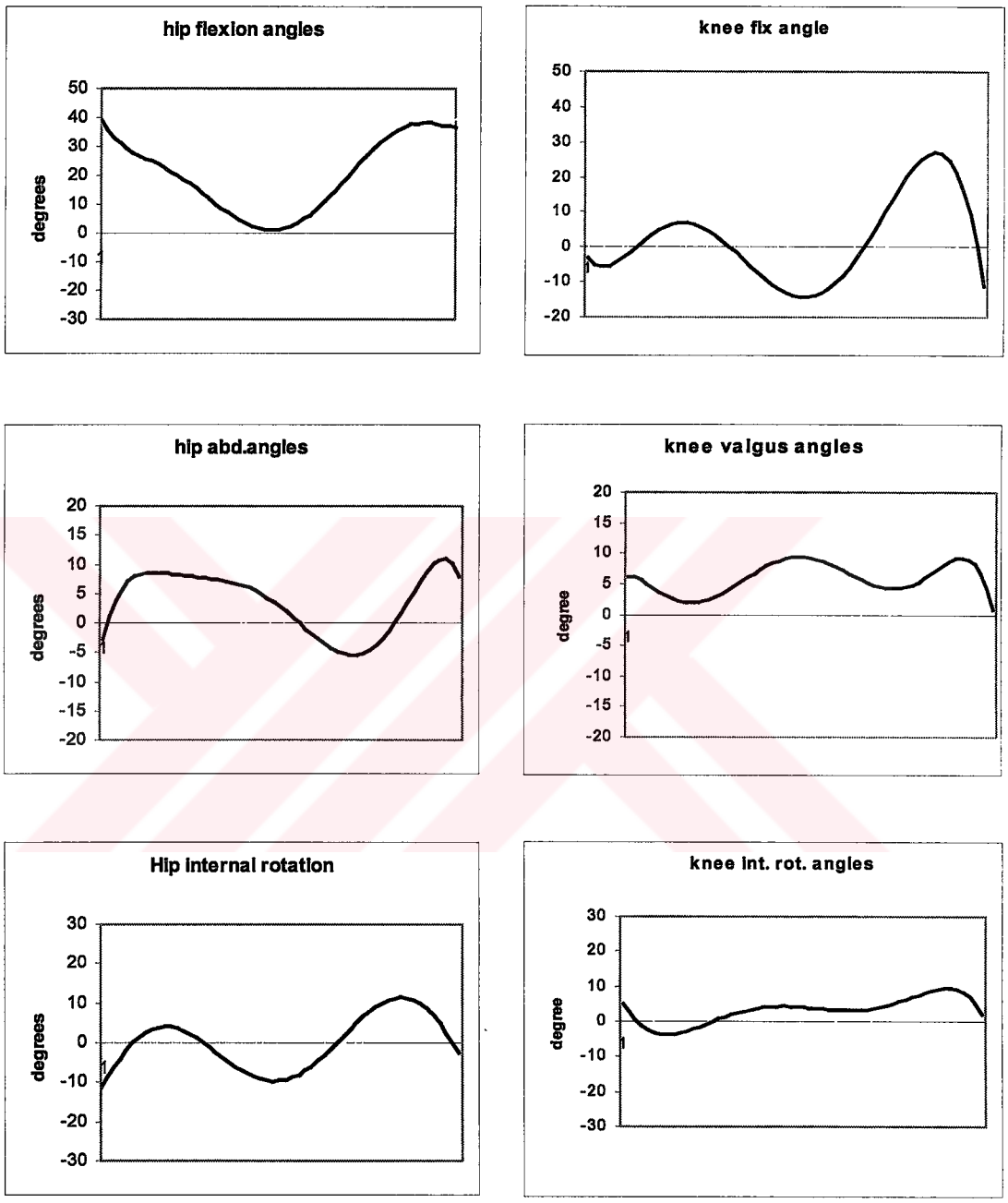

Figure C- 3: Joint angles using instantaneous axis of rotation method

1.2.2 RODRIGUES' FORMULA FOR FINITE ROTATIONS

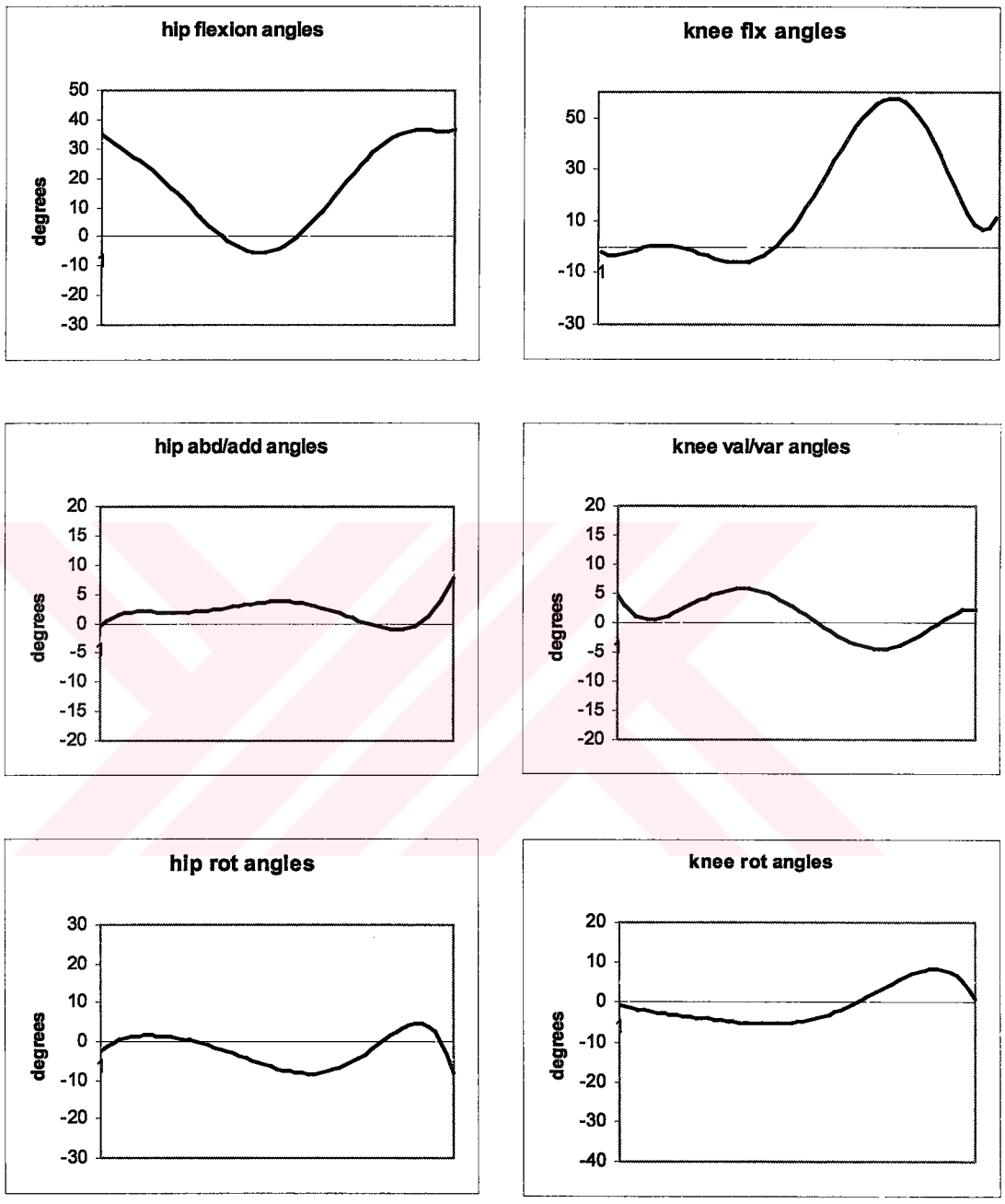

Figure C- 4: Joint angles using Rodrigues' formula

1.3 Results Of KissGAIT

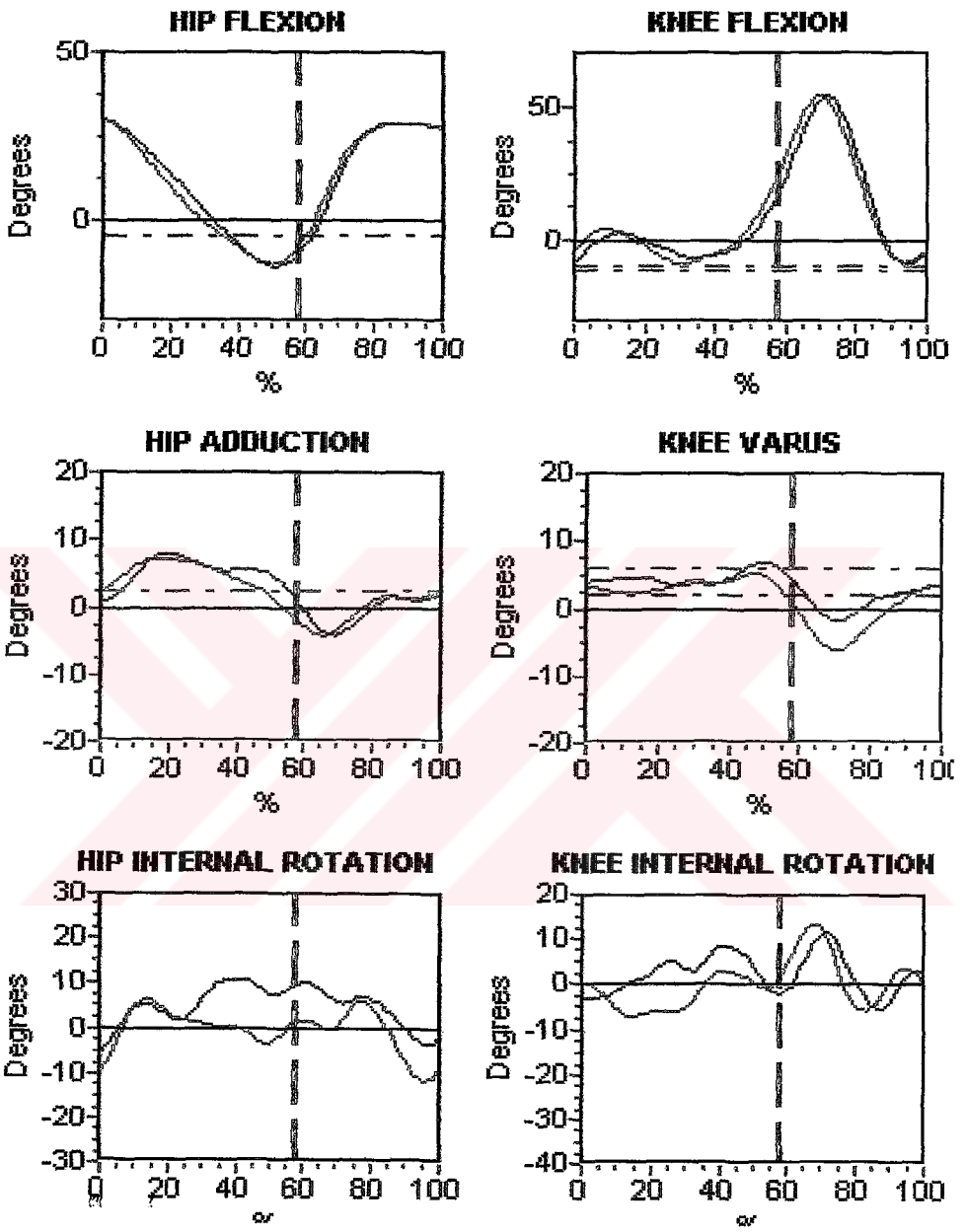

Figure C- 5: Joint angles from KissGAIT

2 Second Subject

2.1 First Experiment

2.1.1 INSTANTANEOUS AXIS OF ROTATION METHOD

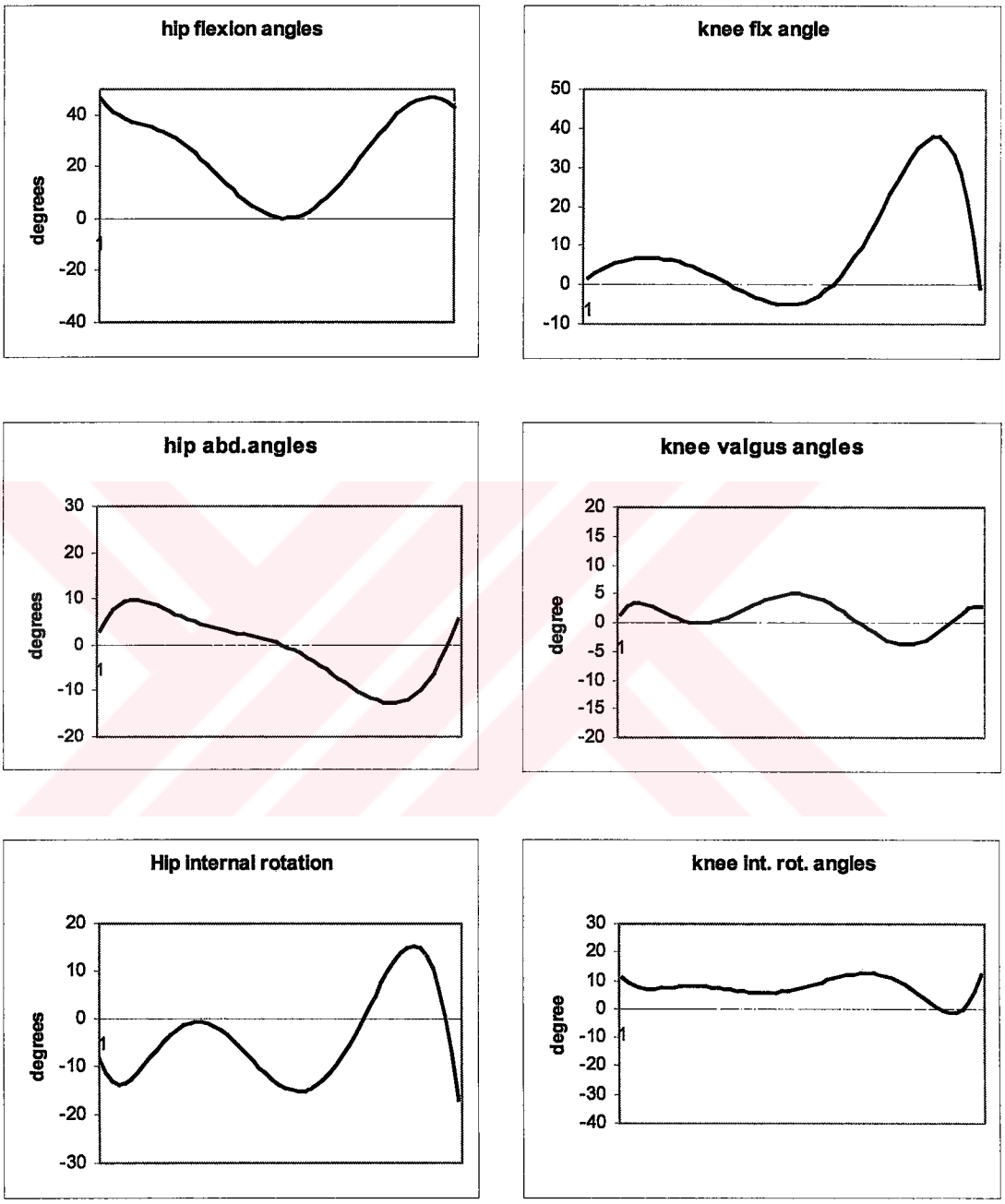

Figure C- 6: Joint angles using instantaneous axis of rotation method

2.1.2 RODRIGUES' FORMULA FOR FINITE ROTATIONS

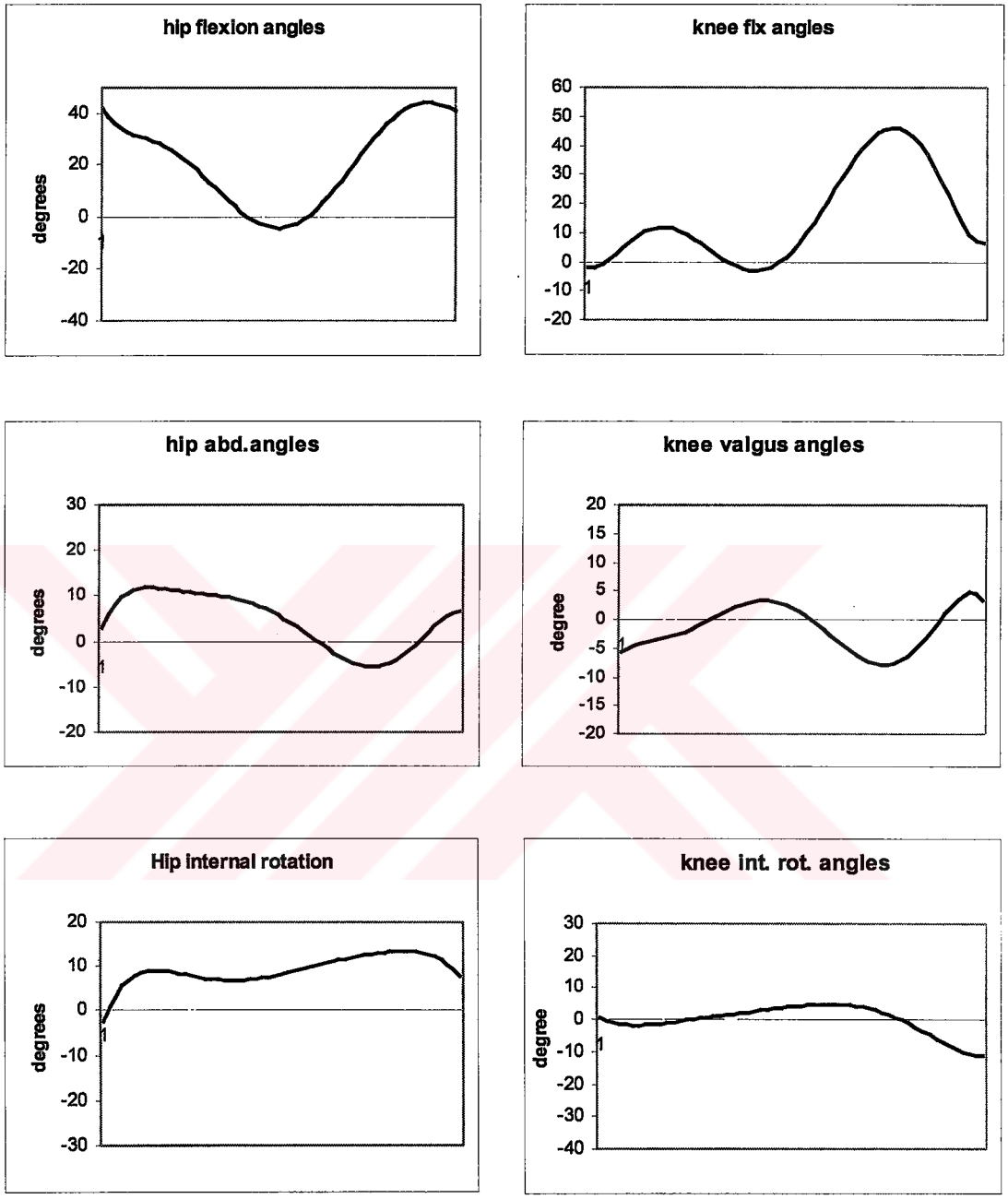

Figure C- 7: Joint angles using Rodrigues' formula

2.2 Second Experiment

2.2.1 INSTANTANEOUS AXIS OF ROTATION

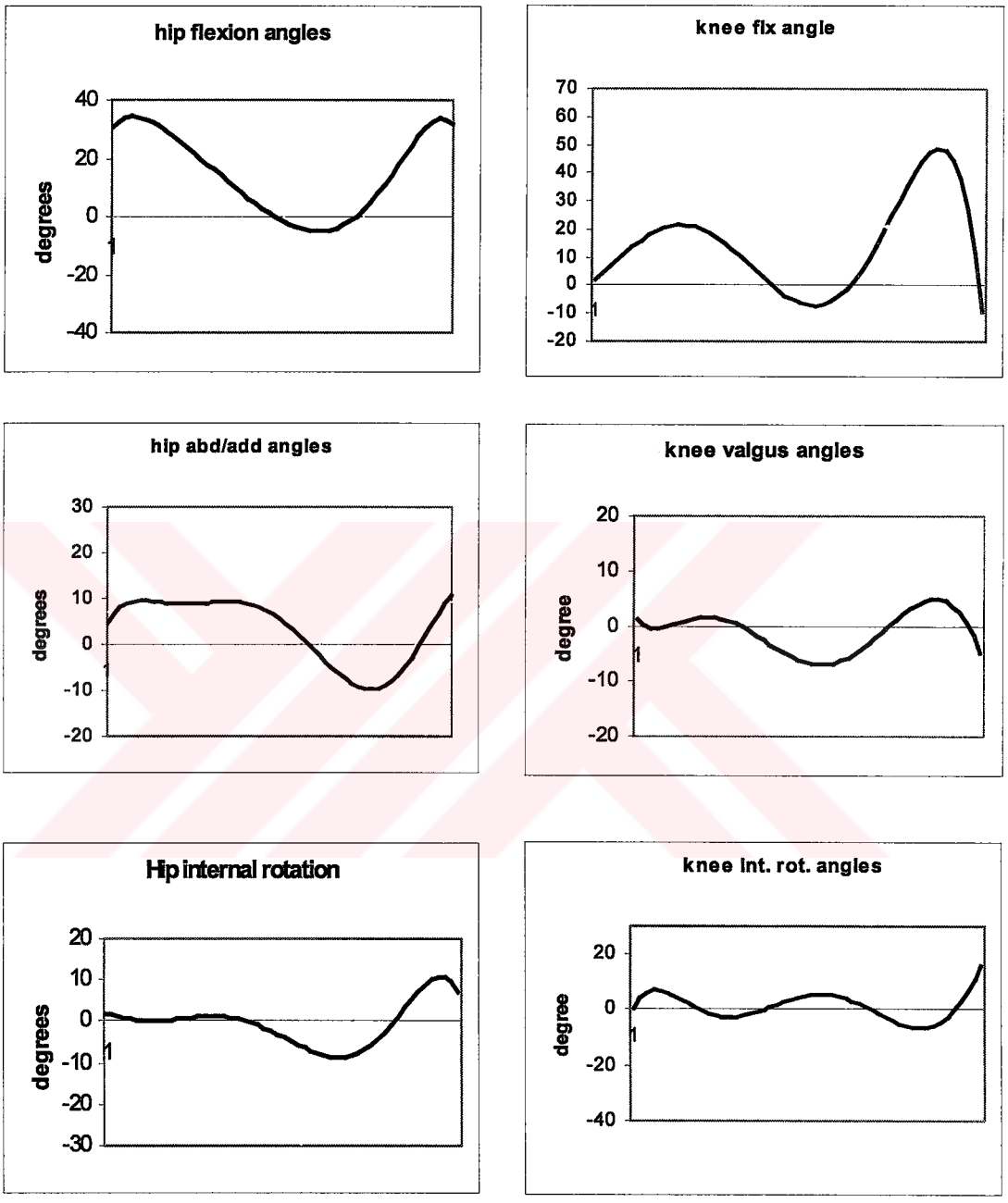

Figure C- 8: Joint angles using instantaneous axis of rotation method

2.2.2 RODRIGUES' FORMULA FOR FINITE ROTATIONS

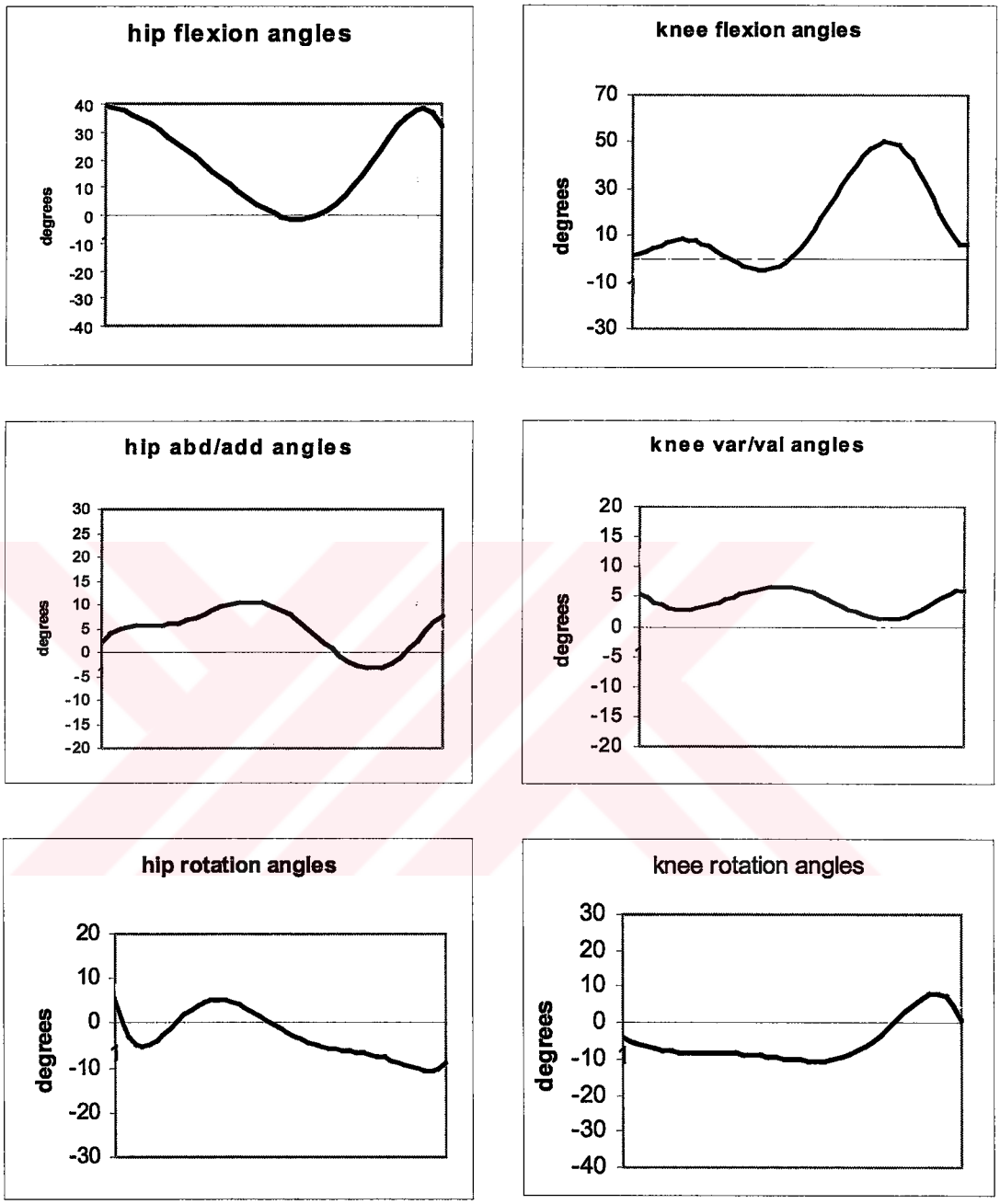

Figure C- 9: Joint angles using Rodrigues' formula

2.3 Results Of KissGAIT

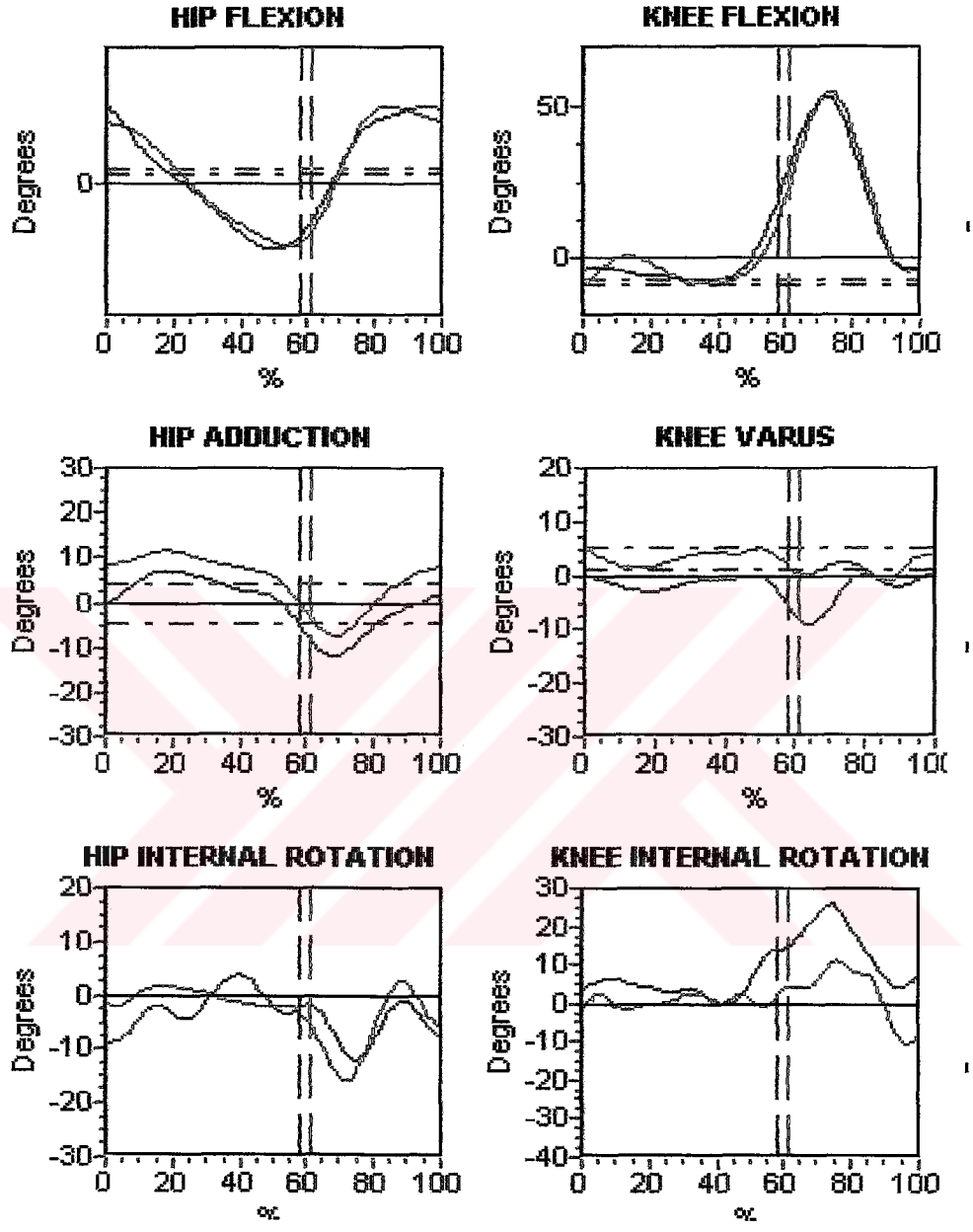

Figure C- 10: Joint angles from KissGAIT

3 Third Subject

3.1 First Experiment

3.1.1 INSTANTANEOUS AXIS OF ROTATION METHOD

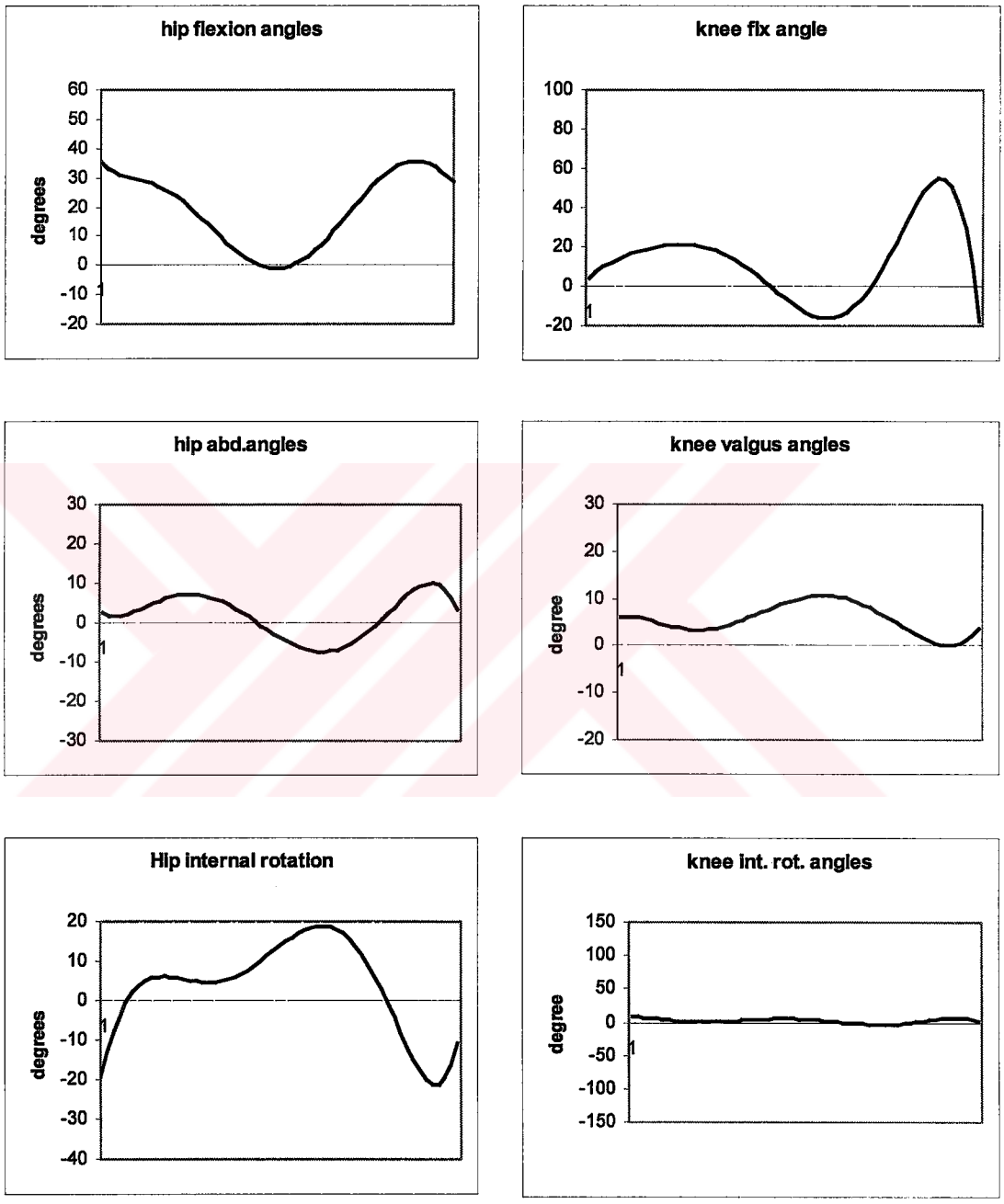

Figure C- 11: Joint angles using instantaneous axis of rotation method

3.1.2 RODRIGUES' FORMULA FOR FINITE ROTATIONS

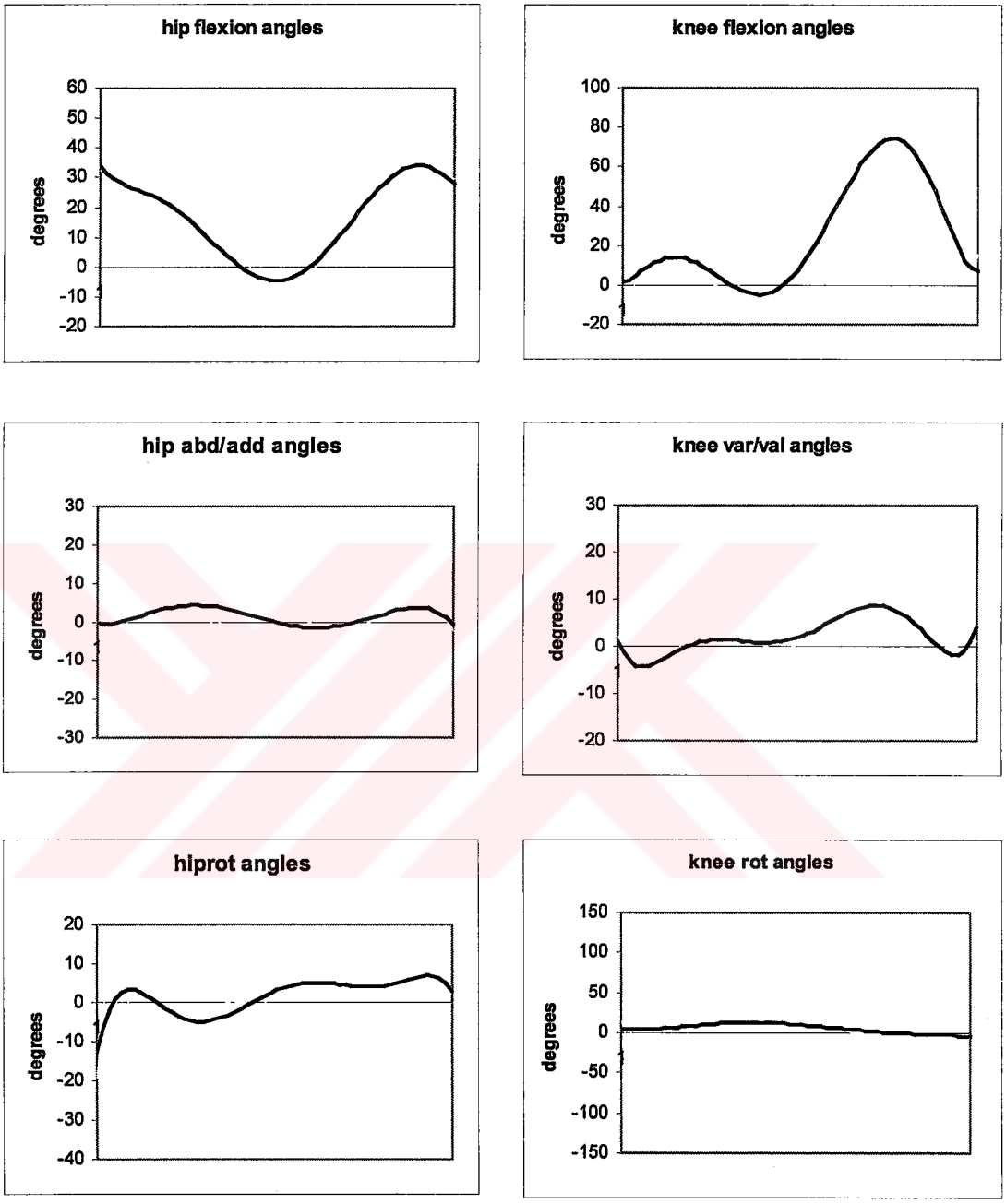

Figure C- 12: Joint angles using Rodrigues' formula

3.2 Second Experiment

3.2.1 INSTANTANEOUS AXIS OF ROTATION METHOD

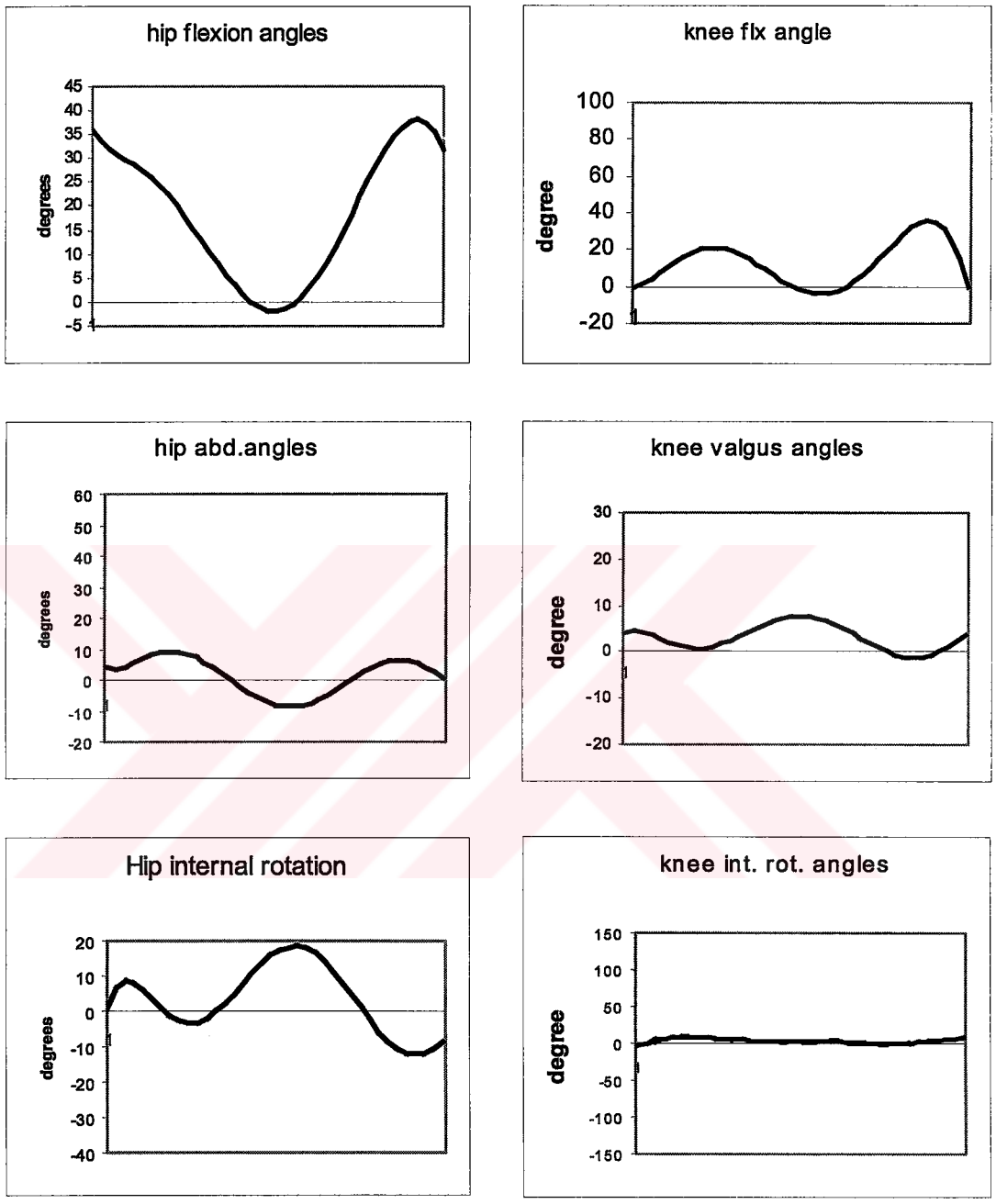

Figure C- 13: Joint angles using instantaneous axis of rotation method

3.2.2 RODRIGUES' FORMULA FOR FINITE ROTATIONS

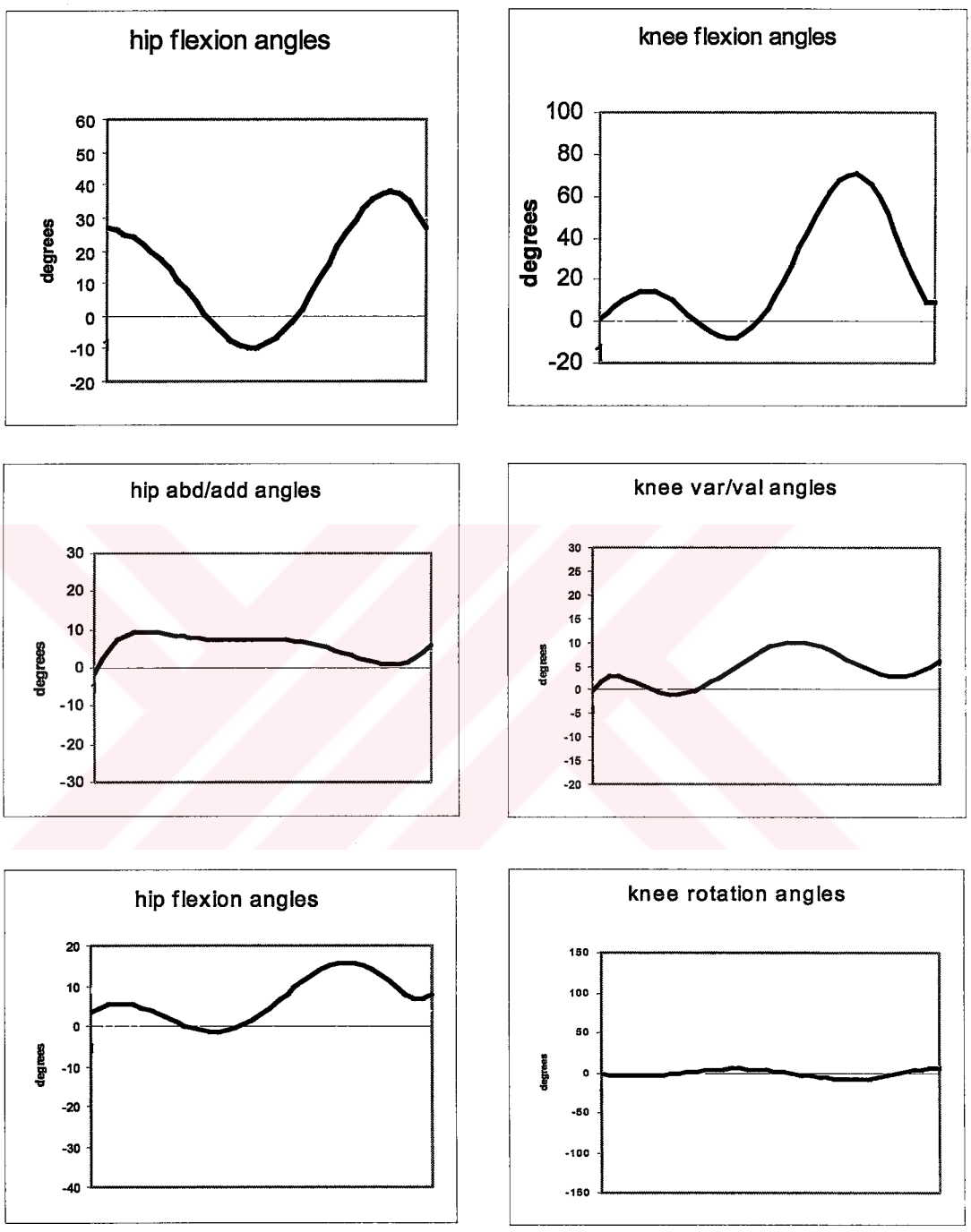

Figure C- 14: Joint angles using Rodrigues' formula

3.3 Results Of KissGAIT

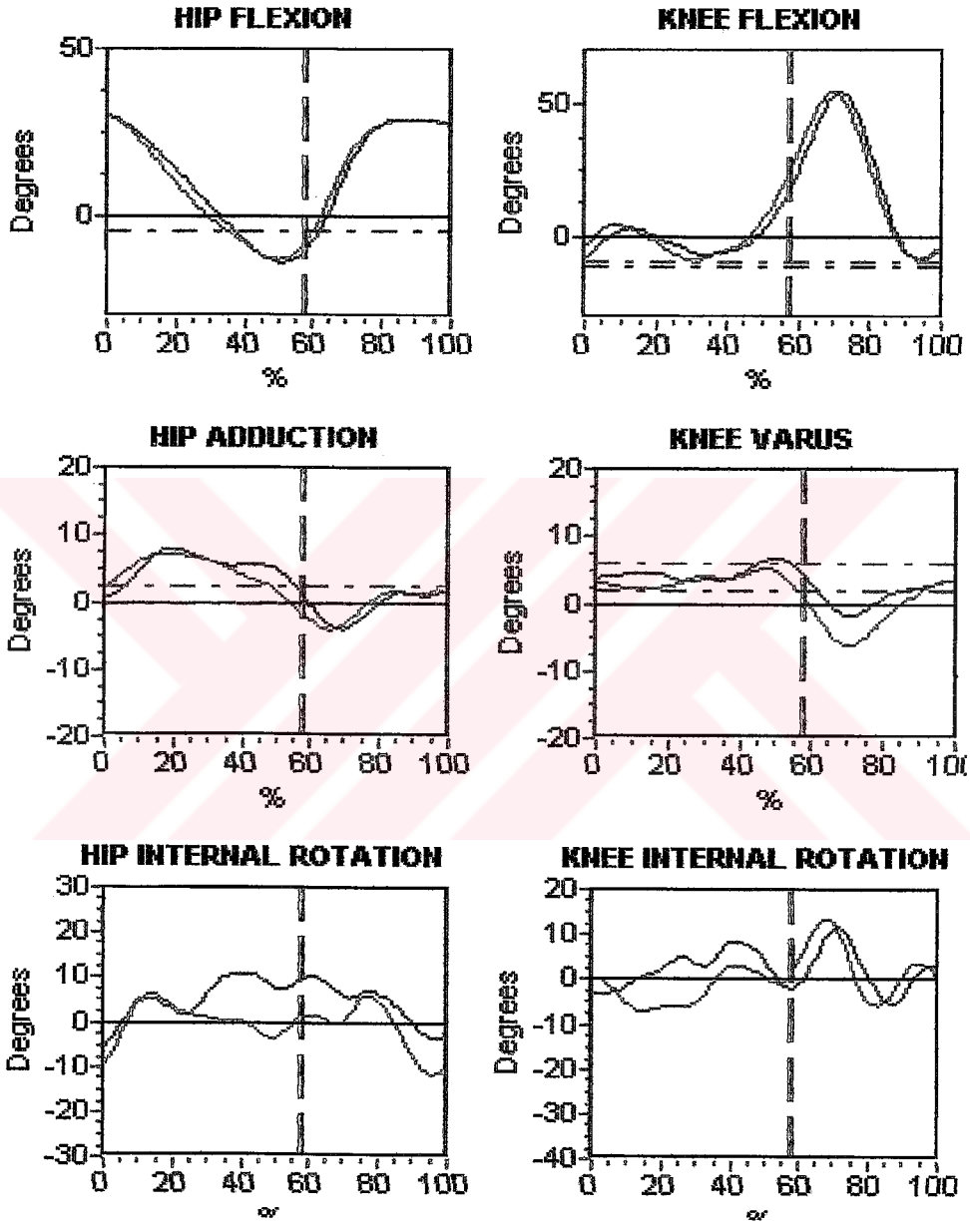

Figure.C- 15: Joint angles from KissGAIT

4 Fourth Subject

4.1 First Experiment

4.1.1 INSTANTANEOUS AXIS OF ROTATION METHOD

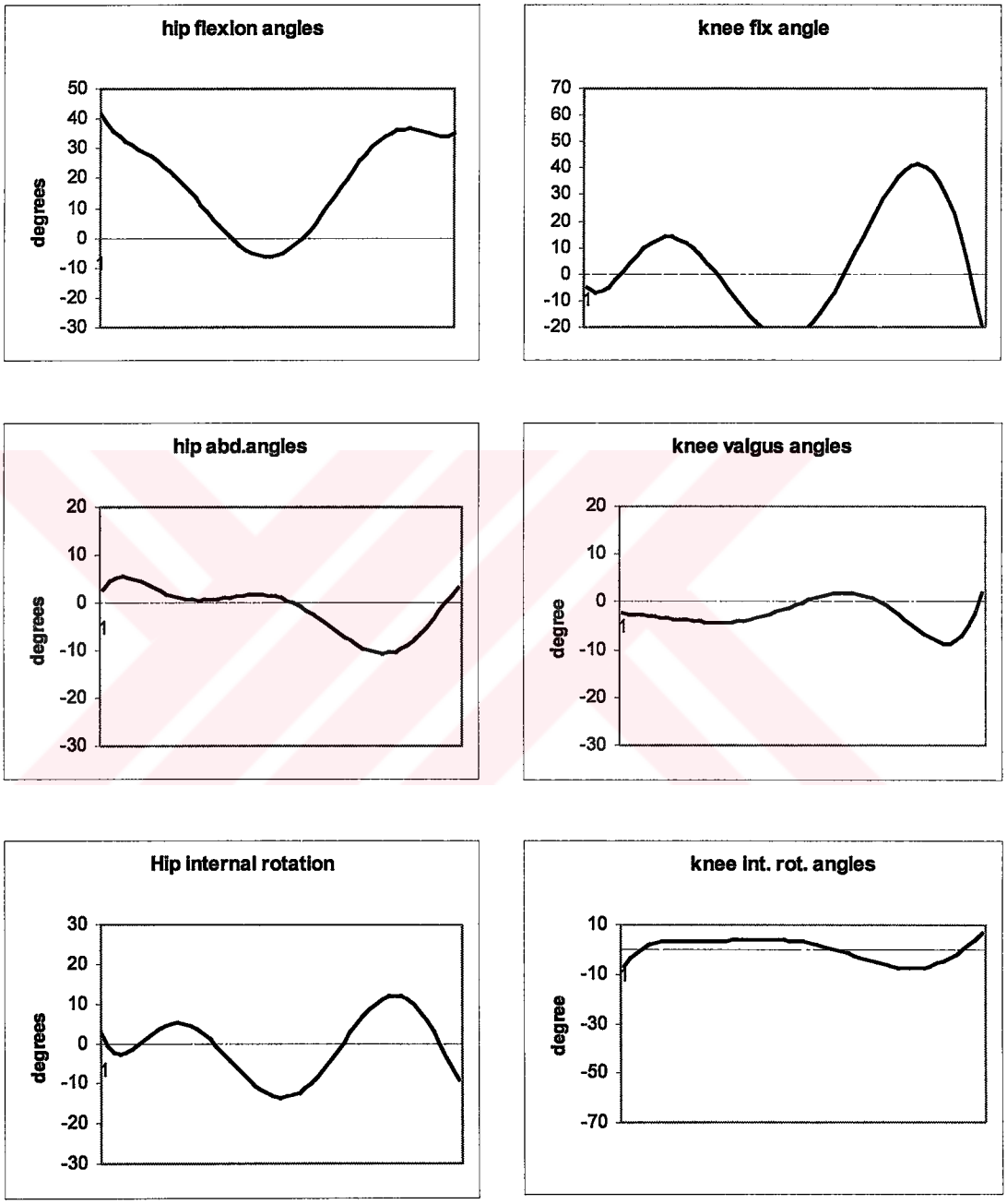

Figure C- 16: Joint angles using instantaneous axis of rotation method

4.1.2 RODRIGUES' FORMULA FOR FINITE ROTATIONS

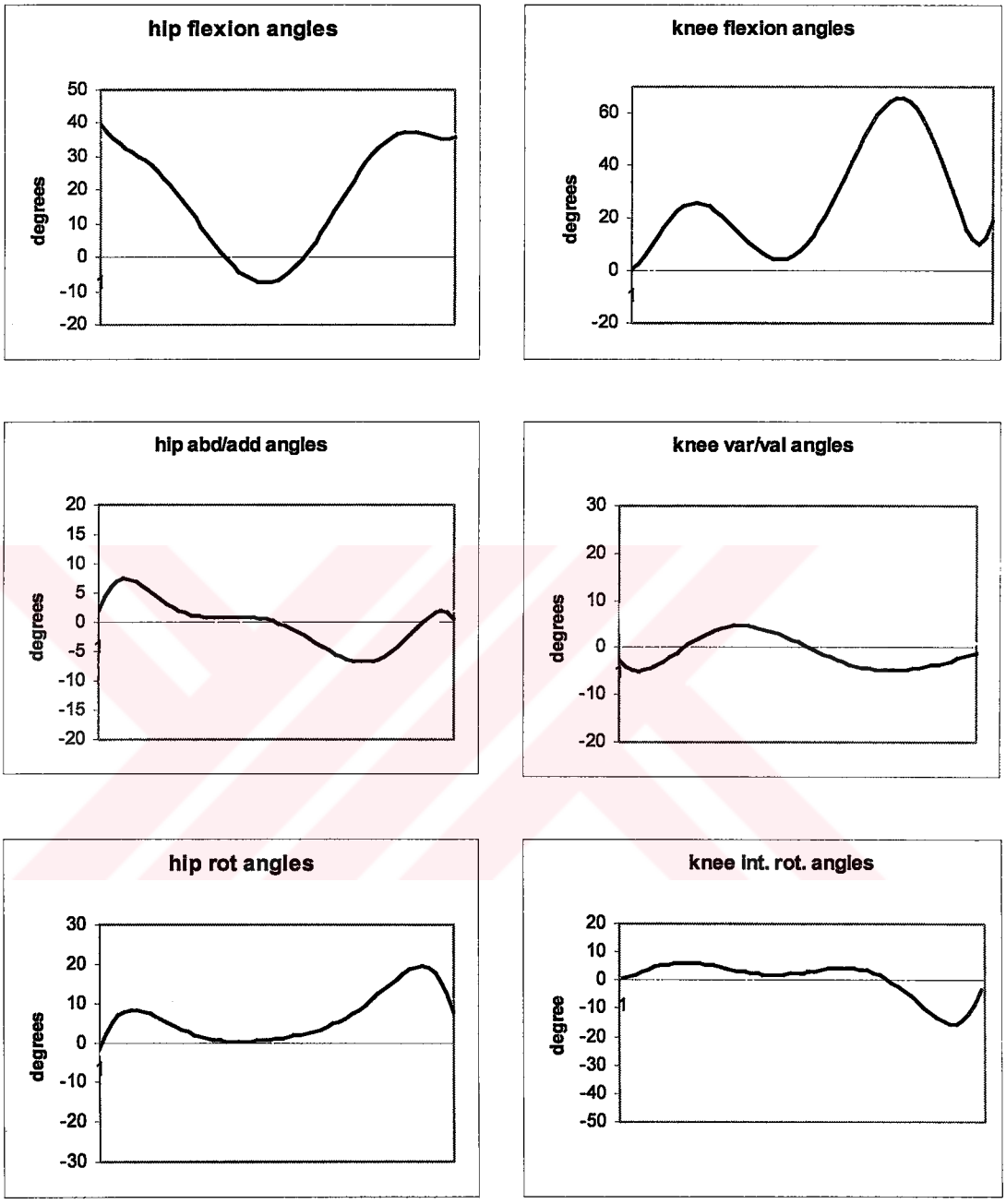

Figure C- 17: Joint angles using Rodrigues' formula

4.2 Second Experiment

4.2.1 INSTANTANEOUS AXIS OF ROTATION METHOD

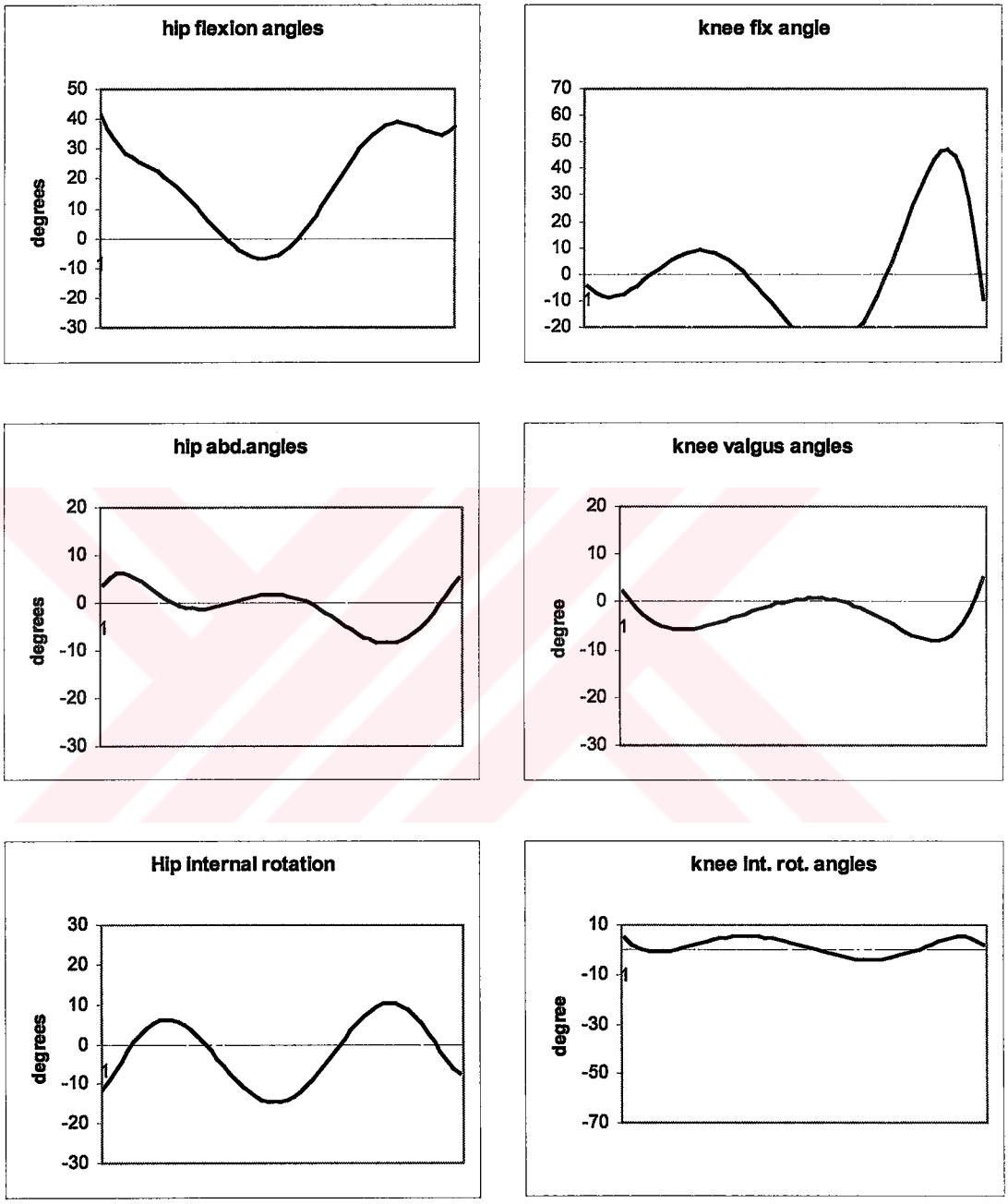

Figure C- 18: Joint angles using instantaneous axis of rotation method

4.2.2 RODRIGUES' FORMULA FOR FINITE ROTATIONS

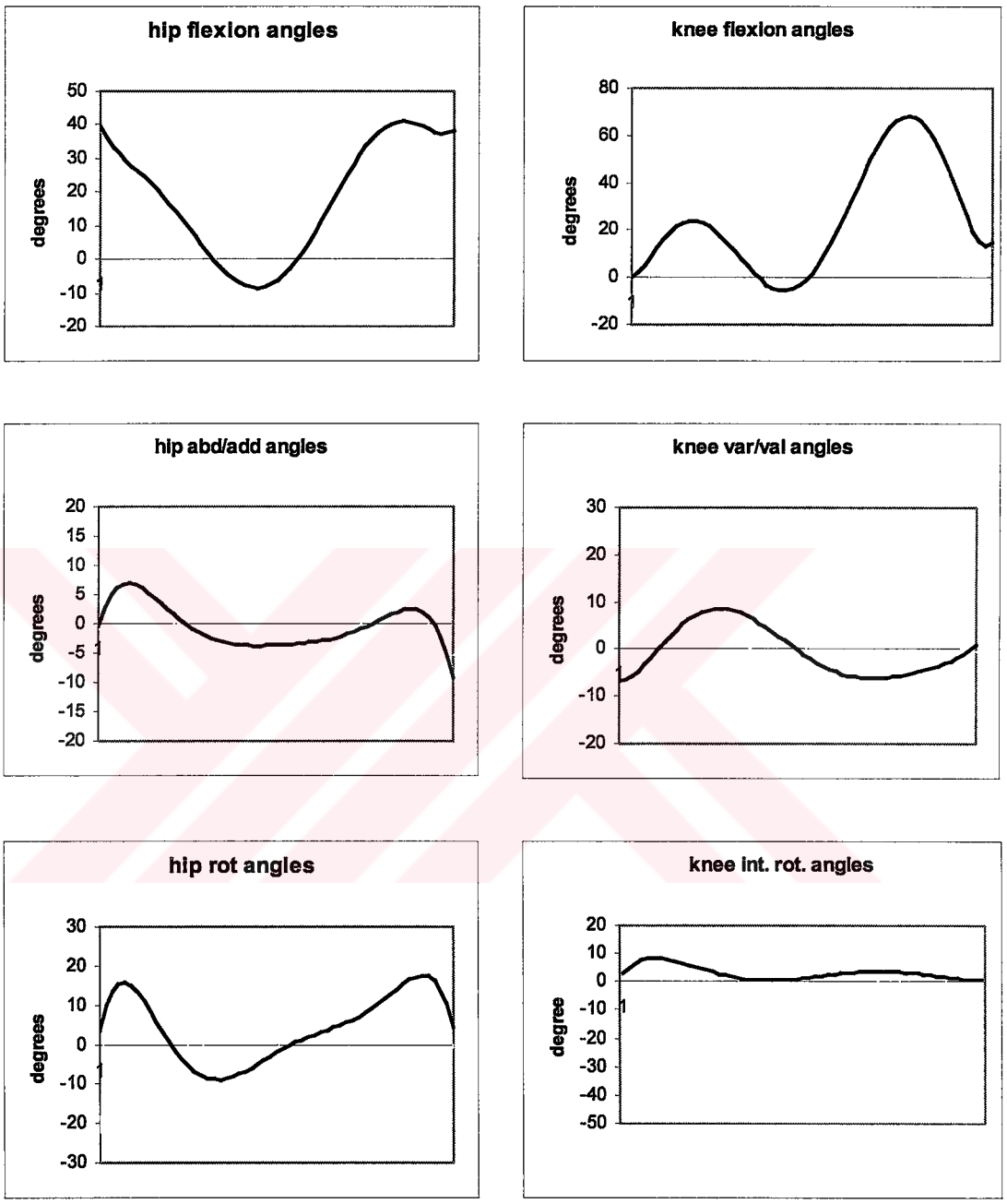

Figure C- 19: Joint angles using Rodrigues' formula

4.3 Results Of KissGAIT

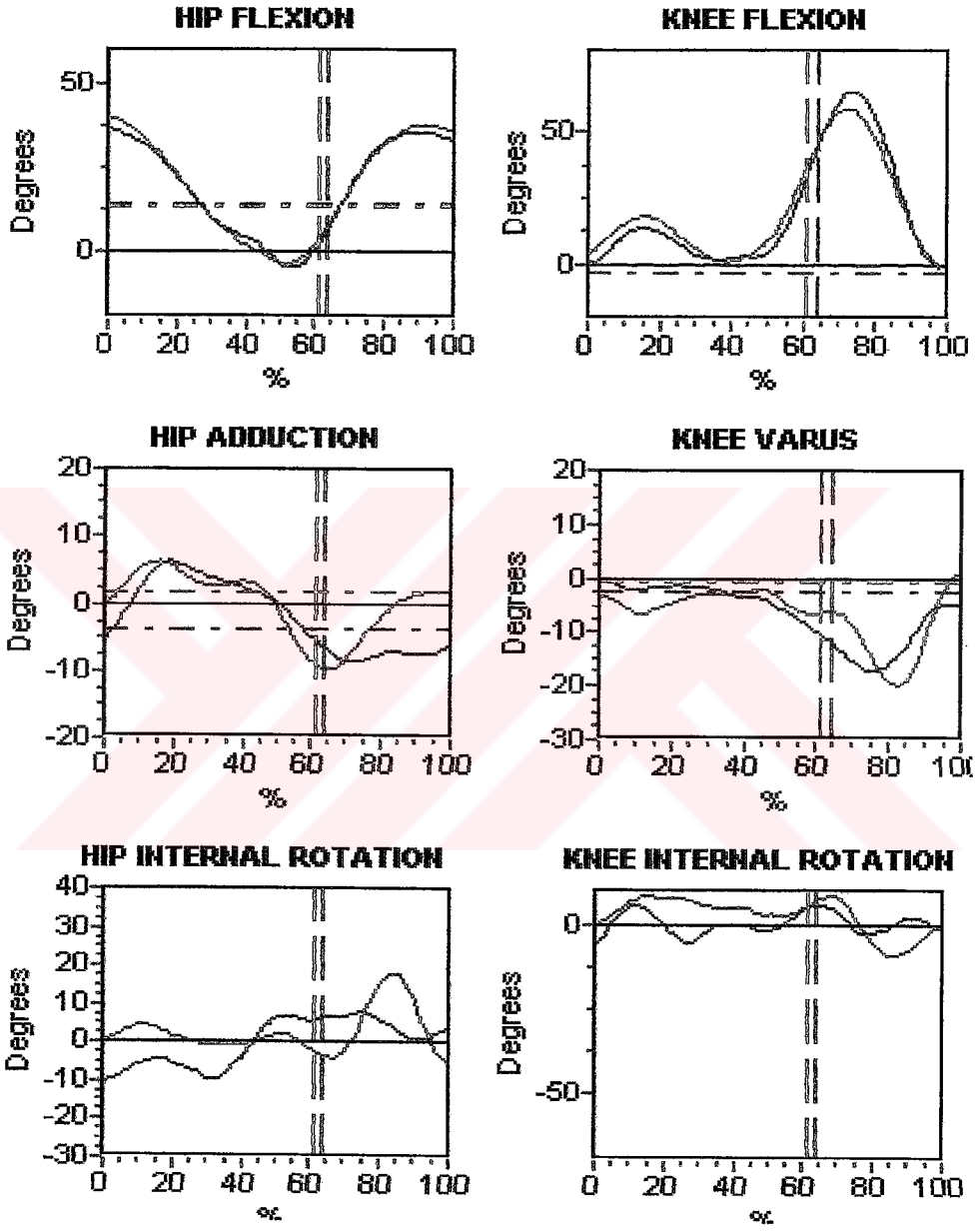

Figure C- 20: Joint angles from KissGAIT

5 Fifth Subject

5.1 First Experiment

5.1.1 INSTANTANEOUS AXIS OF ROTATION METHOD

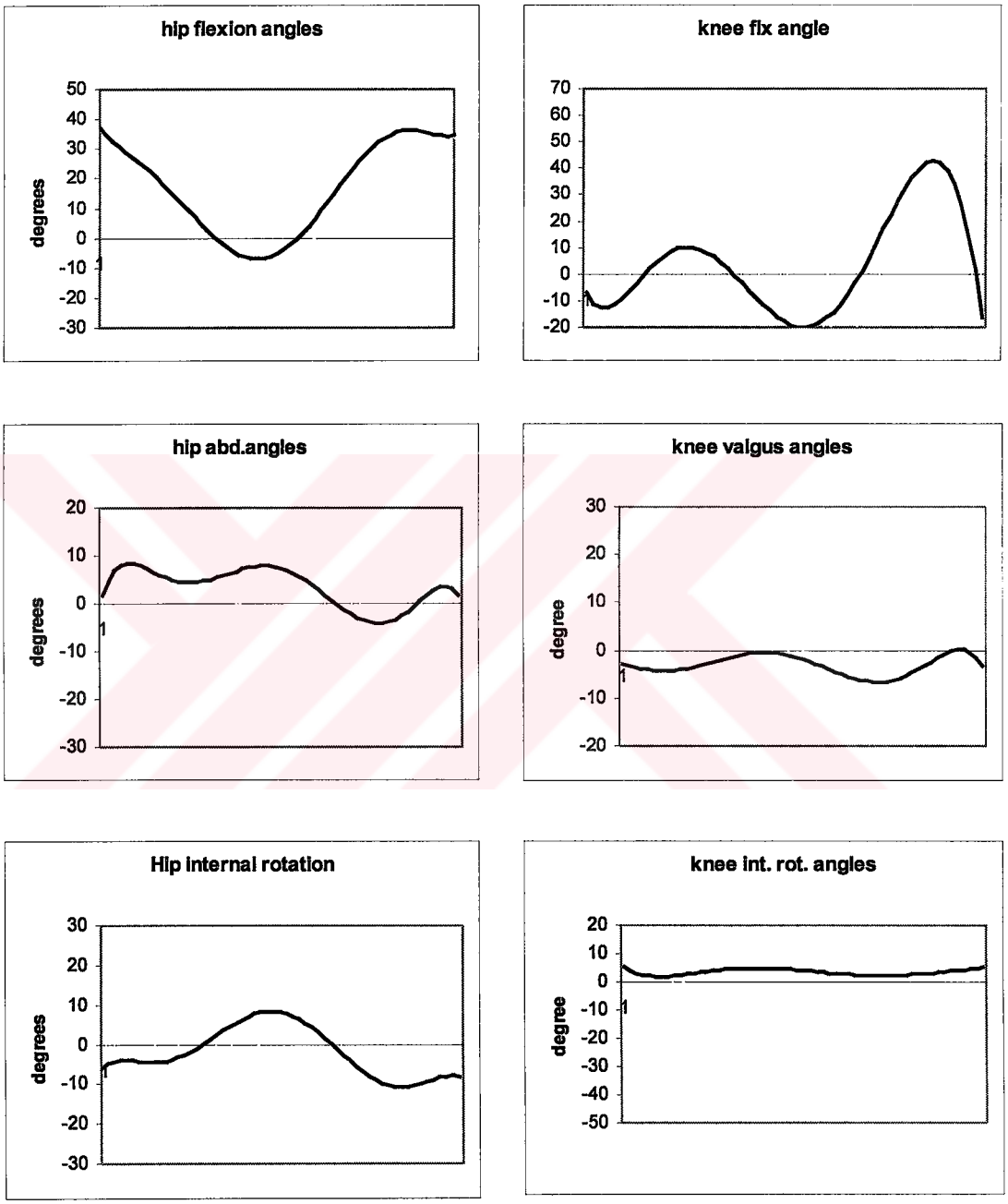

Figure C- 21: Joint angles using instantaneous axis of rotation method

5.1.2 RODRIGUES' FORMULA FOR FINITE ROTATIONS

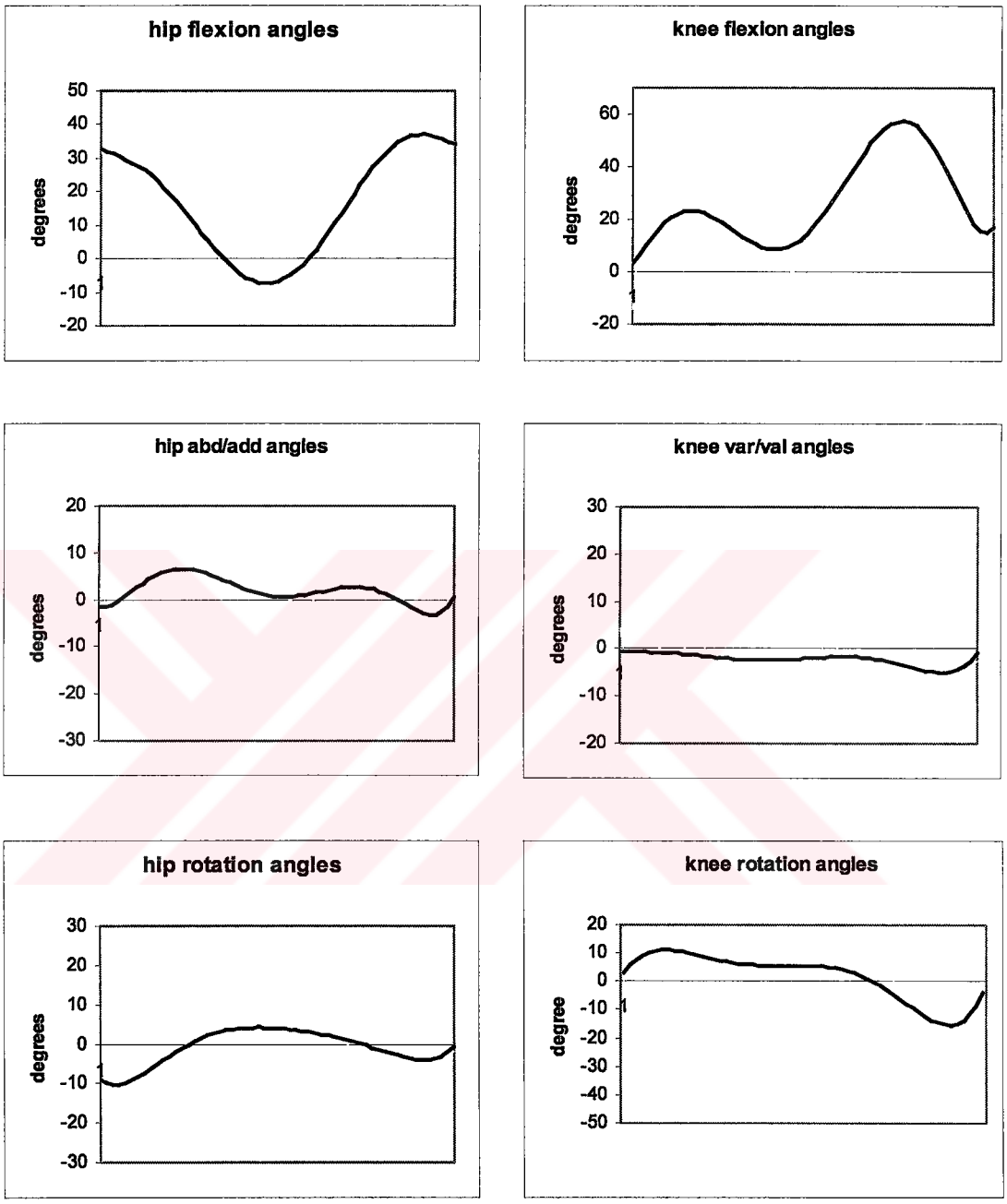

Figure C- 22: Joint angles using Rodrigues' formula

5.2 Second Experiment

5.2.1 INSTANTANEOUS AXIS OF ROTATION METHOD

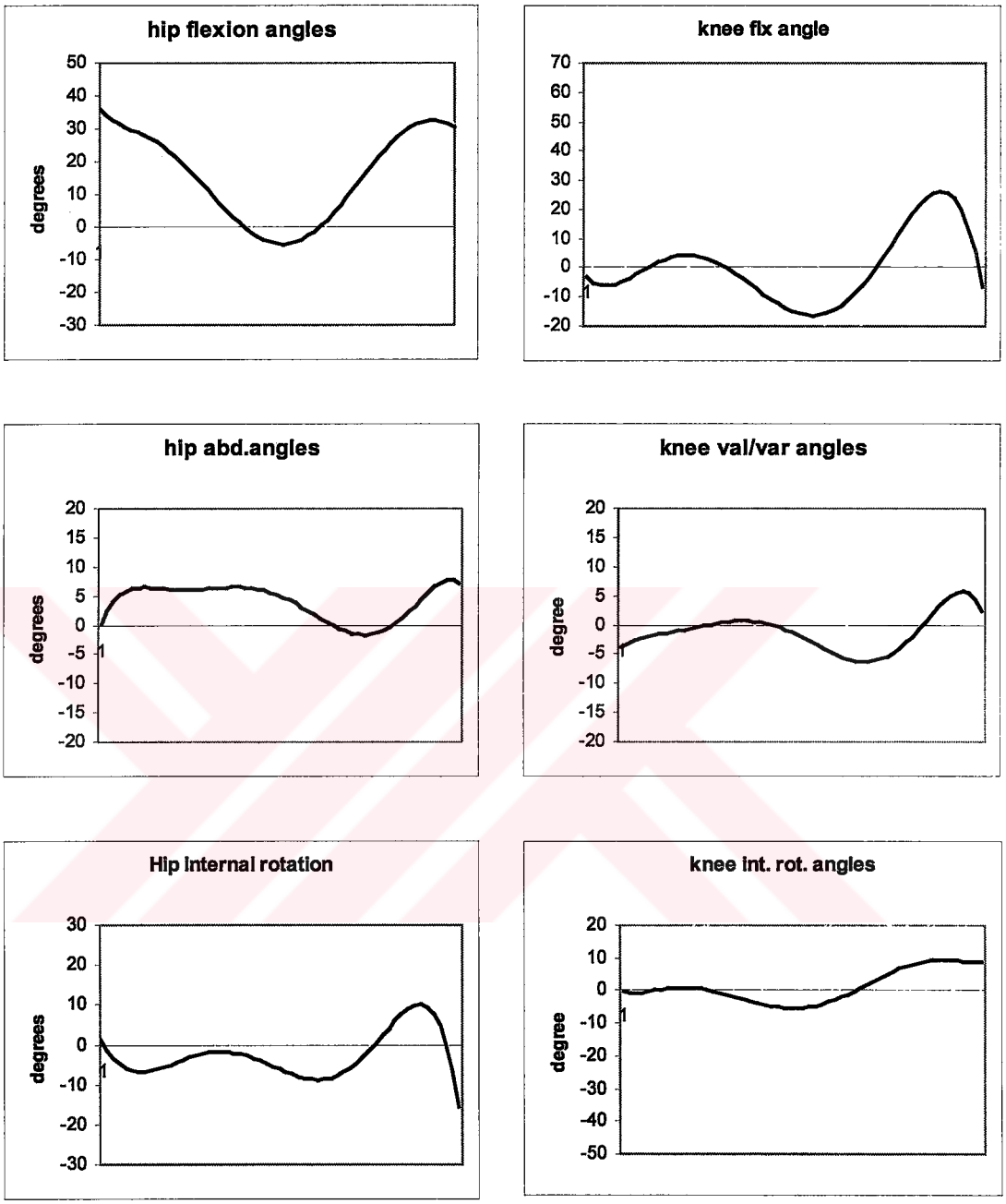

Figure C- 23: Joint angles using instantaneous axis of rotation method

5.2.2 RODRIGUES' FORMULA FOR FINITE ROTATIONS

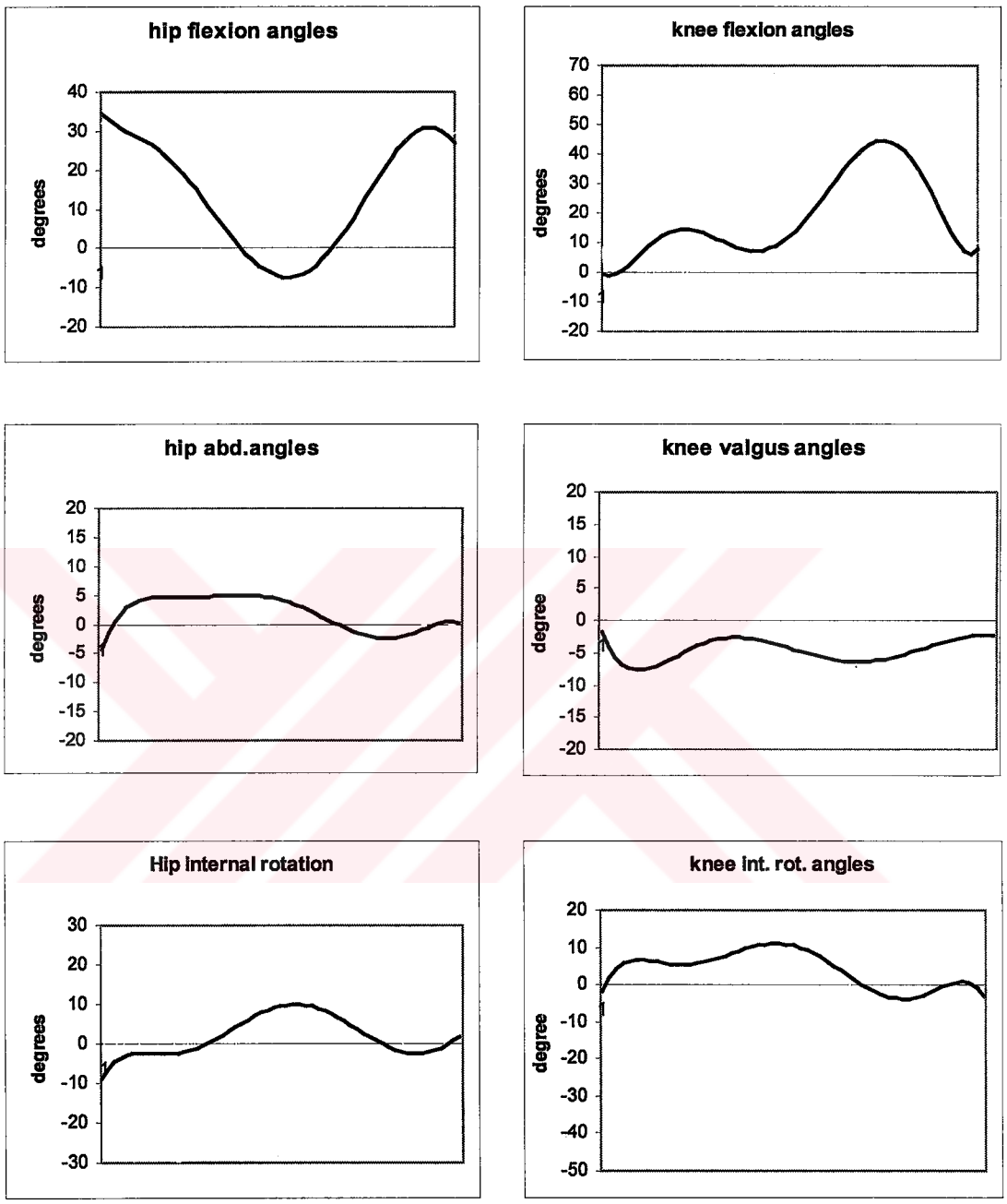

Figure C- 24: Joint angles using Rodrigues' formula

5.3 Results Of KissGAIT

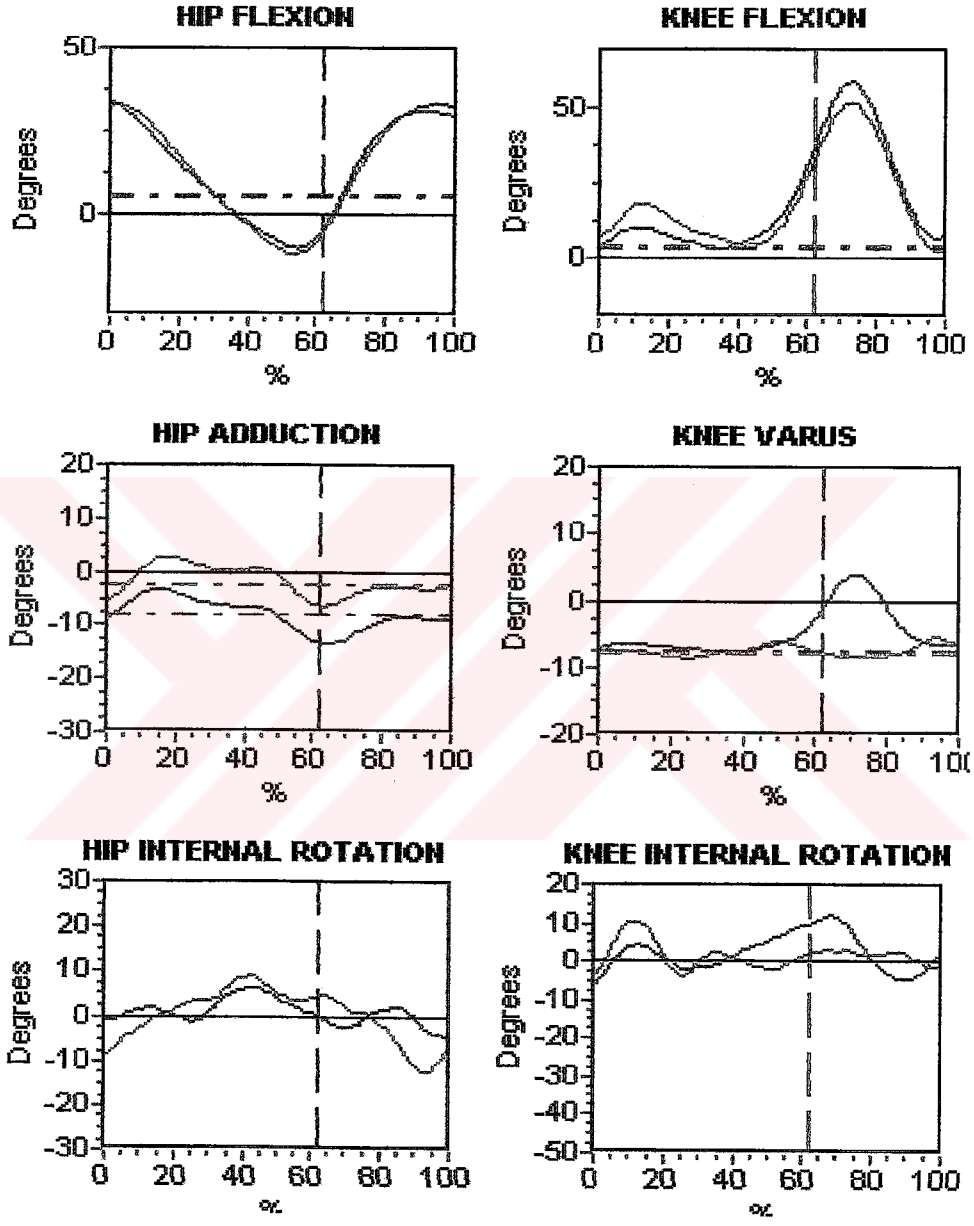

Figure C- 25: Joint angles from KissGAIT

6 Results From Literature And A Commercial System

6.1 Results From Literature[1]

Figure C-26 shows the hip joint angles estimated by Apkarian *et al.* for 3 different subjects.

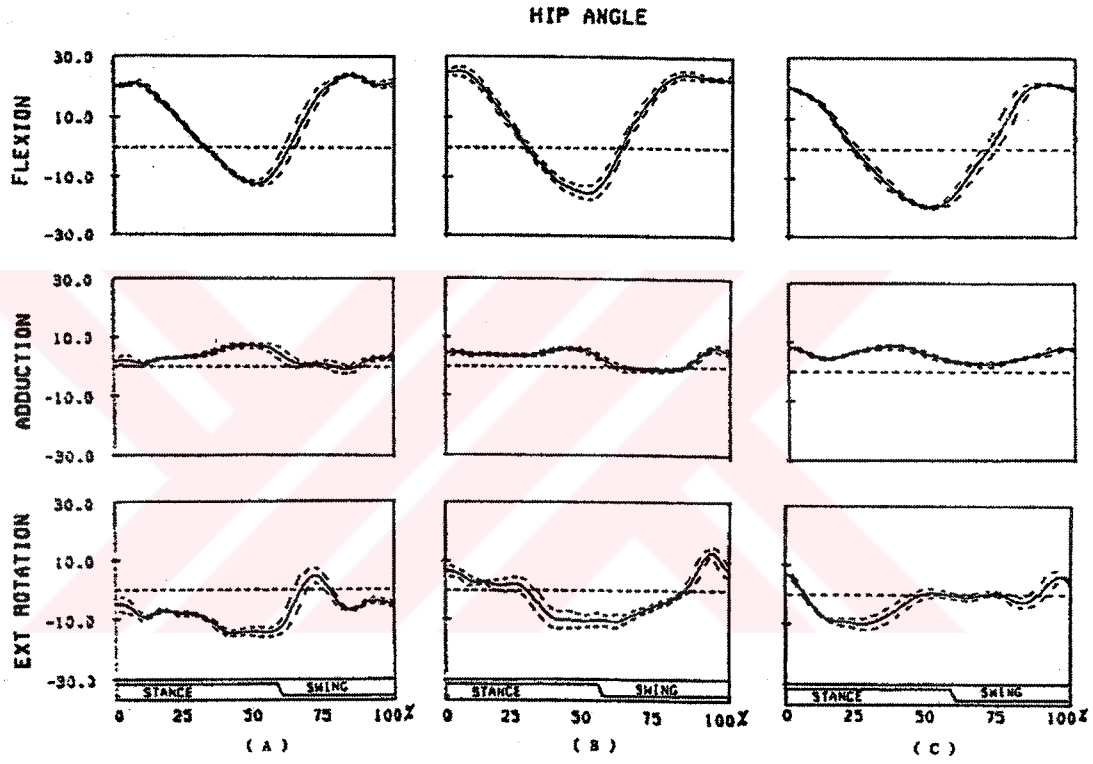

Figure C-26: Hip joint angles

[1] Apkarian *et al.* (1989)

Figure C-27 shows the knee joint angles estimated by Apkarian *et al.* for 3 different subjects.

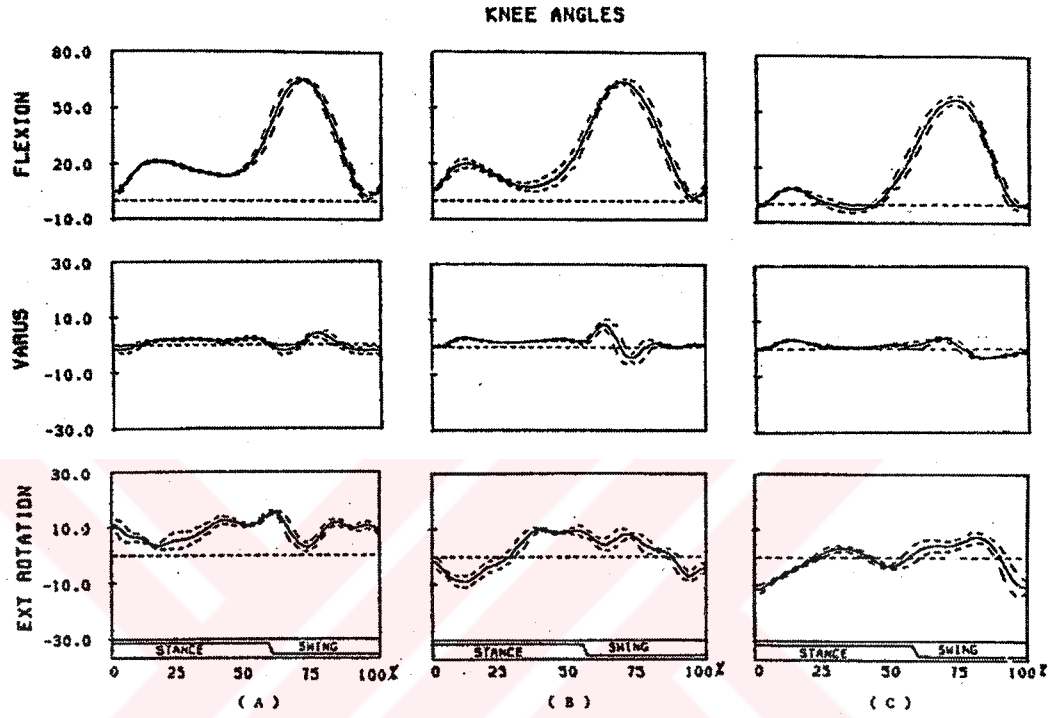

Figure C-27: Knee joint angles

6.2 Results From A Commercial System[2]

The results in Figure C-28 are from Dr. Richard Baker, Musgrave Park Hospital Belfast N. Ireland using a six-camera Vicon© system. Knee rotation angle is not defined in this system.

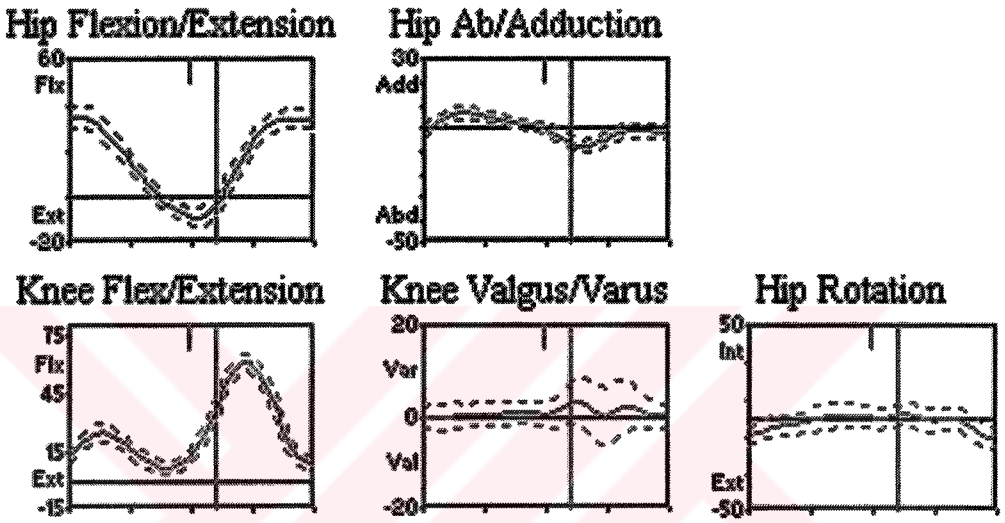

Figure C-28: Joint angles by Vicon©-1

The second results are from Dr. ChrisKirtley, Honkong Polytechnic University again using a six-camera Vicon© system (Figure C-29).

[2] Vicon© using laboratories around the world

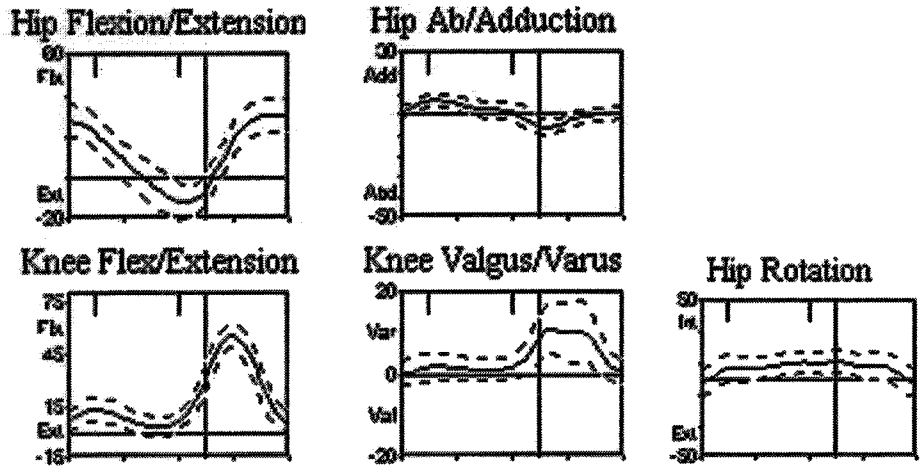

Figure C-29: Joint angles by Vicon©-2